AD_____

Award Number: DAMD17-00-C-0026

TITLE: Characterization and Modulation of Proteins Involved in SM Vesication

PRINCIPAL INVESTIGATOR: Dean S. Rosenthal, Ph.D.

CONTRACTING ORGANIZATION: Georgetown University
Washington, DC 20057-1411

REPORT DATE: May 2005

TYPE OF REPORT: Annual, Phase II

PREPARED FOR: U.S. Army Medical Research and Materiel Command
Fort Detrick, Maryland 21702-5012

DISTRIBUTION STATEMENT: Approved for Public Release;
Distribution Unlimited

REPORT DOCUMENTATION PAGE

Form Approved
OMB No. 0704-0188

1. REPORT DATE *(DD-MM-YYYY)*	**2. REPORT TYPE**	**3. DATES COVERED** *(From - To)*
01-05-2005	Annual, Phase II	1 May 2004 – 30 Apr 2005

4. TITLE AND SUBTITLE
Characterization and Modulation of Proteins Involved in SM Vesication

5a. CONTRACT NUMBER
DAMD17-00-C-0026

5b. GRANT NUMBER

5c. PROGRAM ELEMENT NUMBER

6. AUTHOR(S)
Dean S. Rosenthal, Ph.D.

E-mail: rosenthd@georgetown.edu

5d. PROJECT NUMBER

5e. TASK NUMBER

5f. WORK UNIT NUMBER

7. PERFORMING ORGANIZATION NAME(S) AND ADDRESS(ES)

Georgetown University
Washington, DC 20057-1411

8. PERFORMING ORGANIZATION REPORT NUMBER

9. SPONSORING / MONITORING AGENCY NAME(S) AND ADDRESS(ES)
U.S. Army Medical Research and Materiel Command
Fort Detrick, Maryland 21702-5012

10. SPONSOR/MONITOR'S ACRONYM(S)

11. SPONSOR/MONITOR'S REPORT NUMBER(S)

12. DISTRIBUTION / AVAILABILITY STATEMENT
Approved for Public Release; Distribution Unlimited

13. SUPPLEMENTARY NOTES
Original contains color plates: All DTIC reproductions will be in black and white.

14. ABSTRACT

We defined the molecular events leading to SM vesication to develop medical countermeasures for exposure of military personnel and civilians. We blocked SM-induced toxicity using a genetic approach, and are now adopting a chemical inhibitor-based strategy to block these pathways. We made significant headway in elucidating important pathways of SM-induced cell death in cultured human keratinocytes (KC) and in intact mouse and grafted human skin (Rosenthal *et al.,* 2002). SM induces terminal differentiation markers as well as apoptosis in KC and involves activation of a death receptor pathway for apoptosis, in which Fas plays a role, as well as a calmodulin (CaM)/Bcl-2-mediated mitochondrial apoptotic pathway (Rosenthal *et al*, 1998). Significantly, altering Fas/FADD pathways in human skin grafted onto nude mice reduces vesication and tissue injury in response to SM (Rosenthal *et al*., 2003). We now tested whether CaM mediates the mitochondrial apoptotic pathway induced by SM. RT-PCR and immunoblot analysis revealed rapid modulation in CaM expression following SM treatment. To delineate the potential role of CaM1, the predominant form expressed in KC, in the regulation of SM-induced apoptosis, retroviral vectors expressing CaM1 RNA in the antisense (AS) orientation were used to transduce and derive CaM1 AS cells, which were exposed to SM and subjected to immunoblot analysis for expression of apoptotic markers. Proteolytic activation of "executioner" caspases-3, -6, -7, and the "upstream" caspase-9, as well as caspase-mediated PARP cleavage were inhibited by CaM1 AS expression. Consistent with a mitochondrial apoptotic pathway for CaM, CaM1 AS did not prevent Fas-induced apoptosis. Changes in pro- and anti-apoptotic Bcl-2 family proteins were examined to determine their role in CaM-mediated pathways. CaM1 AS upregulated anti-apoptotic protein Bcl-xL, and blocked Bcl-2 down-regulation. SM-treated CaM1-depleted KC expressed the phosphorylated, non-apoptotic sequestered form of Bad, whereas Bad was present only as the hypophosphorylated apoptotic form in SM-exposed control KC. To determine if pharmacological CaM inhibitors could mediate SMinduced apoptosis *via* Bad dephosphorylation, KC were pretreated with the CaM-specific inhibitor W-13, along with its inactive analogue W-12. Following SM, KC exhibited Bad dephosphorylation, which was inhibited by W-13, but not with W-12. W-13 also attenuated SM-induced proteolytic activation of caspase-3, indicating that the CaM/mitochondrial pathway plays a role in SM-induced apoptosis, and is therefore a target for therapeutic intervention to reduce SM injury. Peptide inhibitors of caspases 3, 8, and 9 are also currently being utilized in an attempt to reduce SM-induced cytotoxicity and vesication in human skin grafts.

15. SUBJECT TERMS
Mustard, Chemical Defense

16. SECURITY CLASSIFICATION OF:			**17. LIMITATION OF ABSTRACT**	**18. NUMBER OF PAGES**	**19a. NAME OF RESPONSIBLE PERSON**
					USAMRMC
a. REPORT	**b. ABSTRACT**	**c. THIS PAGE**			**19b. TELEPHONE NUMBER** *(include area code)*
U	U	U	UU	78	

Standard Form 298 (Rev. 8-98)
Prescribed by ANSI Std. Z39.18

FOREWORD

Opinions, interpretations, conclusions and recommendations are those of the author and are not necessarily endorsed by the U.S. Army.

✓ Where copyrighted material is quoted, permission has been obtained to use such material.

✓ Where material from documents designated for limited distribution is quoted, permission has been obtained to use the material.

✓ Citations of commercial organizations and trade names in this report do not constitute an official Department of Army endorsement or approval of the products or services of these organizations.

N/A In conducting research using animals, the investigator(s) adhered to the "Guide for the Care and Use of Laboratory Animals," prepared by the Committee on Care and use of Laboratory Animals of the Institute of Laboratory Resources, national Research Council (NIH Publication No. 86-23, Revised 1985).

N/A For the protection of human subjects, the investigator(s) adhered to policies of applicable Federal Law 45 CFR 46.

N/A In conducting research utilizing recombinant DNA technology, the investigator(s) adhered to current guidelines promulgated by the National Institutes of Health.

N/A In the conduct of research utilizing recombinant DNA, the investigator(s) adhered to the NIH Guidelines for Research Involving Recombinant DNA Molecules.

N/A In the conduct of research involving hazardous organisms, the investigator(s) adhered to the CDC-NIH Guide for Biosafety in Microbiological and Biomedical Laboratories.

11/15/05

DAMD 17-00-C-0026 PI - Signature Date

TABLE OF CONTENTS

1. OVERVIEW

Sulfur mustard (bis-(2-chloroethyl) sulfide; SM), the highly reactive vesicant agent used in 1988/89 in the Iraq/Iran conflict and presumably in the Gulf War, produces severe skin blisters *via* its ability to induce the death and detachment of the basal cells of the epidermis from the basal lamina (Meier *et al.*, 1984; Gross *et al.*, 1988; Petrali *et al.*, 1990; Smith *et al.*, 1990; Papirmeister *et al.*, 1991; Smith *et al.*, 1991). We have shown that SM induces both terminal differentiation and apoptosis in human keratinocytes (KC; Rosenthal *et al.*, 1998b), while human dermal fibroblasts contribute to the vesication response by releasing degradative cytosolic components after a PARP-dependent SM-induced necrosis (Rosenthal *et al.*, 2001).

Changes in intracellular Ca^{2+} (Ca_i) and calmodulin (CaM) have been implicated in SM cytotoxicity (Ray *et al.*, 1993; Ray *et al.*, 1995; Mol and Smith, 1996; Rosenthal *et al.*, 1998c). In cultured KC, elevation of extracellular Ca^{2+} and other differentiating agents raise Ca_i due to increased activity of phospholipase C isoforms γ1 and ∂1 (Punnonen *et al.*, 1993), both of which are bound and stimulated by CaM, (Lowry *et al.*, 1996; Richard *et al.*, 1997), generating IP3 (along with DAG) and release of Ca_i from ER stores. Elevated Ca_i, in conjunction with DAG, activates PKC, and subsequently the expression of KC differentiation-specific markers (Hennings *et al.*, 1980; Stanley and Yuspa, 1983; Rosenthal *et al.*, 1991), while agents that chelate and buffer Ca_i can block markers of terminal differentiation (Li *et al.*, 1995). The response of cultured KC to CaM and Ca^{2+} is physiologically relevant, since a gradient of Ca^{2+} increases in the upper layers of the epidermis (Malmqvist *et al.*, 1983; Menon *et al.*, 1985), and malignant transformation of KC is closely associated with the loss of the ability of KC to respond to Ca^{2+}

CaM also directly regulates other Ca^{2+} transport processes controlling differentiation and apoptosis. All four isoforms of the plasma membrane Ca^{2+} pump are stimulated by Ca^{2+}-CaM (Carafoli, 1992). Other Ca^{2+}-permeable channels within the plasma membrane, including cyclic-nucleotide-gated channels (Liu *et al.*, 1994), those encoded by the *trp* and *trpl* genes, and N-methyl D-aspartate receptors (Ehlers *et al.*, 1996), expressed in

KC (Morhenn *et al*., 1994), are directly regulated by Ca^{2+}-CaM. CaM indirectly regulates other Ca^{2+} channels *via* CaM kinases, phosphatases, and cAMP (Gnegy, 1993).

Published studies, including ours, utilizing inhibitors of CaM have implicated the importance of Ca^{2+}-CaM complexes in programmed cell death (Pan *et al*., 1996; Sasaki *et al*., 1996; Rosenthal *et al*., 1998c). CaM may also play a role in the induction of an endonuclease responsible for internucleosomal DNA cleavage, yielding the characteristic apoptotic DNA ladders (Jones *et al*., 1989; McConkey *et al*., 1989), and studies have shown that the apoptotic endonuclease AP-24 is activated via CaM-dependent protein kinase II (Wright *et al*., 1998a; Wright *et al*., 1998b). A cytoskeletal-associated CaM-binding death-domain-containing protein termed DAP kinase induces apoptosis in a CaM-dependent fashion (Cohen *et al*., 1997), and thus indicates another important direct role for CaM in apoptosis. Another pathway that modulates Ca^{2+}-CaM-related apoptosis involves CaM-dependent kinase IV (CaMKIV), which is cleaved during apoptosis (McGinnis *et al*., 1998).

To help develop medical countermeasures for potential exposure of military personnel and civilians to SM, we have been defining the molecular series of events leading to SM toxicity in cell culture and in grafted human epidermis. We have shown that SM-induced apoptosis in KC proceeds via both death receptor and mitochondrial pathways (Rosenthal *et al*., 2000b; Rosenthal *et al*., 2003). Blocking the death receptor signaling by stable expression of FADD-DN can suppress SM-induced markers of KC apoptosis, as shown by diminished caspase-3 activity and proteolytic processing of procaspases-3, -7, and –8, internucleosomal DNA cleavage, and caspase-6-mediated nuclear lamin cleavage (Rosenthal *et al*., 2003).

An early event in DNA-damaged cells involves release of cytochrome c and other apoptogenic factors from mitochondria, which occurs prior to caspase activation (Bossy-Wetzel *et al*., 1998). Pro-apoptotic members of the Bcl-2 family, including Bax and Bak can oligomerize and insert into the mitochondrial cell membrane and directly or indirectly induce the release of apoptogenic factors from the mitochondria. Bcl-2 and Bcl-xL form inactive heterodimers with Bax and Bak, while BH3-only Bcl-2 family members, including the hypophosphorylated form of Bad, help dissociate these inactive heterodimers and/or induce active Bax or Bak homo-oligomers. Thus, the activation of the mitochondrial pathway of apoptosis depends ultimately on the

relative levels and modifications of the pro- and anti-apoptotic Bcl-2 family proteins. CaM activates the serine/threonine phosphatase calcineurin, which induces apoptosis (Shi *et al*., 1989), probably *via* its ability to interact with different Bcl-2 family members (Shibasaki *et al*., 1997) and to dephosphorylate Bad (Yang *et al*., 1995; Datta *et al*., 1997; del Peso *et al*., 1997; Hsu *et al*., 1997; Wang *et al*., 1997; Zha *et al*., 1997; Scheid and Duronio, 1998; Zundel and Giaccia, 1998), allowing it to interact with Bcl-2 or Bcl-xL and induce apoptosis (Yang *et al*., 1995). These interactions are significant, since calcineurin has narrow substrate specificity.

In the present contract, we investigated the role of CaM in the apoptotic responses in KC, and whether these pathways can be modulated to alter SM toxicity in cell culture models. We have now utilized CaM1 antisense (AS) and demonstrate that SM-induced KC apoptosis is CaM-dependent, and involves caspase-3, -6, -7, and -9 activation and a mitochondrial/Bad-mediated pathway. Our experiments indicate that the CaM/Bad pathway is at least in part involved in SM-induced apoptosis, since both CaM1 antisense, as well as specific inhibitors of this pathway block caspase-3 proteolytic activation. Inhibition of the CaM/Bad pathway by specific pharmacological inhibitors such as W13 or CaM1 RNA_i may therefore be of therapeutic value in the treatment of or prophylaxis against SM injury in humans.

We have shown earlier that primary KC as well as an immortalized line, Nco, could be used to establish a histologically and immunocytochemically normal epidermis when grafted onto nude mice (Rosenthal et al., 1995; Rosenthal et al., 1998; Rosenthal et al., 2001). In addition, our recent results have demonstrated that markers of apoptosis are induced in basal cells, particularly in regions where microvesicles are formed. Utilizing the graft system to generate a human epidermis containing keratinocytes expressing FADD-DN, we showed that microvesication is reduced by the inhibition of FADD. Our previous studies with Fas-deficient mice also indicate the viability of this strategy to prevent vesication by using inhibitors of the death receptor pathway. Importantly, our inhibition experiments indicated that the Fas/FADD and CaM pathways converge upstream of caspase-3 processing, since inhibitors of either pathway inhibit SM-induced apoptosis. Since the FADD pathway can be manipulated at the level of a cell surface (Fas/TNF), receptor, Fas/FADD as well as the caspases represent attractive targets for the modulation of the effects of SM. Inhibition of the Fas/FADD

pathway or of CaM/ mitochondrial pathways by specific pharmacological inhibitors such as peptide inhibitors of caspases or CaM inhibitors may therefore be of therapeutic value in the treatment of or prophylaxis against SM injury in humans.

2. RAPID MODULATION OF CAM1 EXPRESSION FOLLOWING SM EXPOSURE OF CULTURED HUMAN KERATINOCYTES

2.1 Introduction

In the previous contract period, we devoted our efforts to investigating the roles of the Fas/FADD death receptor pathway and the sequence of caspase activation during SM-induced apoptosis in cultured human KC, and potentially involved in vesication. Since changes in Ca_i and CaM have been implicated in SM cytotoxicity (Ray *et al.*, 1993; Ray *et al.*, 1995; Mol and Smith, 1996; Rosenthal *et al.*, 1998c), we next focused on the role of CaM in SM-induced apoptosis. We utilized much of the same technology that we successfully employed previously to answer an essential question- How does the CaM/mitochondrial pathway regulate the apoptotic response in human KC, and can these pathways be modulated to alter **SM** vesication in primary human KC and in human skin grafted onto nude mice? Thus, will targeting these pathways using pharmacological inhibitors alter the cytotoxic response of keratinocytes to SM in cell culture, and the vesication response *in vivo?*

Ca^{2+} signaling in KC has been implicated in the activation of PLC and PKC, which may be a major signal for differentiation, and Ca^{2+}-CaM complexes are also generated which modulate this PKC response (Chakravarthy *et al.*, 1995). Consistently, we have demonstrated that induction of KC differentiation-specific markers by SM is Ca^{2+}-dependent, since expression of these markers is blocked by the Ca^{2+}-chelator BAPTA (Rosenthal *et al.*, 1998b; Rosenthal *et al.*, 2000a). Pre-treatment of KC with a CaM inhibitor (W-7) also suppresses the expression of the differentiation-specific marker keratin K1 in the presence of SM (Rosenthal *et al.*, 2000a) suggesting that SM-induced changes in differentiation in these cells is mediated by CaM.

Three human genes encode *bona-fide* CaM, CaM1 (Wawrzynczak and Perham, 1984), CaM2 (SenGupta *et al.*, 1987; Toutenhoofd *et al.*, 1998), and CaM3 (Fischer *et al.*, 1988, Koller, 1990 #5177), which are about 80% coding region homology at the nucleotide level, but encode identical proteins (Fischer *et al.*, 1988). In addition to several pseudogenes (Rhyner *et al.*, 1994), a related functional gene, CALML3/GH6/CLP (Koller

and Strehler, 1988) is expressed only in the epithelium of the tissues including thyroid, breast, prostate, kidney, and skin; in the latter, CLP expression increased in the upper differentiating layers (Rogers *et al.*, 2001). To determine which of the CaM genes is primarily involved in the SM-induced apoptotic response as well as alterations in CaM protein levels in response to SM, we first monitored the endogenous levels of CaM protein and mRNA during SM-induced apoptosis by RT-PCR and immunoblot analysis.

2.2 Materials and Methods

(1) Culture of primary and immortalized human keratinocytes, and exposure to SM.

a. Cells. Primary human KC were derived from neonatal foreskins and grown in KC serum-free medium (SFM) supplemented with human recombinant EGF and bovine pituitary extract (Life Technologies Inc., Rockville, MD). Cells were grown to 60-80% confluency, and then exposed to SM diluted in SFM to final concentrations of 100, 200, or 300 μM, with or without pretreatment with CaM inhibitors. Media was not changed for the duration of the experiments. At indicated time points after SM exposure, cells were harvested for further analyses.

b. Chemicals. SM (bis-(2-chloroethyl) sulfide; >98% purity) was obtained from the US Army Edgewood Research, Development and Engineering Center.

(2) Reverse transcription-polymerase chain reaction (RT-PCR). Unique oligonucleotide primer pairs for CaM1, CaM2, CaM3, and CLP mRNA were designed and prepared. RT-PCR was performed with total RNA, purified from cell pellets with Trizol Reagent (Life Technologies), utilizing a Perkin Elmer Gene Amp EZ rTth RNA PCR kit according to manufacturer's specifications. After RNA was transcribed at 65 ºC for 40 min, DNA was amplified by an initial incubation at 95 ºC for 2 min, followed by 30 cycles of 95 ºC for 1 min, 60 ºC for 1.5 min, and 65 ºC for 0.5 min, and a final extension at 70 ºC for 22 min. PCR products were then separated by electrophoresis in a 1.5% agarose gel and visualized by ethidium bromide staining.

(3) Immunoblot analysis. SDS-polyacrylamide gel electrophoresis and transfer of separated proteins to nitrocellulose membranes were performed according to standard procedures. Proteins were measured (DCA

protein assay; BioRad, Hercules, CA), and normalized prior to gel loading, and all filters were stained with Ponceau-S, in order to reduce the possibility of loading artifacts. After blocking of nonspecific sites, the blots were incubated with monoclonal or polyclonal antibodies (below) and then detected with appropriate peroxidase-labeled secondary antibodies (1:3000 dilution) and enhanced chemiluminescence (ECL, Amersham). Immunoblots were sequentially stripped by incubation for 30 min at 50 ˚C with a solution containing 100 mM 2-mercaptoethanol, 2% SDS, and 62.5 mM Tris-HCl (pH 6.7), blocked again, and reprobed with additional antibodies to accurately compare different proteins from the same filter. Typically, a filter could be reprobed three times before there was detectable loss of protein from the membrane, which was monitored by Ponceau S staining after stripping.

a. Antibodies. All antibodies indicated in Table 1 were tested and used successfully in our laboratory.

Table 1

Antibody (kDa)	type(clone)	Source	Dilution (conc.
CaM	polyclonal	Sigma	1:1000
Caspase 3	monoclonal	Santa Cruz Biotech	1:200
Caspase 7	polyclonal	PharMingen	1:1000
Caspase 6	polyclonal	Trevigen	1:1000
Caspase 8	monoclonal	PharMingen	1:1000
Caspase 9	monoclonal (SY5)	Trevigen	1:1000
DFF 45	monoclonal	PharMingen	1:500
PARP	monoclonal	PharMingen	1:1000
Bcl-xL	monoclonal	Calbiochem	1:400
Bcl-2	monoclonal	BioMol	1:200
Bax	monoclonal	Calbiochem	1:50
Bad	monoclonal	NEB	1:1000
Phospho-Bad	monoclonal	NEB	1:1000
GAPDH			

2.3 Results and Discussion

Primary human KC were exposed to indicated doses (100, 200, and 300 μM) of SM and extracts were derived at indicated times and subjected to immunoblot analysis with epitope specific antibodies as well as to RT-PCR, as described in Materials and Methods. When levels of CaM protein and mRNA during SM-induced apoptosis were monitored by RT-PCR and immunoblot analysis, we observed a rapid modulation in CaM expression following SM treatment. Prior to and 24 h following SM exposure CaM1 is the predominant form expressed in KC is (Fig. 1A). A time course experiment also showed a transient increase in CaM1 protein for 2 h following exposure to SM, followed by a subsequent decrease to negligible levels by 6 h. A marked decrease in CaM1 transcript levels in SM-exposed KC at 24 h, as shown by RT-PCR analysis correlates with decreased abundance of CaM protein in these cells 6 to 24 h after SM exposure. In contrast, untreated KC exhibited lower transcript levels of CaM2 compared to CaM1 and showed no change in CaM2 expression after SM. There were also no differences in mRNA or protein levels of GAPDH, as normalization or loading control, in these cells before or after SM exposure. This, together with our previous results, indicated that CaM1 might play a role in the response of KC to SM.

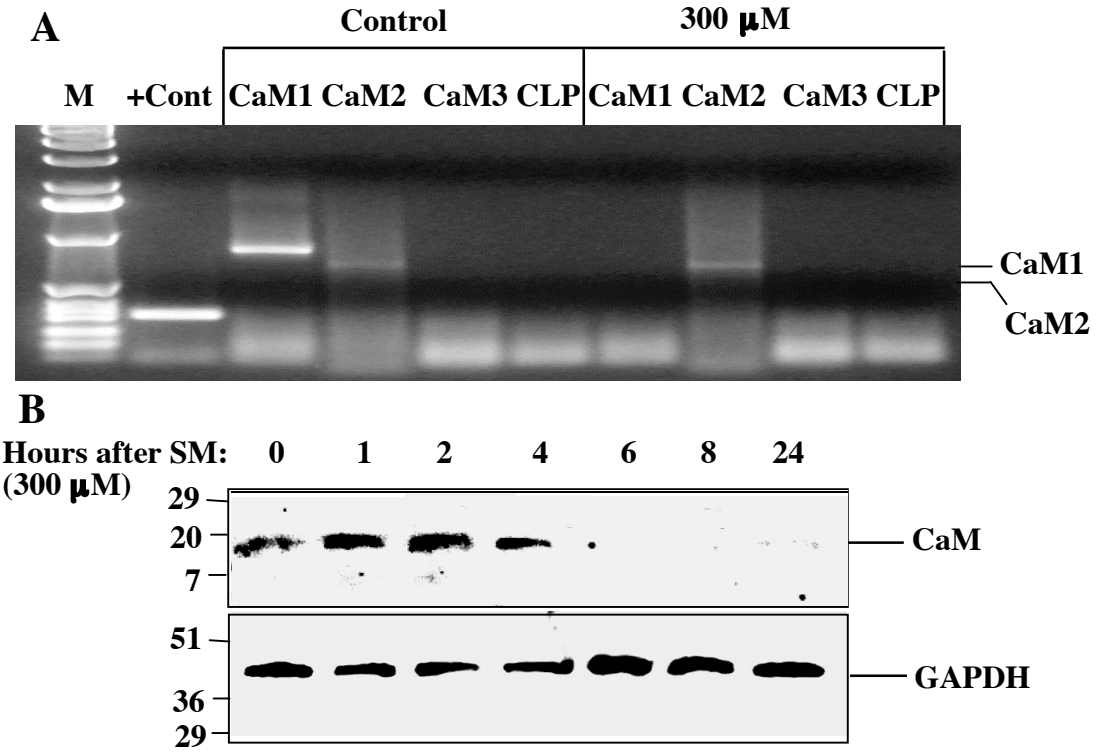

Fig. 1 *CaM1, the predominant CaM in KC, is induced and subsequently suppressed by SM.*
(A) Primary human KC were incubated for 16 h with a vesicating dose (300 mM) of SM in SFM, after which cells were harvested and subjected to RT-PCR analysis with specific primers for three *CaM* genes and *CLP*.
(B) Primary human KC were incubated with 300 mM SM in SFM and, after the indicated times, cell extracts were prepared and assayed for CaM protein levels by immunoblot analysis. The positions of molecular size standards (in kilodaltons) and of the various proteins and DNA are indicated.

3. ROLE OF CAM1 IN PROGRESSION OF SM-INDUCED APOPTOSIS OF HUMAN KERATINOCYTES: CASPASE ACTIVATION

3.1 Introduction

To further delineate the role of CaM1 in the regulation of SM-induced apoptosis in primary KC, we utilized an AS RNA approach to determine the effect of constitutive depletion of CaM1 protein in these cells. A retroviral vector was constructed expressing CaM1 RNA in the AS orientation. A 900 bp CaM1 cDNA fragment, derived by RT-PCR with KC mRNA and specific primers, was ligated in the AS orientation into the retroviral vector, LXSN (Fig. 2A; Clontech). Following transient transfection of an amphotropic retrovirus packaging cell line (ϕNX; Gary Nolan; Stanford), high-titer viral supernatants (>10^6/ml) were derived, filtered, and used to infect KC. After selection in neomycin to ensure that 100% of the cells are expressing CaM AS RNA, resistant colonies were pooled from each transduction and used for subsequent experiments. These pooled cells were exposed to 100, 200, or 300 μM SM. Immunoblot analysis with antibodies to CaM was first performed to confirm depletion of endogenous CaM1 protein in the CaM1 AS-expressing cells. Compared to vector-transduced cells, significantly diminished levels of endogenous CaM protein was noted in CaM1 AS cells prior to and after SM exposure (Fig. 2B). We next determined whether these CaM1 AS constructs could alter the response of KC to SM with respect to apoptosis.

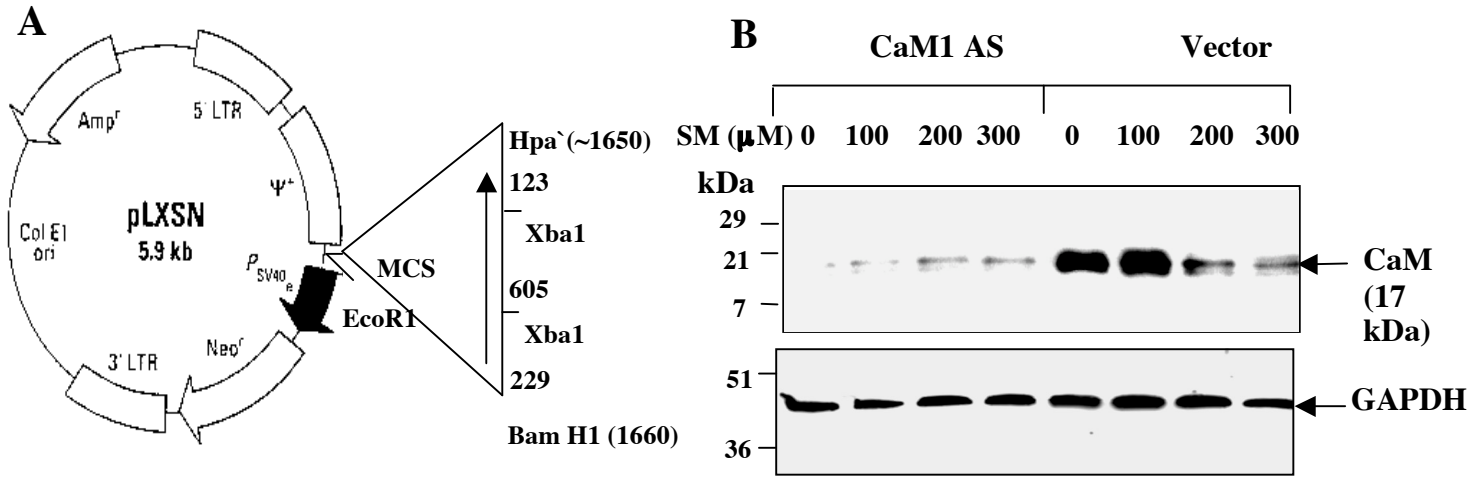

FIG. 2. *Expression of CaM1 AS reduces endogenous levels of CaM. A*. Restriction map of CaM1 cloned into LSXN retroviral vector in AS orientation. A 900 base pair cDNA was derived from KC mRNA and cloned into the Bam H1-Hpa I site of pLXSN as shown. (B) Immunoblot analysis of CaM protein levels prior to and following SM exposure. KC were incubated with indicated doses of SM in SFM and, after 16 h, cell extracts were prepared and assayed for

endogenous CaM levels by immunoblot analysis with antibodies to CaM. The positions of molecular size standards (in kilodaltons) and of CaM are indicated.

3.2 Materials and Methods

(1) Culture of primary and immortalized human keratinocytes, and exposure to SM.

a. Cells, Plasmids, Transfection. Primary human KC were prepared from neonatal foreskins and maintained in serum-free medium (SFM) supplemented with human recombinant EGF and bovine pituitary extract (Life Technologies). A replication-deficient recombinant retroviral construct expressing *CaM1* AS was constructed by subcloning into the retroviral vector pLXSN (Fig. 2A). Correct insertion of CaM1 AS cDNA in the pLXSN vector was confirmed by restriction enzyme digestion mapping, as well as by DNA sequencing. This retroviral construct, as well as empty vector pLXSN were then packaged and propagated in the amphotropic producer cell line ϕNX by transfection using Lipofectamine 2000 (Life Technologies) according to manufacturer's protocols; viral supernatants were derived, filtered, and used to transduce KC. Retrovirus-infected cells were selected for 10 days in G418, and resistant colonies were pooled from each transduction. Immunoblot analysis was performed on expanded pooled cells to confirm loss of CaM1 expression.

b. Chemicals. SM (bis-(2-chloroethyl) sulfide; >98% purity) was obtained from the US Army Edgewood Research, Development and Engineering Center.

c. Exposure to SM. Cells were grown to 60-80% confluency and exposed to SM diluted in KGM to final concentrations of 100, 200, or 300 μM. Media was not changed for the duration of the experiments, and at different times after SM exposure, cells were derived for further analyses.

(2) Immunoblot analysis. SDS-PAGE, transfer of separated proteins to nitrocellulose membranes, and immunoblot analysis were performed according to standard protocols as described above (section 2.2.3).

3.3 Results and Discussion

CaM1 AS blocks SM-induces proteolytic processing of caspases-3 and –6, -7, -8 and –9, and PARP.

To determine the effects of CaM1 depletion by AS expression on the sequence of events involved in SM-induced apoptosis, KC were exposed to various doses of SM and extracts were derived after 24 h and subjected to immunoblot analysis for expression of apoptotic markers. We assayed for the activation of key caspases, in particular the "upstream" caspases -8 and -9, and the "executioner" caspases -3, -6, and -7. The executioner caspases-3 and –6, and -7 were all proteolytically activated after exposure to increasing doses of SM. When the immunoblot was stripped of antibodies and reprobed with antibodies to the initiator caspases -8 and -9, SM-induced proteolytic processing of caspases -8 and –9, as shown by the disappearance of the intact form, was noted in cells exposed to all doses of SM (Fig. 3). Immunoblot analysis using antibodies that recognize both the full length (116 kDa) and 89 kDa cleavage products of PARP, which has been shown to be a substrate of caspase-3 and –7, also revealed that SM-induced apoptosis is accompanied by complete cleavage of PARP at vesicating SM doses (200 and 300 μM).

More significantly, activation of caspases-3, -6, -7, -8, and –9, as well as the caspase-mediated cleavage of PARP were inhibited by the expression of CaM1 AS. Partial proteolytic processing of caspase-3 to p20 at lower doses (100 and 200 mM) and complete processing to p17 after 300 μM SM was noted in vector-transduced cells, but not in CaM1 AS cells. While proteolytic activation of caspase-6 and –8 were observed after 100 and 200 mM SM, only the highest dose (300 mM) induced this response in CaM1-depleted cells. Proteolytic processing of caspase-7 was completely suppressed in CaM1-AS cells at all SM doses tested. Furthermore, caspase-mediated PARP cleavage was noted at 100 mM SM in vector-transduced cells, but not CaM1 AS cells. The depletion of endogenous CaM protein by the CaM1 AS RNA expression was accompanied as well by decreased apoptotic nuclear morphology (data not shown). These results indicate that SM-induced apoptosis is CaM1-dependent, and involves the activation of a number of caspases implicated in both death receptor and mitochondrial pathways of apoptosis. These results further suggest that inhibition of CaM can protect KC from SM-induced apoptosis.

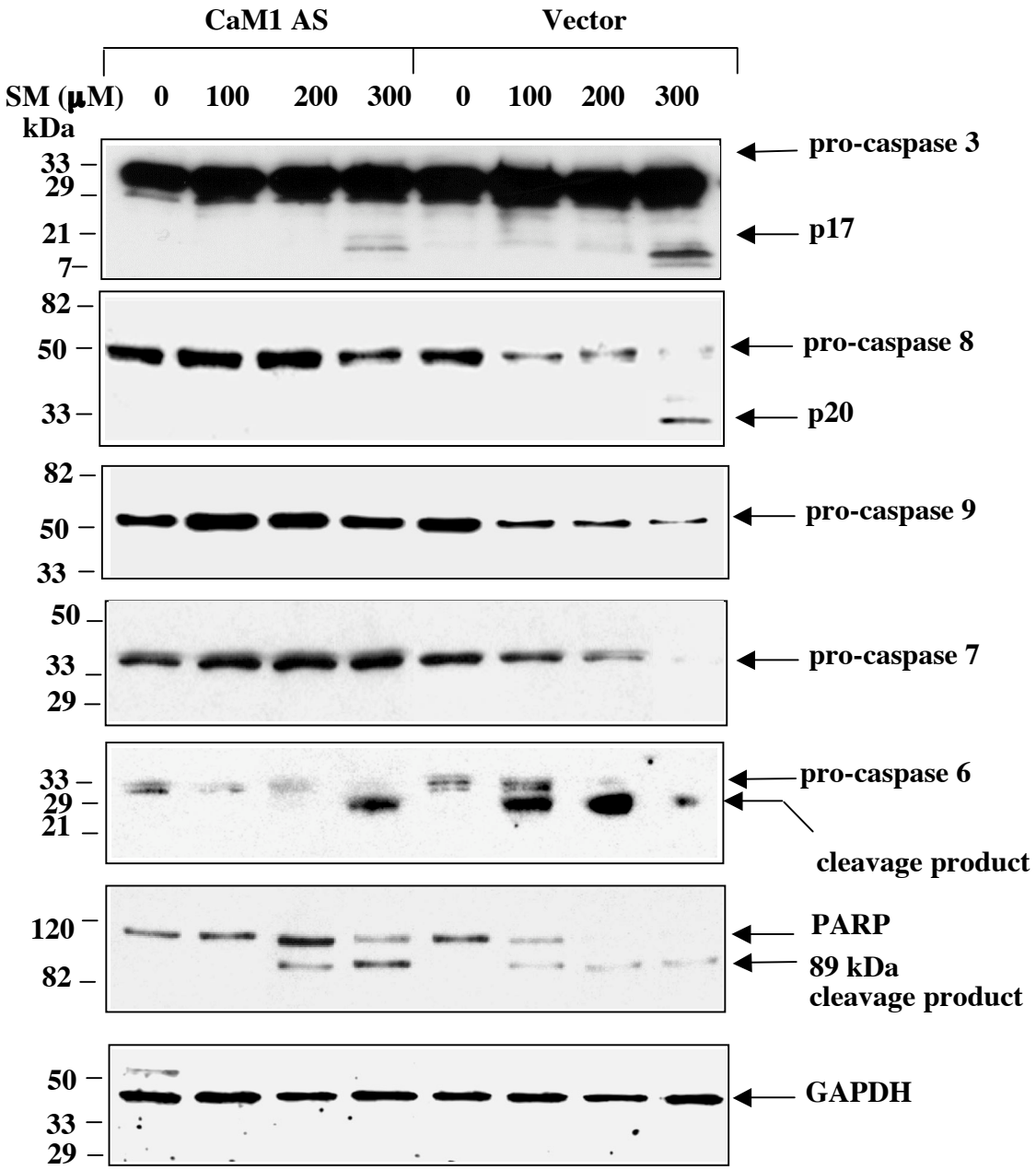

Fig. 3. *CaM1 AS blocks SM-induces proteolytic processing of caspases-3 and –6, -7, -8 and –9, and PARP.* KC were exposed to the indicated doses of SM and extracts were derived after 24 h and subjected to immunoblot analysis using antibodies specific for of "upstream" caspases -8 and -9, the "executioner" caspases -3, -6, and –7, and PARP. Immunoblots were stripped of antibodies and reprobed with antibodies to GAPDH for loading control. The positions of the immunoreactive proteins as well as the molecular size standards are indicated.

CaM1 AS attenuates caspase-3 proteolytic processing induced by SM but not Fas

To determine whether CaM was mediating a death receptor or mitochondrial pathway of SM-induced apoptosis, the response of KC expressing CaM1 AS to SM was compared to that of Fas activation. Figure 4 shows that while CaM1 AS attenuates SM-induced caspase-3 proteolytic processing, no effect was observed on Fas-induced apoptosis, suggesting that CaM1 acts *via* a mitochondrial pathway of apoptosis.

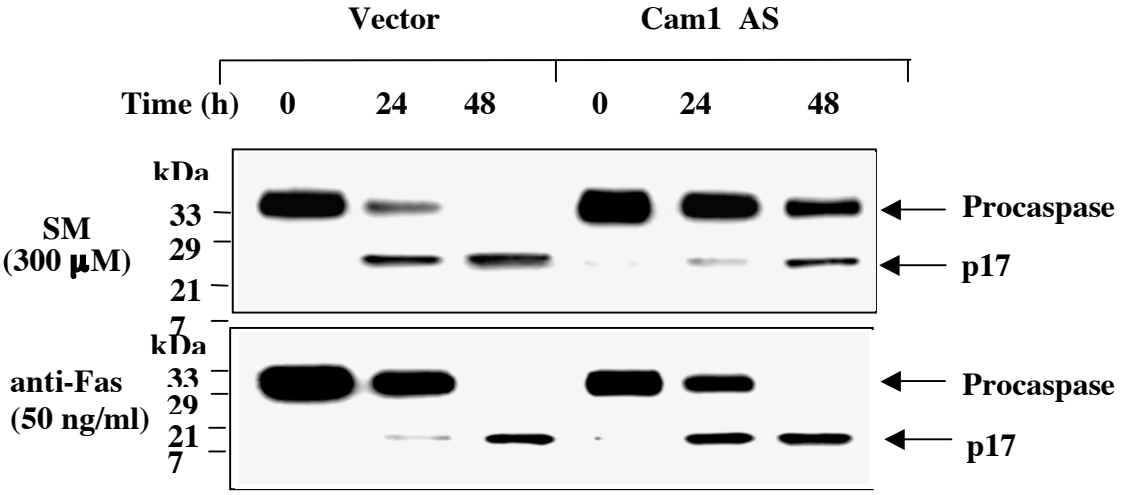

Fig. 4. *CaM1 AS attenuates caspase-3 proteolytic processing induced by SM but not Fas*. KC were exposed to the indicated doses of SM or Fas agonist antibody and extracts were derived after the indicated times and subjected to immunoblot analysis using antibodies specific for the active form of caspase-3. The positions of the immunoreactive proteins as well as the molecular size standards are indicated.

4. EFFECT OF CAM1 ANTISENSE ON THE ENDOGENOUS LEVELS OF BCL-2 FAMILY MEMBERS

4.1 Introduction

Release of cytochrome c and other apoptogenic factors from mitochondria, an early event in DNA-damaged cells, occurs prior to caspase activation (Bossy-Wetzel *et al*., 1998). Pro-apoptotic members of the Bcl2 family, including Bax and Bak can oligomerize and insert into the mitochondrial cell membrane and directly or indirectly induce the release of apoptogenic factors from the mitochondria. Bcl-2 and Bcl-xL form inactive heterodimers with Bax and Bak, while BH3-only Bcl2 family members, including the hypophosphorylated form of Bad, help dissociate these inactive heterodimers and/or induce active Bax or Bak homo-oligomers. Thus, the activation of the mitochondrial pathway of apoptosis depends ultimately on the relative levels and modifications of the pro- and anti-apoptotic Bcl-2 family proteins. CaM has been shown to

activate the serine/threonine phosphatase calcineurin, which induces apoptosis (Shi *et al.*, 1989), probably *via* its ability to interact with different Bcl-2 family members (Shibasaki *et al.*, 1997) and to dephosphorylate Bad (Yang *et al.*, 1995; Datta *et al.*, 1997; del Peso *et al.*, 1997; Hsu *et al.*, 1997; Wang *et al.*, 1997; Zha *et al.*, 1997; Scheid and Duronio, 1998; Zundel and Giaccia, 1998), allowing it to interact with Bcl-2 or Bcl-xL and induce apoptosis (Yang *et al.*, 1995). These interactions are significant, since calcineurin has narrow substrate specificity.

In the results described above, we demonstrate by CaM1 AS that SM-induced human KC apoptosis is CaM-dependent, and involves caspase-3, -6, -7, and -9 activation and a mitochondrial- mediated pathway. We next examined possible mechanisms by which CaM1 may mediate SM-induced apoptotic death. Since CaM has been implicated in regulation of the levels of Bcl-2 family members and thus the mitochondrial pathway of apoptosis, we focused on the role of the Bcl-2 family of proteins, which are involved in the mitochondrial pathway of apoptosis, leading to the activation of caspase-9. Since the ratio of pro- and anti-apoptotic members of the Bcl-2 family determine the stability of the mitochondria, and subsequent release of cytochrome c and caspase-9 activation, changes in the levels of Bcl-2-related proteins were examined to determine their role in CaM mediated pathways.

4.2 Materials and Methods

(1) Culture of primary and immortalized human keratinocytes, and exposure to SM.

a. Cells, Plasmids, Transfection. Primary human KC were prepared from neonatal foreskins and maintained in serum-free medium (SFM) supplemented with human recombinant EGF and bovine pituitary extract (Life Technologies). A retroviral construct expressing *CaM1* AS was constructed as described in section 2.2.1, and along with the empty vector pLXSN, were packaged and propagated in producer cell line ϕNX by transfection. Viral supernatants were derived, filtered, and used to transduce KC. Retrovirus-infected cells were then selected for 10 days in G418, and resistant colonies were pooled from each transduction.

b. Chemicals. SM (bis-(2-chloroethyl) sulfide; >98% purity) was obtained from the US Army Edgewood Research, Development and Engineering Center.

c. Exposure to SM. Cells were grown to 60-80% confluency and exposed to SM diluted in KGM to final concentrations of 100, 200, or 300 μM. Media was not changed for the duration of the experiments, and at different times after SM exposure, cells were derived for further analyses.

(2) Immunoblot analysis. SDS-PAGE, transfer of separated proteins to nitrocellulose membranes, and immunoblot analysis were performed according to standard protocols as described above (section 2.2.3).

4.3 Results and Discussion

In a dose response, primary KC transduced with CaM1 AS or empty vector LXSN were exposed to 0, 100, 200, or 300 μM SM, and extracts were subjected to immunoblot analysis with antibodies specific for anti-apoptotic Bcl2 family members, such as Bcl-2 and Bcl-xL, as well a proapoptotic members, including Bax. While levels of Bcl-xL were undetectable in control KC at all levels of SM tested, CaM1 depletion by AS expression upregulated Bcl-xL expression following exposure to vesicating doses of SM (200 μM and 300 μM; Fig. 5). Bcl-2 was expressed at higher levels in control KC, but levels were markedly reduced in the presence of 200 μM and 300 μM SM. Following CaM depletion by AS RNA expression, however, Bcl-2 was maintained at high levels following treatment with SM at all doses. Whereas levels of Bax increased dose-dependently in control KC, in CaM1-depleted cells, Bax levels were reduced at higher doses of SM.

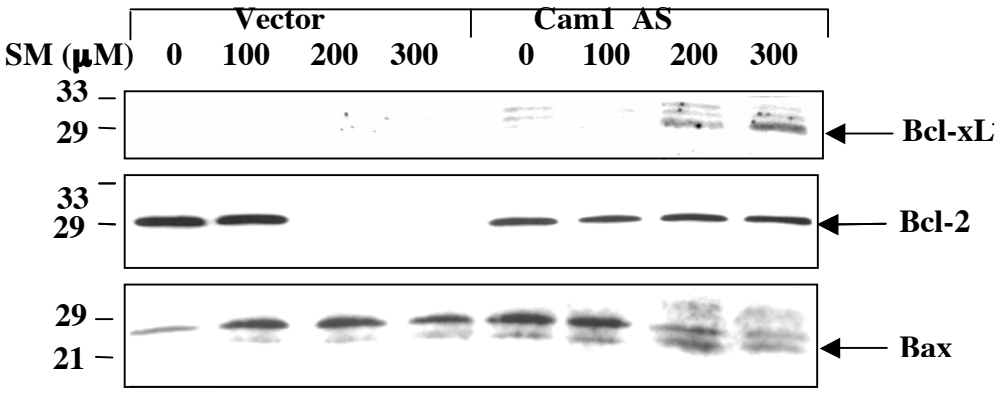

Fig. 5. *CaM1 AS expression upregulates anti-apoptotic Bcl-xL and Bcl-2 expression and blocks upregulation of Bax following exposure to vesicating doses of SM.* Human KC were exposed to the indicated doses of SM and extracts were derived after 24 h and subjected to immunoblot analysis using antibodies specific for Bcl2, BclxL, or Bax. The positions of the immuno-reactive proteins as well as the molecular size standards are indicated.

The abundance of Bad protein was unaffected in CaM1-depleted cells exposed to vesicating doses of SM. However since the phosphorylation status of Bad determines its apoptotic activity, we examined this aspect further in later experiments (see below).

CaM1 depletion may therefore block the mitochondrial pathways of SM-induced apoptosis via upregulation of the anti-apoptotic proteins Bcl-2 and Bcl-xL, as well as the down regulation of the pro-apoptotic protein Bax. This is consistent with previous studies showing that CaM is involved in regulating the levels, intracellular localization, and stability of Bcl-2 family members (Haldar *et al.*, 1995; Shibasaki *et al.*, 1997; Gomez *et al.*, 1998). Thus, depletion of CaM by AS RNA results in the stabilization of mitochondria and inhibits the activation of caspase-9. This finding has direct implications for the utilization of pharmacologically relevant CaM inhibitors to reduce SM toxicity.

5. EFFECT OF CAM1 AS AND PHARMACOLOGICAL CAM INHIBITORS ON THE PHOSPHORYLATION STATUS OF BAD PROTEN AND CASPASE ACTIVATION DURING SM-INDUCED APOPTOSIS OF HUMAN KERATINCYTES

5.1 Introduction

The CaM-regulated protein, calcineurin interacts with the Bcl-2 family members (Shibasaki *et al.*, 1997) and dephosphorylates the proapoptotic protein Bad (Wang *et al.*, 1997). The dephosphorylated form of Bad interacts with Bcl-2 or Bcl-xL to induce apoptosis (Zha *et al.*, 1997). We sought to determine if CaM mediates SM-induced apoptosis *via* dephosphorylation of Bad and if this process can be blocked depleting endogenous CaM levels by antisense RNA. Thus, a time course experiment was performed in which CaM1 AS or control KC were exposed to SM.

As discussed above, we tested the effects of blocking the CaM-mediated mitochondrial pathway on **SM**-induced apoptosis and cytotoxicity in cultured human KC by CaM1 AS approach. We showed that the expression of CaM1 AS blocked **SM**-induced apoptosis and cytotoxicity. In order to adopt a more practical approach for *in vivo* inhibition of CaM, we utilized pharmacological CaM inhibitors that can be potentially topically administered. The advantage of such technology applied to the skin is that topical application can

localize treatment. Systemic treatment can also be performed with pharmacological agents that have already been shown to be safe in human use. The use of pharmacological inhibitors to study **SM** pathology, in the context of the whole animal grafted with human skin will later offer a better understanding of the mechanism of this damage for human personnel.

5.2 Materials and Methods

Culture of cells, exposure to SM and immunoblot analysis were performed as described in previous sections.

5.3 Results and Discussion

To determine if CaM mediates SM-induced apoptosis *via* dephosphorylation of Bad and if this process can be blocked using specific inhibitors of CaM, we performed a time course experiment in which CaM1 AS or control KC transduced with the empty vector LXSN were exposed to SM. Figure 6A shows that by 24 h after SM exposure of control human KC, almost all Bad is dephosphorylated. In CaM1 AS KC, however, there is no detectable reduction in the levels of phosphorylated Bad.

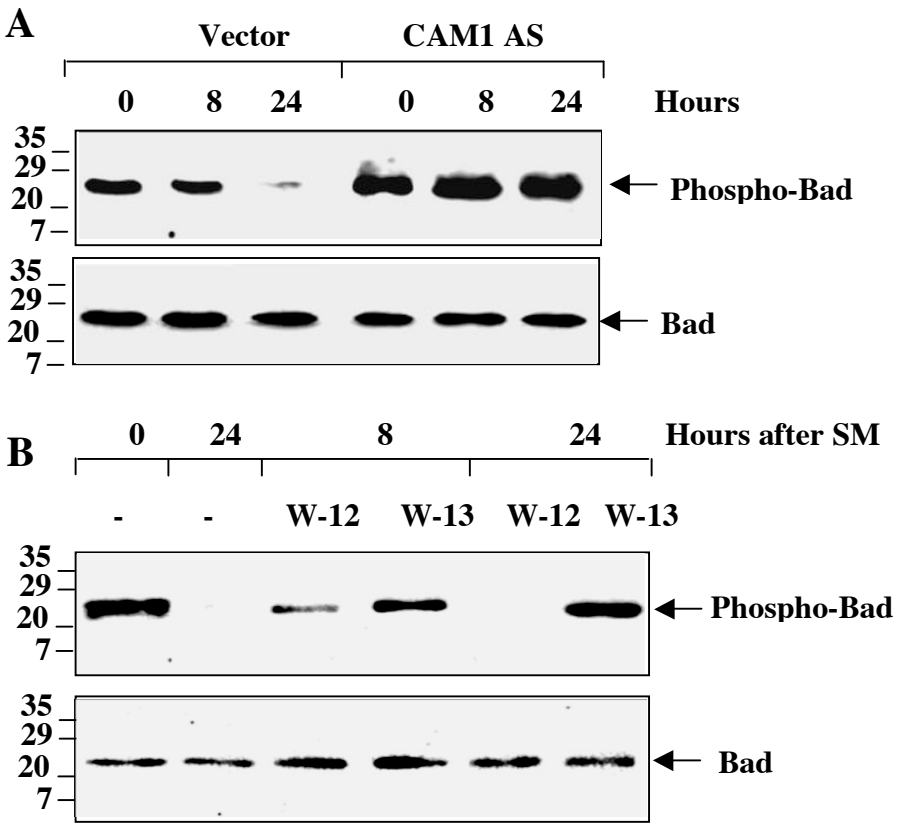

FIG. 6. CaM1 AS and pharmacological inhibitors of CaM prevent dephosphorylation of Bad and caspase-3 activation during SM-induced apoptosis. CaM1 AS (A) or control KC (A, B, C) were exposed to the indicated doses of SM with (B, C) or without pretreatment with the CaM-specific inhibitor W-13, along with its structurally similar, but inactive control analogue, W-12. Extracts were derived after 24 h (C) or the indicated time points (A, B) and subjected to immunoblot analysis using antibodies specific for the phosphorylated form of Bad, or total Bad protein (A B) or the p17 active form of caspase-3 (C). The positions of the immunoreactive proteins as well as the molecular size standards are indicated.

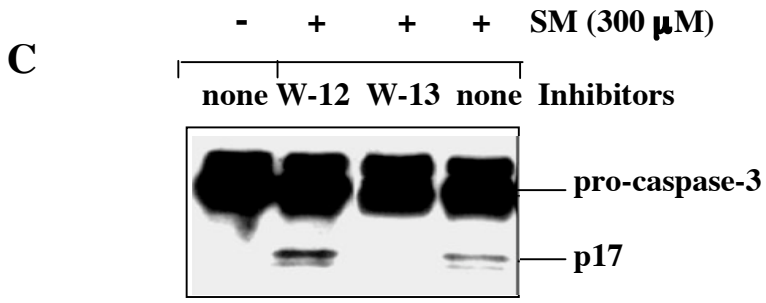

To determine whether pharmacological inhibitors of CaM could replicate this effect, the CaM-specific inhibitor W-13, along with its structurally similar, but inactive control analogue, W-12, which does not bind to CaM, as a control. Primary KC exposed to SM exhibited a decrease in the phosphorylation level of Bad, as determined by specific antibody against phospho-Bad (Fig. 6B, top right panel). This dephosphorylation occurred as early as 8 h after SM exposure, and was complete by 24 h. In the presence of the specific CaM inhibitor, W-13, this dephosphorylation was inhibited, but not with the control structural analogue W-12. On the other hand, the total levels of Bad were fairly constant for all times after SM exposure and all inhibitor treatments. Thus, the phosphorylation status of Bad appears to be more important for the induction of apoptosis than the abundance of the protein.

We then utilized W-13 as well as W-12 to abrogate any CaM-response pathways for SM-induced apoptosis. Immunoblot analysis of cytosolic extracts from cells pretreated with these CaM inhibitors and subsequently exposed to 300 μM SM for 24 h revealed that W-13, but not W-12, suppressed the processing of procaspase-3 into its active form. In control KC (untreated and W-12-treated), one of the two subunits of the active form of caspase-3, p17, can clearly be detected 24 h following treatment with SM. In the presence of W-13, p17 is markedly reduced in SM-exposed KC (Fig. 6C). These results with CaM inhibitors indicate that SM induces apoptosis via a CaM-dependent pathway that involves the activation of procaspase-3 and that inhibition of the CaM/Bcl-2/mitochobdrial apoptotic pathway by specific pharmacological inhibitors such W-13 may therefore be of therapeutic value in the treatment of SM injury in humans.

6. EFFECTS OF RETROVIRAL VECTORS EXPRESSING DOMINANT-NEGATIVE CASPASE-9 ON HUMAN KERATINOCYTE APOPTOSIS

6.1 Introduction

We have previously devoted our efforts to developing molecular probes to determine the relative contribution of both mitochondrial and death receptor pathways leading to sulfur mustard vesication. The targets of these apoptotic pathways are the caspases. Caspase-3, which appears to be a converging point for different apoptotic pathways, is proteolytically activated, and in turn cleaves key proteins involved in the structure and integrity of the cell, including PARP. In addition to the CaM / mitochondrial pathway, utilizing a combination of techniques including the stable expression of a dominant-negative inhibitor of Fas-associated death domain protein (FADD), we demonstrated in our previous annual report a role for the Fas/TNF receptor family in mediating the response of human keratinocytes to SM. Stable expression of FADD-DN blocks SM-induced markers of keratinocyte apoptosis, such as caspase-3 activity and proteolytic processing of procaspases-3, -7, and -8, internucleosomal DNA cleavage, and caspase-6-mediated nuclear lamin cleavage in both cell culture and in human skin grafts on the backs of nude mice.

Accordingly, as part of the contract (ending April 30, 2005), we also focused primarily on developing a dominant-negative retroviral construct of caspase-9 to delineate the contribution of the mitochondrial pathway of apoptosis. We therefore designed retroviral viral constructs expressing dominant-negative caspase-9 (caspase-9-DN), and together with the dominant-negative FADD (FADD-DN), we established stable keratinocyte cell lines expressing these DN inhibitors to determine the relative contributions of the death receptor and mitochondrial pathways as well as to further examine which caspases are apical and essential in human keratinocyte apoptosis. As a model system to test these constructs, the human keratinocyte cell lines stably expressing these DN inhibitors were induced into UVB-mediated apoptosis.

6.2 Materials and Methods

(1) Plasmids and recombinant viruses; infection of keratinocytes with retroviral constructs. Replication-deficient recombinant retrovirus constructs were cloned and utilized to establish stable cell lines.

These retrovirus constructs expressing constitutively active dominant negative FADD mutant lacking the N-terminal death effector domain (FADD-DN) and dominant negative caspase-9 (caspase-9-DN) were constructed by subcloning the cDNA for these genes into the retroviral vector pLHCX. These retroviral constructs, as well as empty vector pLHCX were then packaged and propagated in the amphotropic producer cell line ΦNX by transfection with 25 mg of the retroviral constructs using Lipofectamine 2000 (Life Tech); viral supernatants were derived, filtered, and used to infect immortalized KC in 100 mm plates in the presence of polybrene (10 μg/ml) for 4 h. Retrovirus-infected cells were selected in hygromycin (10 μg/ml) for 10 days, and hygromycin-resistant colonies were pooled from each transduction and passaged every 4 days. Immunoblot analysis was performed on expanded pooled cells to confirm FADD-DN and caspase-9-DN expression.

(2) Fluorometric assay of caspase activity. At indicated times after induction of UVB-induced apoptosis, cytosolic extracts were derived from pooled floating and attached cells and subjected to fluorometric caspase-3 activity assays using fluorescent tetrapeptide substrate specific for caspases-3 (Ac-DEVD-aminomethylcoumarin (AMC), BioMol) as previously described (6). For the fluorometric caspase-8 and -9 activity assays, the tetrapeptide substrates specific for caspases-8 and -9 (Ac-IETD-AMC and Ac-LEHD-AMC, respectively; BioMol), were utilized in essentially the same reaction assay conditions as for caspase 3. Free AMC, generated as a result of cleavage of the aspartate-AMC bond, was monitored over 30 min with a Wallac Victor^{3}V fluorometer (Perkin Elmer) at excitation and emission wavelengths of 360 and 460 nm, respectively. The emission from each sample was plotted against time, and linear regression analysis of the initial velocity (slope) for each curve yielded the activity.

(3) Immunoblot analysis. SDS-PAGE, transfer of separated proteins to nitrocellulose membranes, and immunoblot analysis were performed according to standard protocols as described above (section 2.2.3).

6.3 Results and Discussion

To further elucidate the pathways of SM apoptosis and vesication, we aimed to investigated whether the initiator caspase for the mitochondrial pathway, caspase-9, is indispensable for human keratinocyte apoptosis by

cloning and utilizing retroviral constructs constitutively expressing a dominant-negative caspase-9 (caspase-9-DN). The dominant negative form of caspase-9 was designed by making a point mutation in a critical position in the active site of the catalytic domain of caspase-9. Since the CARD domain of caspase-9 is present, replacing cysteine 287 (QACGG) by a serine (QASGG) and producing the mutant form DN9-C287S allows binding between caspase-9, Apaf1, and cytochrome c, but suppresses caspase-9 processing by forming an inactive apoptosome. Overexpression of this dominant negative caspase-9 mutant titers the endogenous caspase-9, thus, blocking the mitochondrial pathway in apoptotic cells. Immunoblot analysis with antibodies specific to caspase-9 confirms the increased expression of the mutant form DN9-C287S, which is the same size as caspase-9, in caspase 9-DN cells (Fig. 7A). Whereas control LHCX cells had no significant effect on the activation of caspases-9, -8, or -3 after induction into apoptosis, stable expression of this dominant negative form of caspase-9 completely abrogated this response (Fig. 7B). Caspase-3 and -8 activation, therefore, occurs downstream of caspase-9 and is dependent on caspase-9. The effects of caspase-9-DN on caspase 3-mediated cleavage of DNA fragmentation factor 45 (DFF45) were also assessed. Immunoblot analysis with antibodies to the intact form of DFF45 revealed caspase-3-mediated cleavage of DFF45, as shown by the disappearance of the intact form, in control LHCX cells after apoptosis induction (Fig. 7C). On the other hand, this proteolytic cleavage of DFF45 was completely suppressed in cells stably expressing caspase-9-DN.

To further analyze the effect of dominant negative caspase-9 on the proteolytic activation of caspase-3, immunoblot analysis of extracts from LHCX or caspase-9-DN cells exposed to UVB was performed using an antibody specific for the p17 subunit of caspase-3. In UVB-irradiated LHCX cells, caspase-3 is proteolytically processed to its active form (p17), but this processing is completely blocked in caspase-9-DN cells (Fig. 7D). The fact that control LHCX cells, but not caspase-9 DN cells, induced a time-dependent increase in caspase-8 activity (Fig. 7B), provides evidence that caspase-8 acts downstream of caspase-9 activation. These results together indicate that the mitochondrial pathway and caspase-9 activation is required and plays a pivotal role in apoptosis in human keratinocytes.

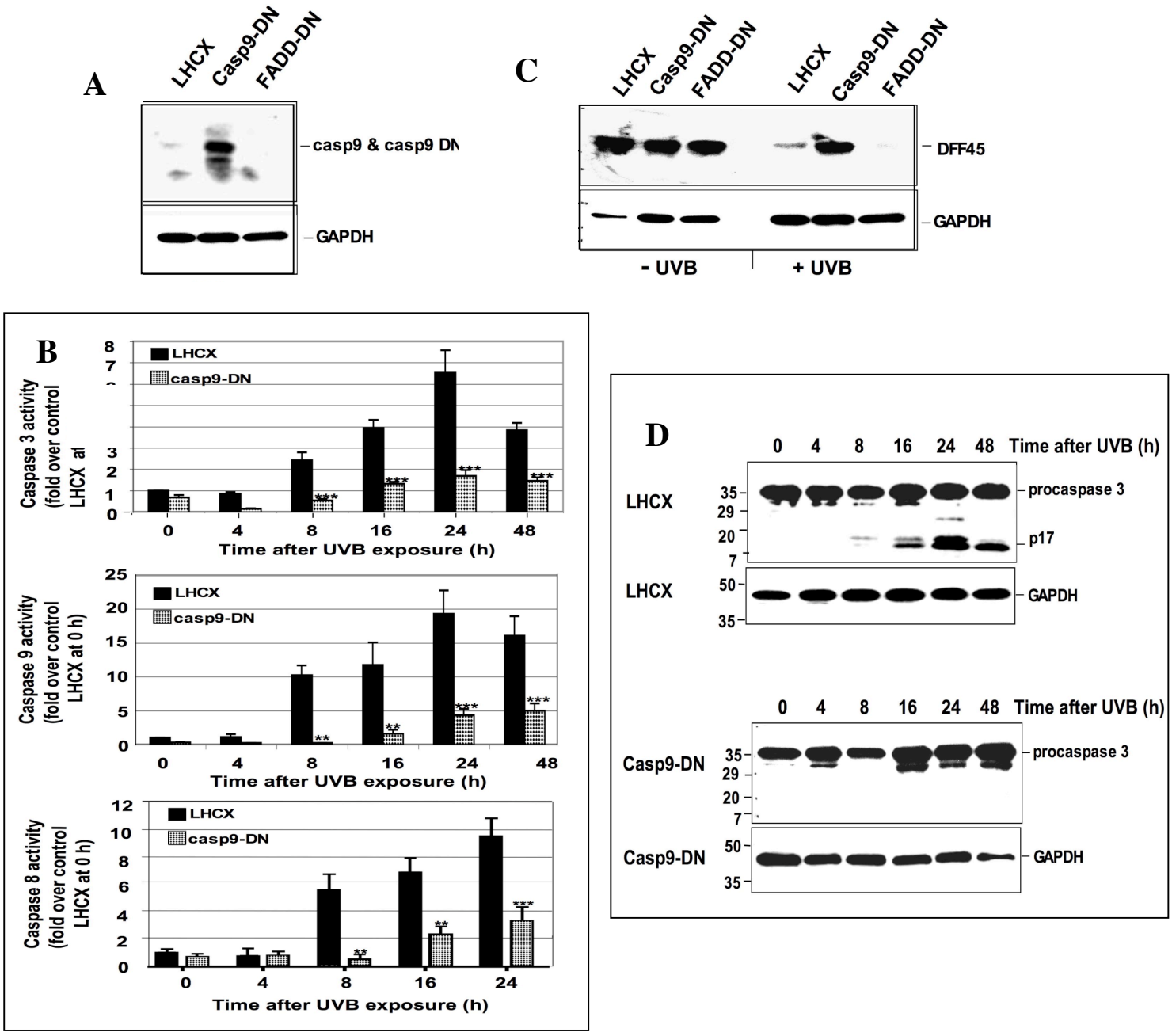

FIG. 7. Stable expression of caspase-9-DN blocks activation of caspase-3, -8, and -9 in human keratinocytes. Retroviral constructs constitutively expressing caspase-9-DN were cloned in pLHCX and used to infect HPV16 E6/7-immortalized KC; retrovirus-infected cells were selected in hygromycin as described in Materials and Methods.

Control LHCX cells were induced into apotosis and after the 16 h, cytosolic extracts were assayed for the presence of caspase-9-DN (A) by immunoblot analysis (a); the immunoblot in A was stripped of antibodies and reprobed with antibodies to full-length DFF45 (C) or to GAPDH (protein loading control). B, Control LHCXand caspase-9-DN cells were induced into apoptosis, and after the indicated times, cytosolic extracts were assayed for caspase-3 activity with the specific substrate DEVD-AMC (top), for caspase-9 activity with LEHD-AMC (middle), or for caspase-8 activity with the specific substrate IETD-AMC (bottom). All data are presented as means ± SEM of three replicates of a representative experiment; essentially the same results were obtained in three independent experiments. *** Denotes p<.001; ** denotes p<.01 for all figures. D, Cells were induced into apoptosis, and after the indicated times, cytosolic extracts were assayed for the presence of the large active p17 subunit of caspase-3 or GAPDH (loading control) by immunoblot analysis.

7. USE OF TOPICAL APPLICATION OF PEPTIDE CASPASE INHIBITORS TO BLOCK SM-INDUCED APOPTOSIS IN GRAFTED HUMAN SKIN (PRELIMINARY RESULTS)

7.1 Introduction

We have successfully established that caspases play a role in SM toxicity in cultured cells throughout the Phase I and Phase II periods of the research. In the current Phase II research, we have utilized specific and potent inhibitors of different caspases to determine the most effective means of preventing toxicity in vitro and vesication in vivo. Thus, we obtained tetrapeptide inhibitors to each of the caspases and treated keratinocytes for 30 min prior to SM exposure. In addition to determining total SM toxicity, we were also able to delineate the specific pathway for the activation of each of the caspases. In the previous annual report, we showed that when primary keratinocytes were treated for each of the caspase inhibitors, prior to SM exposure and assayed for activation of each caspase, IETD and LEHD (caspase-8 and caspase-9 inhibitors) were found to be the most effective caspase inhibitors for human keratinocytes in culture. Surprisingly, these worked more effectively than the pan-caspase inhibitor, ZVAD. Using these peptide caspase inhibitors, we were also able to delineate that caspase-8 activation is most upstream, and activates caspase-9 via "crosstalk" between the death receptor and mitochondrial pathways, dependent on activation of caspase-3 (via Bid cleavage**). In the current annual report for 2005, we have now utilized these inhibitors as compounds for testing in the *in vivo* human skin graft for their ability to block SM vesication.** We have previously used primary human keratinocytes to establish a histologically and immunocytochemically normal epidermis when grafted onto nude mice (Rosenthal et al., 1995; Rosenthal et al., 1998; Rosenthal et al., 2001, Rosenthal, et al., 2003). The correct expression of human keratins K1, K10 and K14 have been confirmed in the grafted epidermis utilizing human keratin-specific antibodies (Rosenthal et al., 1995). To test the effects of the peptide inhibitors of caspases on apoptosis and vesication in intact human epidermis, we utilized this system to graft normal human skin onto the back of athymic mice, and 6-8 weeks after grafting, we inhibited the activity of caspases in vivo by topical application of the inhibitors at the graft site 30 min prior to SM exposure. These human grafts were then exposed to SM by vapor cup method, and showed a vesication response.

The immediate purpose is to devise prevention or treatment strategy for soldiers and civilians who may be exposed to this debilitating substance, and the long term goal is to understand how similar, warfare and non-warfare alkylating agents (UV, chemical carcinogens), are involved in epithelial lesions and carcinogenesis. In order to do this, we are using the following model system:

Nude mice grafted with human keratinocytes. The keratinocytes can be stably transfected with control vector, or vector expressing a "dominant negative" inhibitor of the Fas receptor pathway (truncated FADD protein). The tetrapeptide inhibitors and controls will be dissolved in DMSO at a concentration of 50 μM and 75 μl will be applied with a micropipettor to 6-7 week grafted skin on the morning prior to shipment to Aberdeen. The peptide inhibitors include:

a. *Z-DEVD-FMK (Benzyloxycarbonyl-aspartyl-glutamyl-valyl-aspartyl-fluoromethyl ketone) is a cell and skin-permeable non-pain-inducing specific inhibitor of caspase-3, the executioner caspase of apoptosis. In cultured cells, this inhibitor partially blocks the toxicity of SM to keratinocytes and is the converging point for most apoptotic pathways.

b. *Z-IETD-FMK (Benzyloxycarbonyl-isoleucyl-glutamyl-threonyl-aspartyl-fluoromethyl ketone) is a cell and skin-permeable non-pain-inducing specific inhibitor of caspase-8, the initiator caspase of the death receptor pathway. In cultured cells, this inhibitor blocks the toxicity of SM to keratinocytes and also blocks the activation of caspase-3.

c. *Z-LEHD-FMK (Benzyloxycarbonyl-leucyl-glutamatyl-histidinyl-aspartly-fluoromethyl ketone) is a cell and skin-permeable non-pain-inducing specific inhibitor of caspase-9, the initiator caspase of the mitochondrial pathway. In cultured cells, this inhibitor partially blocks the toxicity of SM to keratinocytes, and in the presence of FADD-DN may hopefully inhibit SM toxicity *in vivo*.

d. *Z-VAD-FMK (Benzyloxycarbonyl--valyl-alanyl-aspartyl-fluoromethyl ketone) is a cell and skin-permeable non-pain-inducing specific inhibitor of all caspases. Surprisingly, in cultured cells, this inhibitor does not block the toxicity of SM to keratinocytes as effectively as the above inhibitors.

e. *Z-FA-FMK (Benzyloxycarbonyl--phenylalanyl-asparty-fluoromethyl ketone) is a cell and skin-permeable non-pain-inducing dipeptide that does not inhibit caspases but resembles the above inhibitors and thus serves as a good negative control. As expected, in cultured cells, this inhibitor does not block the toxicity of SM to keratinocytes.

f. DMSO- vehicle control.

SM exposure: After the graft is complete (6-7 weeks), the animals are shipped, under the supervision of DCM and the PI, to USAMRICD at the Aberdeen Proving Ground. The goal of project is to determine the role of Fas in SM blistering. There is no cell culture model that can even approximate the blistering response, including monolayer, or stratified raft cultures of keratinocytes. In order to study blistering, one needs intact, physiological normal epidermis, and intact basal lamina (since this is the primary site of detachment of the skin), and an underlying dermis that contributes attachment proteins. In addition, it is important to know if an immune response and lymphocytic infiltration into the skin occurs following different treatments; this can only be studied in the intact animal.

We have data that show that we can graft genetically modified keratinocytes (i.e., containing plasmids that alter the function of Fas as described above) and these keratinocytes form a well-organized stratified squamous epithelium that is indistinguishable from normal human skin both histologically and biochemically. The grafted skin also forms a bona fide basal lamina above the dermis, and is thus a good model to study the blistering effects of SM.

The mice represent 2 different cell types (FADD-DN vs. control keratinocytes) x 6 peptide inhibitor treatment groups (Z-DEVD-FMK, Z-IETD-FMK, Z-LEHD-FMK, Z-VAD-FMK, Z-FA-FMK, and no inhibitor) x 15 replicate mice per treatment group (10 mice with 6 min. vapor cup exposure plus 5 untreated controls) x 2 collection times after exposure (24 and 48h after exposure) = 360 nude mice total. A sample size of 5 in the control group and 10 in the treated group will have 88% power to detect a shift in histopathology scores of 1 category using a Wilcoxon (Mann-Whitney) rank-sum test with a 0.050 two-sided significance level. In addition

to histological analysis for blistering, inflammation, and necrosis, all SM-exposed and control skin grafts are analyzed by histological, immunocytochemical, immunoblot, and RNA analysis. All grafts will be utilized.

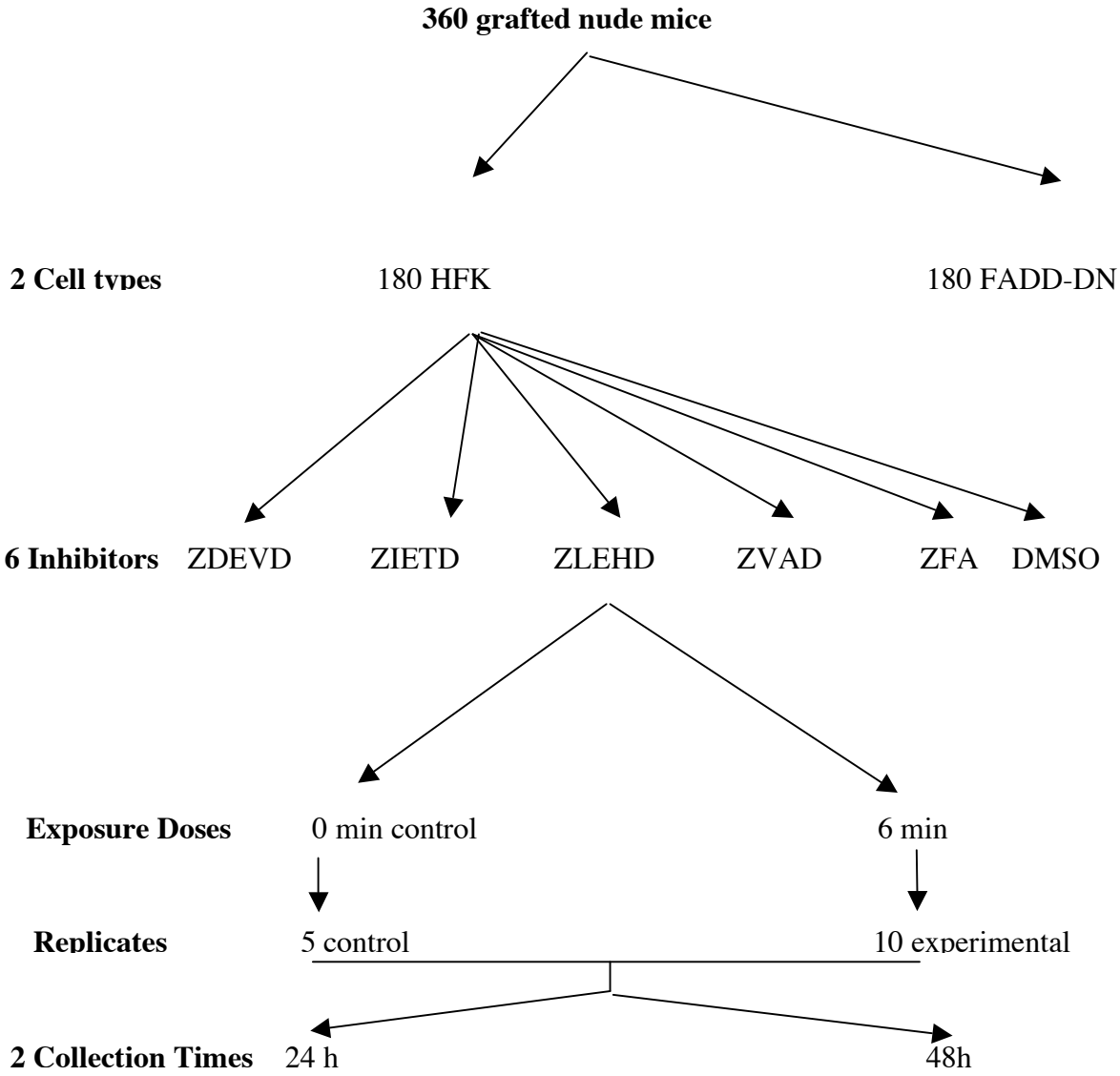

FIG. 8 Strategy for determining effective caspase inhibitors

Abbrev.	Inhibitor	Specificity	Caspase "Type"
DEVD	ZDEVD-FMK	Caspase-3	Executioner
IETD	ZIETD-FMK	Caspase-8	Upstream Death Receptor
LEHD	ZLEHD-FMK	Caspase-9	Upstream Mitochondrial
ZVAD	ZVAD-FMK	All	All Caspases
ZFA	ZFA-FMK	None	Control Compound for all above
CON	Untreated		

7.2 Materials and Methods

a. Culture of primary human keratinocytes. Culture of primary human keratinocytes cells were performed as described in previous sections.

b. Chemicals. SM (bis-(2-chloroethyl) sulfide; >98% purity) was obtained from the US Army Edgewood Research, Development and Engineering Center.

c. Grafting Protocols and Exposure of Human Skin Grafts to SM. A piece of skin (1 cm diameter) was removed from the dorsal surface of athymic mice, and a cell pellet containing 8 x 10^6 fibroblasts + 5 x 10^6 keratinocytes (KC) was pipetted on top of the muscular layer within a silicon dome to protect the cells. The dome was removed after a week and the graft was allowed to develop for 6-8 weeks. SM exposure was performed by placing a small amount of SM liquid into an absorbent filter at the bottom of a vapor cup, which was then inverted onto the dorsal surface of the animal, to expose the graft site to the SM vapor. Frozen and fixed sections were derived from punch biopsies taken from the graft site. Histological analysis of the SM-exposed human skin grafts transplanted onto nude mice was also performed utilizing an end point of micro or macro blisters or SM-induced microvesication.

d. Assays for In Vivo Markers of Apoptosis on Human Skin Grafts. Paraffin-embedded sections derived from SM-exposed human skin grafts were subjected to analysis for markers of *in vivo* apoptosis, including immunofluorescence microscopy with antibodies to the active form of caspase-3 (Cell Signaling). Sections were deparaffinized, incubated overnight in a humid chamber with antibodies to active caspase-3 (1:250) in PBS containing 12% BSA, washed with PBS, incubated for 1 h with biotinylated anti-mouse IgG (1:400), washed again, incubated for 30 min with streptavidin-conjugated Texas red (1:800 dilution), mounted with PBS with 80% glycerol, and observed with a Zeiss fluorescence microscope. DNA breaks late stage of apoptosis were detected *in situ* using a Klenow fragment-based assay system (DermaTACS; Trevigen). For fixation, slides were dried for 2 h on a slide warmer at 45° C, rehydrated in 100%, 95%, then 70% ethanol, washed in PBS, fixed in 3.7% buffered formaldehyde for 10 min at room temp, and washed in PBS. Slides were

then incubated with 50 µl of Cytonin for 15 min, washed in water, immersed in quenching solution containing 90% methanol and 3% H_2O_2 for 5 min, washed with PBS, incubated in TdT labeling buffer, and visualized under a bright field microscope.

7.3 Results and Discussion

Human skin grafts transplanted onto nude mice have been used successfully to examine SM-induced biochemical alterations, utilizing an end point of micro or macro blisters (Gross et al., 1988; Meier et al., 1984; Papirmeister et al., 1991; Petrali et al., 1990; Smith et al., 1990; Smith et al., 1991; Smulson, 1990; van Genderen and Wolthuis, 1986). The model has also been used to assess the protection afforded against SM-induced biochemical alterations by the systemically administered inhibitors. Frozen and fixed sections derived from graft sites of these animals were thus analyzed for the apoptosis markers.

We now demonstrate that upon histological analysis of SM-exposed animals grafted with primary KC, SM microvesication can be reduced by topical application of the pan-caspase peptide inhibitor zVAD-fmk. While there was no difference in the DMSO (vehicle)-treated and ZFA-treated control skin grafts, there was a notable decrease in the amount of microvesication in grafts treated with zVAD-fmk (Figs. 9-11). A summary of the pathology report is shown in Table 2.

Table 2

		Pustular Epidermitis	Epidermal Necrosis	Vesicle	Follicular damage	Dermal Necrosis	Punch Weight
Graft	DMSO	1	3.5	2.5		3.5	79.8
	ZFA	0	3.7	1.7		4	74.8
	ZVAD	0.7	2.3	0.7		3.7	79.2
Recipient	DMSO	2.5	3.5	2.5	2.5	3	
	None	1.5	4	0.5	3.5	4	
	ZFA	1.3	3.7	0.7	3.3	3.7	
	ZVAD	1.7	3.7	1	3.3	3.7	

Values averaged for n=10 mice

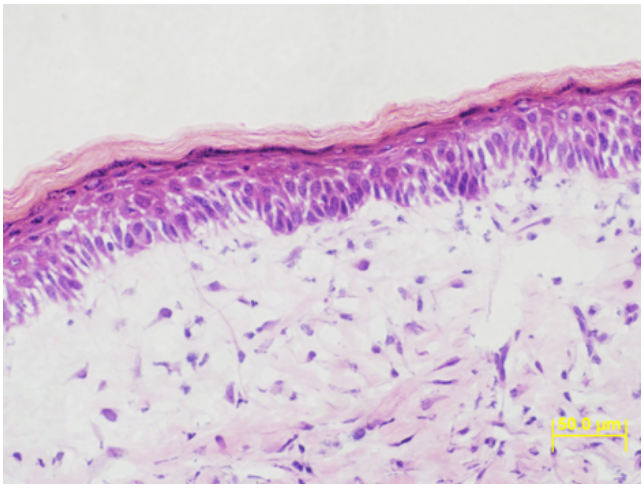

FIG. 9: Skin Graft treated with ZVAD prior to SM

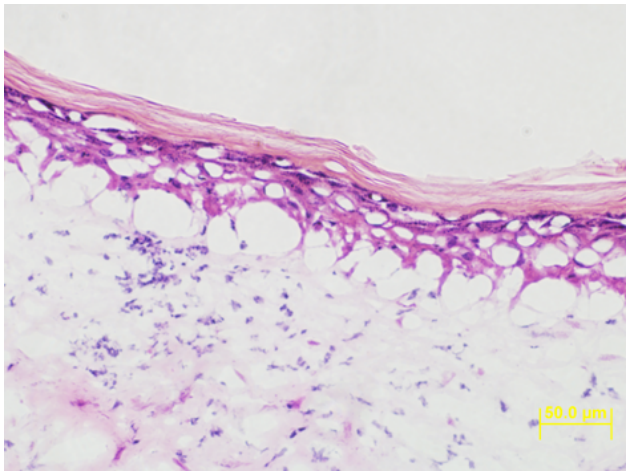

FIG. 10: Skin Graft pretreated with DMSO

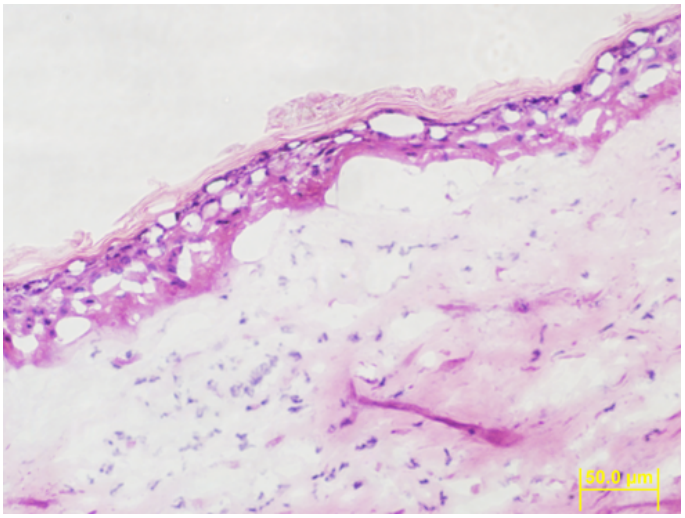

FIG 11: Skin Graft pretreated with ZFA

DNA breaks can be detected *in situ* using a Klenow fragment-based assay system (TUNEL staining). We then tested the relationship between apoptotic DNA breaks, vesication and the effect of topical peptide inhibitors of caspases. We pretreated human skin grafts on the back of athymic mice with different peptide inhibitors of caspases 3, 8, 9, and the pan-caspase inhibitor for 30 min prior to SM exposure by the vapor cup method. Animals were sacrificed 24 h after exposure and skin biopsies were obtained, fixed, and sectioned. DNA breaks were then detected by the TUNEL staining as described in Materials and Methods. As noted in our previous studies, apoptotic cells were concentrated in the areas of microvesication. **Interestingly, SM induced apoptotic DNA breaks primarily in the basal cells of DMSO-treated control human skin grafts, but was significantly attenuated in the grafts treated with the pan-caspase inhibitor z-VADfmk. However, pretreatment of the skin grafts with the individual peptide inhibitors specific for caspases-8 or -9 were not as effective in modulating this response (in progress).** Taken together, the data indicate that SM activates both a death receptor and mitochondrial apoptotic pathway resulting in the activation of multiple caspases and apoptosis of basal cells, contributing to the vesication response. **Thus, inhibition of one of the caspases is insufficient in blocking the cytotoxic effects because other caspases are still active and can compensate . This may explain how a pan-caspase peptide inhibitor, which inhibits all the caspases is more effective.**

To examine the expression of markers within individual cells and to localize and identify the cell type within the epidermis undergoing apoptosis (i.e. basal, spinous, granular, or cornified), immunocytochemistry of the grafted skin was then performed. Double immunostaining allowed further detection of multiple markers within individual cells, and thus determination of pathways of apoptosis. This information coupled with the vesication data ultimately permits determination of the correlation between each of the apoptotic pathways and blistering. To observe activation of caspase-3 in skin sections, we performed immunofluorescent staining with antibodies to the cleavage product of caspase-3 but not the intact protein thus localizing active caspase-3 in individual cells following exposure of human skin grafts to SM. Immunostaining of mouse epidermis treated with SM by vapor cup exposure, using anti-active caspase-3 or phase contrast reveals that caspase-3 is activated

in basal epidermal cells of control mouse skin treated with SM vapor cup, but not in skin pretreated with ZVAD (in progress).

8. CONCLUSIONS

Using CaM1 AS in the current study, we have shown that CaM depletion may block the mitochondrial pathways of SM-induced apoptosis *via* upregulation of the anti-apoptotic proteins Bcl2 and Bcl-xL, as well as dephosphorylation of Bad. This is consistent with previous studies in which CaM was implicated in the regulation of Bcl-2 family members and thus the mitochondrial pathway of apoptosis. Bcl2 family members have been shown to interact directly with the CaM-regulated phosphatase calcineurin, which can dephosphorylate (Wang *et al.*, 1997) and regulate the intracellular localization (Shibasaki *et al.*, 1997) and stability (Haldar *et al.*, 1995) of Bcl-2 family proteins. Bcl-2 transcription is also regulated *via* a CaM-dependent pathway (Gomez *et al.*, 1998). Further, Ca^{2+}-CaM binds to FKBP38 and induces apoptosis in neuronal tissue by binding Bcl-2 and modulating its activity (Edlich *et al.*, 2005). Ca^{2+}-CaM also binds and activates CaMK IV (Soderling, 1999); nuclear CaMK IV in turn phosphorylates and activates CREB, which results induces transcription of apoptotic genes (Enslen *et al.*, 1994) such as *bax*.

To better understand the contribution of CaM-regulated pathways in the cutaneous response to SM, we blocked this pathway utilizing KC stably expressing CaM1 AS. Because there are three different human and murine genes that encode CaM, elimination of all CaM protein is problematical. Two groups of investigators have used a CaM1 AS vector in rat glioblastoma cells (Prostko *et al.*, 1997) as well as in PC-12 cell (Davidkova *et al.*, 1996). Likewise, we found that CaM1 is by far the predominantly expressed gene in primary as well as immortalized KC, and, thus, used a retroviral vector expressing CaM1 AS to substantially reduce the endogenous levels of CaM in KC. Using AS, the present study demonstrates that SM induces CaM-dependent apoptosis in KC mediated by CaM, and involves the activation of caspases-3, -6, -7 and -9. These responses may, in part, explain the death and detachment of basal cells of the epidermis that occurs following exposure to

SM. Using a cell culture model in the present study, we describe a potential mechanism for SM-induced KC basal cell death and detachment: apoptosis in KC via a CaM/Bad/Bcl-2 mitochondrial pathway.

KC expressing CaM1 AS exhibited reduced levels of SM-induced PARP cleavage and proteolytic processing of caspases-3, -6, -7, and -9 into their active forms. In most apoptotic systems, caspase-3, the primary executioner caspase, is proteolytically activated, and in turn cleaves key proteins involved in the structure and integrity of the cell, including PARP, DFF 45, fodrin, gelsolin, receptor-interacting protein (RIP), X-IAP, topoisomerase I, vimentin, Rb, and lamin B (Nicholson *et al*., 1995; Tewari *et al*., 1995; Casciola-Rosen *et al*., 1996; Song *et al*., 1996; Slee *et al*., 2001). Caspase-3 is also essential for apoptosis-associated chromatin margination, DNA fragmentation, and nuclear collapse (Slee *et al*., 2001).

Our model system has demonstrated a novel role for CaM in SM toxicity. In addition, we have also shown the validity of the use of chemical inhibitors of CaM to block this response. While SM alters the absolute levels of Bcl-2, Bcl-xL, and Bax, Bad is dephosphorylated following SM exposure. Therefore, one mechanism for the action of CaM inhibitors is to block the dephosphorylation of Bad, preventing it from complexing with and inactivating Bcl-2, and thereby blocking activation of downstream caspases and cell death. An understanding of the mechanisms for SM vesication will hopefully lead to therapeutic strategies for prevention or treatment of SM toxicity. Our results suggest that CaM inhibition may protect the epidermis from SM-induced apoptosis, by blocking mitochondrial pathways of apoptosis. Although the mechanism for their protection has not been described, CaM inhibitors have already been used successfully in the treatment of both thermal burns and frostbite (Beitner *et al*., 1989; Beitner *et al*., 1991) and may prove effective for SM as well, either alone, or in combination with caspase-3 inhibitors. We used antisense oligonucleotide and chemical inhibitors of CaM and have successfully attenuated the apoptotic response in cultured cells, and these inhibitors can be used *in vivo* as well.

Our results have also shown the utility of zVAD-fmk for the prevention of SM blistering and vesication, consistent with our cell culture studies. Likewise, pretreatment with the pan-caspase inhibitor zVAD-fmk

reduced DNA fragmentation in vivo (as revealed by TUNEL staining) as well as activation of caspase-3 (as revealed by immunofluorescence using antibody specific for the active form of the enzyme.

Plans/Milestones for the Next Quarter

Subsequent studies would now utilize additional caspase inhibitors to determine their effectiveness in reducing SM pathology and apoptosis

- Continuing the use of pharmacological peptide inhibitors of caspases 3, 8, and 9 on grafted human keratinocytes prior to SM exposure

10. ACCOMPLISHMENT OF TASKS

KEY RESEARCH ACCOMPLISHMENTS PHASE I AND PHASE II

- Discovery that SM induces keratinocyte cell death in large part via a CaM-dependent apoptosis.
- Blocking vesication by inhibiting these pathways in animal models
- Testing of dominant-negative caspase-–9 retroviral vectors to further determine the relative contributions of the death receptor and mitochondrial pathways of SM apoptosis, and to design inhibitors based on these experiments to inhibit SM toxicity and vesication.
- **Successful use of pharmacological inhibitors of caspases and death receptors to block the SM apoptotic response – PHASE II**

C.5 Phase II Specific Aim I: To utilize specific inhibitors of the Fas-FADD-caspase pathway in cultured human keratinocytes to suppress SM toxicity: To apply our understanding of the death receptor pathway of SM-induced apoptosis in order to determine if its cytotoxic effects can be reduced by using clinically applicable antibodies or peptide inhibitors that inhibit death receptor signaling.

C.5.1 Task 1: Keratinocytes will be incubated with neutralizing antibodies to death receptors (Fas, TNFR1) and their ligands (Fas, TNFa) to reduce **SM** toxicity.
C5.1.1 Task 1.1: Cell viability will be tested following SM exposure with each of these antibodies.
C5.1.2 Task 1.2: Biochemical markers of apoptosis will be tested following SM exposure with each of these antibodies.
C5.1.3 Task 1.3: Apoptotic morphology will be tested following SM exposure with each of these antibodies.\
C5.1.4 Task 1.4: Internucleosomal fragmentation will be assessed following SM exposure with each of these antibodies.
C5.1.5 Task 1.5: Membrane alterations typical of apoptosis will be tested by FACS analysis following SM exposure with each of these antibodies.
C5.1.6 Task 1.6: The ratio of apoptotic/necrotic cells will be compared between antibody-treated versus control **SM**-exposed keratinocytes?

C.5.1 TASK HAS BEEN ADDRESSED IN RESULTS RELATING TO MAY 2004 ANNUAL REPORT, FIG. 7.

C.5.2 Task 2 Keratinocytes will be incubated with peptide inhibitors of caspases to reduce **SM** toxicity.
C5.2.1 Task 2.1 Cell viability will be tested following SM exposure with each of these caspase inhibitors.
C5.2.2 Task 2.2: Biochemical markers of apoptosis will be tested following SM exposure with each of these caspase inhibitors.
C5.2.3 Task 2.3: Apoptotic morphology will be tested following SM exposure with each of these caspase inhibitors.
C5.2.4 Task 2.4: Internucleosomal fragmentation will be assessed following SM exposure with each of these caspase inhibitors.
C5.2.5 Task 2.5: Membrane alterations typical of apoptosis will be tested by FACS analysis following SM exposure with each of these caspase inhibitors.
C5.2.6 Task 2.6: The ratio of apoptotic/necrotic cells will be compared between caspase inhibitors-treated versus control **SM**-exposed keratinocytes?

C5.2 TASK 2 HAS BEEN ADDRESSED IN MAY 2004 ANNUAL REPORT DATA IN FIG. 12, 13, AND 14.

C.6 Phase II Specific Aim II: To utilize specific inhibitors of the CaM pathways, and further explore the related Bcl-2 pathway in cultured human keratinocytes to suppress SM toxicity: To apply our understanding of the mitochondrial pathways of **SM**-induced apoptosis in order to block its cytotoxic effects by using drugs that specifically inhibit CaM signaling and by overexpressing Bcl-2.

C.6.1 Task 1: Keratinocytes will be incubated with pharmacological inhibitors of CaM and calcineurin to block the apoptotic response in keratinocytes.
C.6.1.1 Task 1.1: Biochemical markers of apoptosis will be tested following SM exposure with CaM and calcineurin inhibitors.
C.6.1.2 Task 1.2: Morphological markers of apoptosis will be tested following SM exposure with CaM and calcineurin inhibitors.
C.6.1.3 Task 1.3: Necrotic cell death will be measured following SM exposure in the presence of CaM and calcineurin inhibitors
C6.2 Task 2: The role of Bcl-2 in SM toxicity will be examined

C.6 TASK 1 WAS PARTIALLY ADDRESSED IN DATA FROM MAY 2004 ANNUAL REPORT FIG. 9, 10, AND 11. **THESE RESULTS HAVE BEEN FURTHER ADDRESSED IN FIGS. 1-6 OF THE CURRENT ANNUAL REPORT.**

C.7 **Specific Aim III: To utilize specific inhibitors of the Fas-FADD-caspase and CaM pathways, in grafted human keratinocytes to block SM toxicity:** To test the effects of systemically administered antibody and peptide inhibitors, as well as topical CaM inhibitors, in **SM**-exposed human skin grafted onto nude mice.

C.7.1 Task 1: Systemic antibodies against Fas/TNFR1 will be used to block the vesication response in grafted human keratinocytes.
C.7.1.1 Task 1.1: Markers of apoptosis (TUNEL, active caspases) will be assessed in skin grafts derived in grafts treated with antibodies against Fas/TNFR1.
C.7.2 Task 2: Systemic antibodies against Fas/TNFR1 ligands will be used to block the vesication response in grafted human keratinocytes.
C.7.2.1 Task 2.1: Markers of apoptosis (TUNEL, active caspases) will be assessed in skin grafts derived in grafts treated with antibodies against ligands for Fas/TNFR1.

C.7.3 Task 3: Systemic caspase inhibitors will be used to block the vesication response in grafted human keratinocytes.
C.7.3.1 Task 3.1: Markers of apoptosis (TUNEL, active caspases) will be assessed in skin grafts derived in grafts treated with systemic peptide inhibitors of caspases.
C.7.4 Task 4: Topical caspase inhibitors will be used to block the vesication response in grafted human keratinocytes.
C.7.4.1 Task 4.1: Markers of apoptosis (TUNEL, active caspases) will be assessed in skin grafts derived in grafts treated with topical caspase inhibitors.
C.7.5 Task 5: Topical CaM inhibitors will be used to block the vesication response in grafted human keratinocytes.
C.7.4.1 Task 4.1: Markers of apoptosis (TUNEL, active caspases) will be assessed in skin grafts derived in grafts treated with topical CaM inhibitors.

TASK 3 AND 4 ARE CURRENTLY BEING ADDRESSED IN THE CURRENT ANNUAL REPORT (FIGS 8-11, TABLE I). APPROXIMATELY 100 GRAFTED MICE HAVE NOW BEEN GRAFTED, PRETREATED WITH CASPASE INHIBITORS, SM EXPOSED AND ARE CURRRENTLY BEING ANALYZED FOR PATHOLOGY, APOPTOSIS, AND CASPASE ACTIVATION.

12. REFERENCES

Alnemri, E., Livingston, D., Nicholson, D., Salvesen, G., Thornberry, N., Wong, W., and Yuan, J. (1996). Human ICE/CED-3 protease nomenclature [letter]. Cell *87*, 171.

Beitner, R., Chen-Zion, M., Sofer-Bassukevitz, Y., Morgenstern, H., and Ben-Porat, H. (1989). Treatment of frostbite with the calmodulin antagonists thioridazine and trifluoperazine. Gen Pharmacol *20*, 641-6.

Beitner, R., Chen-Zion, M., Sofer-Bassukevitz, Y., Oster, Y., Ben-Porat, H., and Morgenstern, H. (1989). Therapeutic and prophylactic treatment of skin burns with several calmodulin antagonists. Gen Pharmacol *20*, 165-73.

Casciola-Rosen, L., Nicholson, D., Chong, T., Rowan, K., Thornberry, N., Miller, D., and Rosen, A. (1996). Apopain/CPP32 cleaves proteins that are essential for cellular repair: a fundamental principle of apoptotic death. J Exp Med *183*, 1957-64.

Chinnaiyan, A. M., O'Rourke, K., Tewari, M., and Dixit, V. M. (1995). FADD, a novel death domain-containing protein, interacts with the death domain of Fas and initiates apoptosis. Cell *81*, 505-12.

Choi, K. B., Wong, F., Harlan, J. M., Chaudhary, P. M., Hood, L., and Karsan, A. (1998). Lipopolysaccharide mediates endothelial apoptosis by a FADD-dependent pathway. J Biol Chem *273*, 20185-8.

Datta, S. R., Dudek, H., Tao, X., Masters, S., Fu, H., Gotoh, Y., and Greenberg, M. E. (1997). Akt phosphorylation of BAD couples survival signals to the cell-intrinsic death machinery. Cell *91*, 231-41.

del Peso, L., Gonzalez-Garcia, M., Page, C., Herrera, R., and Nunez, G. (1997). Interleukin-3-induced phosphorylation of BAD through the protein kinase Akt. Science *278*, 687-9.

Gomez, J., Martinez, A. C., Gonzalez, A., Garcia, A., and Rebollo, A. (1998). The Bcl-2 gene is differentially regulated by IL-2 and IL-4: role of the transcription factor NF-AT. Oncogene *17*, 1235-43.

Gross, C. L., Innace, J. K., Smith, W. J., Krebs, R. C., and Meier, H. L. (1988). Alteration of lymphocyte glutathione levels affects sulfur mustard cytotoxicity. In Proceedings of the meeting of NATO Research Study Group, Panel VIII/RSG-3 (Washington, D.C.

Haldar, S., Jena, N., and Croce, C. M. (1995). Inactivation of Bcl-2 by phosphorylation. Proc Natl Acad Sci U S A *92*, 4507-11.

Hockenberry, D., Zutter, M., Hickey, W., Nahm, M., and Korsmeyer, S. J. (1991). Bcl-2 protein is topographically restricted in tissues characterized by apoptotic cell death. Proc. Natl. Acad. Sci. USA *88*, 6961-6965.

Hsu, S. Y., Kaipia, A., Zhu, L., and Hsueh, A. J. (1997). Interference of BAD (Bcl-xL/Bcl-2-associated death promoter)-induced apoptosis in mammalian cells by 14-3-3 isoforms and P11. Mol Endocrinol *11*, 1858-67.

Imai, Y., Kimura, T., Murakami, A., Yajima, N., Sakamaki, K., and Yonehara, S. (1999). The CED-4-homologous protein FLASH is involved in Fas-mediated activation of caspase-8 during apoptosis [In Process Citation]. Nature *398*, 777-85.

Kischkel, F. C., Hellbardt, S., Behrmann, I., Germer, M., Pawlita, M., Krammer, P. H., and Peter, M. E. (1995). Cytotoxicity-dependent APO-1 (Fas/CD95)-associated proteins form a death-inducing signaling complex (DISC) with the receptor. Embo J *14*, 5579-88.

Marthinuss, J., Lawrence, L., and Seiberg, M. (1995). Apoptosis in Pam212, an epidermal keratinocyte cell line: a possible role for bcl-2 in epidermal differentiation. .

McLean, W. H., Eady, R. A., Dopping-Hepenstal, P. J., McMillan, J. R., Leigh, I. M., Navsaria, H. A., Higgins, C., Harper, J. I., Paige, D. G., Morley, S. M., and et al. (1994). Mutations in the rod 1A domain of keratins 1 and 10 in bullous congenital ichthyosiform erythroderma (BCIE). J Invest Dermatol *102*, 24-30.

Medema, J. P., Scaffidi, C., Kischkel, F. C., Shevchenko, A., Mann, M., Krammer, P. H., and Peter, M. E. (1997). FLICE is activated by association with the CD95 death-inducing signaling complex (DISC). Embo J *16*, 2794-804.

Meier, H. L., Gross, C. L., Papirmeister, B., and Daszkiewicz, J. E. (1984). The use of human leukocytes as a model for studying the biochemical effects of chemical warfare (CW) agents. In Proceedings of the Fourth Annual Chemical Defense Bioscience Review (Aberdeen Proving Ground, Maryland.

Mol, M. A. E., and Smith, W. (1996). Calcium homeostasis and calcium signalling in sulphur mustard-exposed normal human epidermal keratinocytes. In Chemico-Biological Interactions: Elsevier), pp. 85-93.

Nicholson, D. W., Ali, A., Thornberry, N. A., Vaillancourt, J. P., Ding, C. K., Gallant, M., Gareau, Y., Griffin, P. R., Labelle, M., Lazebnik, Y. A., Munday, N. A., Raju, S. M., Smulson, M. E., Yamin, T. T., Yu, V. L., and Miller, D. K. (1995). Identification and inhibition of the ICE/CED-3 protease necessary for mammalian apoptosis. Nature *376*, 37-43.

Papirmeister, B., Feister, A. J., Robinson, S. I., and Ford, R. D. (1991). Medical defense against mustard gas: toxic mechanisms and pharmacological implications, 1st Edition (Boca Raton: CRC Press).

Petrali, J. P., Oglesby, S. B., and Mills, K. R. (1990). Ultrastructural correlates of sulfur mustard toxicity. J. Toxicol. Cut. Ocul. Toxicol. *9*, 193-214.

Ray, R., Benton, B. J., Anderson, D. R., Byers, S. L., Shih, M. L., and Petrali, J. P. (1996). The intracellular free calcium chelator BAPTA prevents sulfur mustard toxicity in cultured normal human epidermal keratinocytes. In Proc. Med. Defense Biosci. Rev. (Aberdeen Proving Ground: US Army Medical Research Institute of Chemical Defense), pp. 1021-1027.

Ray, R., Legere, R. H., Majerus, B. J., and and Petrali, J. P. (1995). Sulfur mustard-induced increase in intracellular free calcium level and arachidonic acid release from cell membrane. Toxicology and Applied Pharmacology *131*, 44-52.

Ray, R., Majerus, B. J., Munavalli, G. S., and Petrali, J. P. (1993). Sulfur mustard-Induced increase in intracellular calcium: A mechanism of mustard toxicity. In U.S. Army Medical Research Bioscience Review (Aberdeen, MD, pp. 267-276.

Rosenthal, D. S., Simbulan, C. M., and Smulson, M. E. (1995). Model systems for the study of the role of PADPRP in essential biological processes. Biochimie *77*, 439-43.

Rosenthal, D. S., Simbulan-Rosenthal, C. M., Iyer, S., Smith, W., Ray, R., and Smulson, M. E. (1998). Calmodulin, poly(ADP-ribose) polymerase, and p53 are targets for modulating the effects of sulfur mustard. Proceedings of the Medical Defense Bioscience Review

Rosenthal, D. S., Simbulan-Rosenthal, C. M., Iyer, S., Smith, W. J., Ray, R., and Smulson, M. E. (2000). Calmodulin, poly(ADP-ribose)polymerase and p53 are targets for modulating the effects of sulfur mustard. J Appl Toxicol *20*, S43-S49.

Rosenthal, D. S., Simbulan-Rosenthal, C. M., Iyer, S., Spoonde, A., Smith, W., Ray, R., and Smulson, M. E. (1998). Sulfur mustard induces markers of terminal differentiation and apoptosis in keratinocytes via a Ca2+-calmodulin and caspase-dependent pathway. J Invest Dermatol *111*, 64-71.

Rosenthal, D. S., Simbulan-Rosenthal, C. M., Liu, W. F., Velena, A., Anderson, D., Benton, B., Wang, Z. Q., Smith, W., Ray, R., and Smulson, M. E. (2001). PARP determines the mode of cell death in skin fibroblasts, but not keratinocytes, exposed to sulfur mustard. J Invest Dermatol *117*, 1566-73.

Rosenthal, D. S., Simbulan-Rosenthal, C. M. G., Liu, W. F., Stoica, B. A., and Smulson, M. E. (2001) Mechanisms of JP-8 jet fuel cell toxicity. II. Induction of necrosis in skin fibroblasts and keratinocytes and modulation of levels of Bcl-2 family members. Toxicol Appl Pharmacol. 2001 Mar 1;171(2):107-16.

Scheid, M. P., and Duronio, V. (1998). Dissociation of cytokine-induced phosphorylation of Bad and activation of PKB/akt: involvement of MEK upstream of Bad phosphorylation. Proc Natl Acad Sci U S A *95*, 7439-44.

Schlegel, R., Phelps, W. C., Zhang, Y. L., and Barbosa, M. (1988). Quantitative keratinocyte assay detects two biological activities of human papillomavirus DNA and identifies viral types associated with cervical carcinoma. Embo J *7*, 3181-7.

Schwarz, A., Bhardwaj, R., Aragane, Y., Mahnke, K., Riemann, H., Metze, D., Luger, T. A., and Schwarz, T. (1995). Ultraviolet-B-induced apoptosis of keratinocytes: evidence for partial involvement of tumor necrosis factor-alpha in the formation of sunburn cells. J Invest Dermatol *104*, 922-7.

Schwarz, A., Mahnke, K., Luger, T. A., and Schwarz, T. (1997). Pentoxifylline reduces the formation of sunburn cells. Exp Dermatol *6*, 1-5.

Shibasaki, F., Kondo, E., Akagi, T., and McKeon, F. (1997). Suppression of signalling through transcription factor NF-AT by interactions between calcineurin and Bcl-2. Nature *386*, 728-31.

Smith, W. J., Gross, C. L., Chan, P., and Meier, H. L. (1990). The use of human epidermal keratinocytes in culture as a model for studying the biochemical mechanisms of sulfur mustard toxicity. Cell Biol. Toxicol. *6*, 285-91.

Smith, W. J., Sanders, K. M., Gales, Y. A., and Gross, C. L. (1991). Flow cytometric analysis of toxicity by vesicating agents in human cells *in vitro*. Toxicol. *10*.

Smulson, M. E. (1990). Molecular biology basis for the response of poly(ADP-rib) polymerase and NAD metabolism to DNA damage caused by mustard alkylating agents: Georgetown University Medical School).

Song, Q., Lees-Miller, S., Kumar, S., Zhang, Z., Chan, D., Smith, G., Jackson, S., Alnemri, E., Litwack, G., Khanna, K., and Lavin, M. (1996). DNA-dependent protein kinase catalytic subunit: a target for an ICE-like protease in apoptosis. EMBO J *15*, 3238-46.

Stöppler, H., Stöppler, M. C., Johnson, E., Simbulan-Rosenthal, C. M., Smulson, M. E., Iyer, S., Rosenthal, D. S., and Schlegel, R. (1998). The E7 protein of human papillomavirus type 16 sensitizes primary human keratinocytes to apoptosis. Oncogene *17*, 1207-1214.

Takahashi, H., Kobayashi, H., Hashimoto, Y., Matsuo, S., and Iizuka, H. (1995). Interferon-gamma-dependent stimulation of Fas antigen in SV40-transformed human keratinocytes: modulation of the apoptotic process by protein kinase C. J Invest Dermatol *105*, 810-5.

Tewari, M., Quan, L. T., O'Rourke, K., Desnoyers, S., Zeng, Z., Beidler, D. R., Poirier, G. G., Salvesen, G. S., and Dixit, V. M. (1995). Yama/CPP32b, a mammalian homolog of CED-3, is a crmA-inhibitable protease that cleaves the death substrate poly(ADP-ribose) polymerase. Cell *81*, 801-809.

van Genderen, J., and Wolthuis, O. L. (1986). New models for testing skin toxicity. In Skin Models: Models to Study Function and Disease of Skin, R. Marks and G. Plewig, eds. (Berlin: Springer-Verlag).

Wang, H. G., Mckeon, F., and Reed, J. C. (1997). Dephosphorylation of pro-apoptotic protein Bad by calcineurin results in association with intracellular membranes. In Programmed Cell Death (Cold Spring Harbor, NY.

Wang, H. G., Pathan, N., Ethell, I. M., Krajewski, S., Yamaguchi, Y., Shibasaki, F., McKeon, F., Bobo, T., Franke, T. F., and Reed, J. C. (1999). Ca2+-induced apoptosis through calcineurin dephosphorylation of BAD. Science *284*, 339-43.

Yang, E., Zha, J., Jockel, J., Boise, L. H., Thompson, C. B., and Korsmeyer, S. J. (1995). Bad, a heterodimeric partner for Bcl-XL and Bcl-2, displaces Bax and promotes cell death. Cell *80*, 285-91.

Zha, J., Harada, H., Osipov, K., Jockel, J., Waksman, G., and Korsmeyer, S. J. (1997). BH3 domain of BAD is required for heterodimerization with BCL-XL and pro-apoptotic activity. J Biol Chem *272*, 24101-4.

Zhuang, L., Wang, B., and Sauder, D. N. (2000). Molecular mechanism of ultraviolet-induced keratinocyte apoptosis. J Interferon Cytokine Res *20*, 445-54.

Zhuang, L., Wang, B., Shinder, G. A., Shivji, G. M., Mak, T. W., and Sauder, D. N. (1999). TNF receptor p55 plays a pivotal role in murine keratinocyte apoptosis induced by ultraviolet B irradiation. J Immunol *162*, 1440-7.

Zundel, W., and Giaccia, A. (1998). Inhibition of the anti-apoptotic PI(3)K/Akt/Bad pathway by stress. Genes Dev *12*, 1941-6.

13. CHRONOLOGICAL BIBLIOGRAPHY AND PERSONNEL

Publications (2002-2005):

Publications (peer-reviewed):

1. Simbulan-Rosenthal, C. M., Trabosh, V., Velarde, A., Chou, F. P., Daher, A., Tenzin, F., Tokino, T. and **Rosenthal, D. S.** Id2 Protein is selectively upregulated by UVB in primary, but not in immortalized human keratinocytes and inhibits differentiation. *Oncogene*, **24,** 5443-5458 (2005)
2. Daher, A., Simbulan-Rosenthal, C. M., and **Rosenthal, D. S.** Apoptosis induced by UVB in HPV-immortalized human keratinocytes requires caspase-9 and is death receptor-independent. *Experimental Dermatology*, in press (2005)
3. **Rosenthal, D. S.,** Velena, A., Chou, F.P., Schlegel, R., Ray, R., Benton, B., Anderson, D., Smith, W. J., and Simbulan-Rosenthal, C.M. Expression of dominant-negative Fas-associated death domain blocks human keratinocyte apoptosis and vesication induced by sulfur mustard. *J Biol Chem*. **278**:8531-8540 (2003).
4. Simbulan-Rosenthal, C. M., **Rosenthal, D. S.,** Luo, R., Samara, S., Espinoza, L., Hassa, P., Hottiger, M., and Smulson, M.E. PARP-1 binds E2F-1 independently of its DNA-binding and catalytic domains, and acts as a novel coactivator of E2F-1-mediated transcription during reentry of quiescent cells into S-phase. *Oncogene*, **22**; 8460-8471 (2003).
5. Simbulan-Rosenthal, C. M., Velena, A., Veldman, T., Schlegel, R., and **Rosenthal, D. S.** HPV E6/7 immortalization sensitizes human keratinocytes to UVB by altering the pathway from caspase-8 to caspase-9-dependent apoptosis. *J. Biol. Chem*. **277**:24709-16 (2002).

6. Trofimova, I, Dimtchev, A, Jung, M, **Rosenthal, D,** Smulson, M, Dritschilo, A, Soldatenkov, V., Gene therapy for prostate cancer by targeting poly(ADP-ribose) polymerase. *Cancer Res* **62**:6879-6883 (2002).

Chapters

1. Simbulan-Rosenthal, C. M., **Rosenthal, D. S.,** Haddad, B., Ly, D., Zhang, J., and Smulson, M. E. Involvement of PARP-1 and Poly(ADP-ribosyl)ation in the Maintenance of Genomic Stability. In *PARP as a therapeutic target* (Zhang, J. (ed.)), 39-58 (2002).

Abstracts (2002-2005):

1. Simbulan-Rosenthal, C., Bazar, L., Chrikjian, J., and **Rosenthal, D. S.** Detection of high risk oncogenic HPV strains using mismatch repair enzymes. American Association for Cancer Research 96st Annual Meeting, Anaheim, CA (2005).

2. Simbulan-Rosenthal, C., Trabosh, V., Daher, A., Chou F., Tenzin F., and **Rosenthal, D. S.** Id-2 is selectively upregulated by UVB in primary, but not HPV16 E6/7 immortalized human keratinocytes. Cellular Senescence and Cell Death, Keystone, CO (2005).

3. Trabosh, V., Simbulan-Rosenthal, C., and **Rosenthal, D. S**. Id-1 suppression induces apoptosis in aggressive human breast cancer cells. Cellular Senescence and Cell Death, Keystone, CO (2005**).**

4. Ahmad, D., Simbulan-Rosenthal, C., and **Rosenthal, D. S.** Immortalization sensitizes keratinocytes to UVB-induced apoptosis mediated by Id3. Cellular Senescence and Cell Death, Keystone, CO (2005).

5. Chou F., Simbulan-Rosenthal, C., and Rosenthal, D. S. Artemesinin selectively induces apoptosis in tumorigenic human ectocervical and mammary epithelial cells. Cellular Senescence and Cell Death, Keystone, CO (2005).

6. **Rosenthal, D. S.** , Ray, R., Benton, B., Anderson, D., Smith, W., and Simbulan-Rosenthal, C., Characterization and Modulation of Proteins Involved in Sulfur Mustard Vesication. Biosciences 2004 Meeting, Huntvalley, MD (2004).

7. **Rosenthal, D. S**., Smith, W., Benton, B., Ray, R., and Simbulan-Rosenthal, C. Role of Fas/FasL- system in apoptosis and vesication induced by sulfur mustard. International Chemical Medical Defense Conference 2003, Munich, Germany (2003).

8. **Rosenthal, D. S**., Simbulan-Rosenthal, C., Velena, A., Smith, W., Benton, B., and Ray, R. Reduction of SM toxicity by inhibiting death receptor and mitochondrial pathways of apoptosis in human keratinocytes and grafted skin. Biosciences 2002 Meeting, Huntvalley, MD (2002).

9. Smulson, M., Simbulan-Rosenthal, C., Liu, W.F., Velena, A., Anderson, D., Benton, B., Wang, Z-Q., Smith, W., Ray, R., and **Rosenthal, D. S.** PARP determines the mode of cell death in skin fibroblasts, but not keratinocytes, exposed to sulfur mustard. Biosciences 2002 Meeting, Huntvalley, MD (2002)

Personnel

Dean S. Rosenthal, Ph.D.

Cynthia Simbulan-Rosenthal, Ph.D.

Ana Velarde, Technician

Ahmad Daher, Graduate Student

Attachment J.2.

Quarterly Report Format

1. Contract No DAMD17-00-C-0026 2. Report Date Oct. 28, 2005

3. Reporting period from May 1 , 2004 to July, 31, 2004

4. PI ROSENTHAL, DEAN S., Ph.D. Telephone No. (202) 687- 1056

6. Institution Georgetown University School of Medicine

7. Project Title: Characterization and Modulation of Proteins Involved in Sulfur Mustard Vesication

8. Current staff, with percent effort of each on project.

Dean S. Rosenthal, Ph.D.	60 %	Ana Velarde	100 %
Fnu Tenzin	100 %		%

9. Contract expenditures to date (as applicable):

	This Qtr/Cumulative		This Qtr/Cumulative
Personnel	$ 13,067 / $222,301	Travel	$199 / $ 2,764
Fringe Benefits	$2,432 / $ 42,325	Equipment	0 / 0
Supplies	$13,515 / $77,070	Other	$579 / $ 28,109

	This Qtr/Cumulative
Subtotal	$ 29,792 / $ 372,568
Indirect Costs	$16,535 / $ 206,735
Fee	0 / 0
Total:	$ 46,327 / $ 579,303

10. Comments on administrative and logistical matters.

11. Use additional page(s), as necessary, to describe scientific progress for the quarter in terms of the tasks or objectives listed in the statement of work for this contract. Explain deviations where this isn't possible. Include data where possible.

12. Use additional page(s) to present a brief statement of plans or milestones for the next quarter.

Attachment J.2.

Quarterly Report Format

1. Contract No DAMD17-00-C-0026 2. Report Date Oct. 28, 2005

3. Reporting period from Aug. 1 , 2004 to Oct. 31, 2004

4. PI ROSENTHAL, DEAN S., Ph.D. Telephone No. (202) 687- 1056

6. Institution Georgetown University School of Medicine

7. Project Title: Characterization and Modulation of Proteins Involved in Sulfur Mustard Vesication

8. Current staff, with percent effort of each on project.

Dean S. Rosenthal, Ph.D.	30 %	Ana Velarde	100 %
Cynthia Simbulan- Rosenthal, Ph.D.	30 %		%

9. Contract expenditures to date (as applicable):

	This Qtr/Cumulative		This Qtr/Cumulative
Personnel	$ 12,432 / $234,733	Travel	0 / $ 2,764
Fringe Benefits	$3,517 / $ 45,842	Equipment	0 / 0
Supplies	$2,259 / $79,329	Other	$2,579 / $ 30,688

	This Qtr/Cumulative
Subtotal	$ 20,787 / $ 393,356
Indirect Costs	$11,537 / $ 218,312
Fee	0 / 0
Total:	$ 32,324 / $ 611,668

10. Comments on administrative and logistical matters.

11. Use additional page(s), as necessary, to describe scientific progress for the quarter in terms of the tasks or objectives listed in the statement of work for this contract. Explain deviations where this isn't possible. Include data where possible.

12. Use additional page(s) to present a brief statement of plans or milestones for the next quarter.

Attachment J.2.

Quarterly Report Format

1. Contract No DAMD17-00-C-0026 2. Report Date Oct. 28, 2005

3. Reporting period from Nov. 1 , 2004 to Jan. 31, 2005

4. PI ROSENTHAL, DEAN S., Ph.D. Telephone No. (202) 687- 1056

6. Institution Georgetown University School of Medicine

7. Project Title: Characterization and Modulation of Proteins Involved in Sulfur Mustard Vesication

8. Current staff, with percent effort of each on project.

Dean S. Rosenthal, Ph.D.	30 %	Ana Velarde	100 %
Cynthia Simbulan- Rosenthal, Ph.D.	30 %		%

9. Contract expenditures to date (as applicable):

	This Qtr/Cumulative		This Qtr/Cumulative
Personnel	$ 13,068 / $247,801	Travel	0 / $ 2,764
Fringe Benefits	$3,790 / $ 49,632	Equipment	0 / 0
Supplies	$5,562 / $84,891	Other	$80 / $ 30,768

	This Qtr/Cumulative
Subtotal	$ 22,500 / $ 415,856
Indirect Costs	$12,420 / $ 230,732
Fee	0 / 0
Total:	$ 34,920 / $ 646,588

10. Comments on administrative and logistical matters.

11. Use additional page(s), as necessary, to describe scientific progress for the quarter in terms of the tasks or objectives listed in the statement of work for this contract. Explain deviations where this isn't possible. Include data where possible.

12. Use additional page(s) to present a brief statement of plans or milestones for the next quarter.

Attachment J.2.

Quarterly Report Format

1. Contract No DAMD17-00-C-0026 2. Report Date Oct. 28, 2005

3. Reporting period from Feb.1 , 2005 to April 30, 2005

4. PI ROSENTHAL, DEAN S., Ph.D. Telephone No. (202) 687- 1056

6. Institution Georgetown University School of Medicine

7. Project Title: Characterization and Modulation of Proteins Involved in Sulfur Mustard Vesication

8. Current staff, with percent effort of each on project.

Dean S. Rosenthal, Ph.D.	30 %		%
Cynthia Simbulan- Rosenthal, Ph.D.	30 %		%

9. Contract expenditures to date (as applicable):

	This Qtr/Cumulative		This Qtr/Cumulative
Personnel	$9,882 / $257,683	Travel	$1,060 / $ 3,824
Fringe Benefits	$2,866 / $ 52,498	Equipment	0 / 0
Supplies	$527 / $85,418	Other	$929 / $ 31,697

	This Qtr/Cumulative
Subtotal	$ 15,264 / $ 431,120
Indirect Costs	$8,426 / $ 239,158
Fee	0 / 0
Total:	$ 36,854 / $ 670,278

10. Comments on administrative and logistical matters.

11. Use additional page(s), as necessary, to describe scientific progress for the quarter in terms of the tasks or objectives listed in the statement of work for this contract. Explain deviations where this isn't possible. Include data where possible.

12. Use additional page(s) to present a brief statement of plans or milestones for the next quarter.

U.S. Army Medical Research and Materiel Command Animal Use Report

Facility Name: Georgetown University
Address: 3900 Reservoir Rd. NW
Washington DC 20057

Principal Investigator: _____ (Signature)

Principal Investigator: Rosenthal, Dean S., Ph.D. (Typed/Printed Name)

Award Number: DAMD 17-00-C-0026

This Report is for Fiscal Year (01 October - 30 September): 1 May 04- 30 April 05

AAALAC* Accreditation Status (circle one): (Full) Provisional Not Accredited

Date of Last USDA Inspection: July 10, 2002 USDA Registration Number: 10-R-0004

Definitions of Column Headings on Back of Form					
A. Animal	B. Number of animals purchased, bred, or housed but not yet used	C. Number of animals used involving no pain or distress	D. Number of animals used in which appropriate anesthetic, analgesic, or tranquilizing drugs were used to alleviate pain	E. Number of animals used in which pain or distress was not alleviated	F. Total Number of Animals (Columns C+D+E)
Dogs					
Cats					
Guinea Pigs					
Hamsters					
Rabbits					
Non-human Primates					
Sheep					
Pigs					
Goats					
Horses					
Mice	20	0	300	0	300
Rats					
Fish					
List Others:					

*AAALAC - Association for the Assessment and Accreditation of Laboratory Animal Care

Oncogene (2005) 24, 5443–5458

www.nature.com/onc

Id2 protein is selectively upregulated by UVB in primary, but not in immortalized human keratinocytes and inhibits differentiation

Cynthia M Simbulan-Rosenthal[1], Valerie Trabosh[1], Ana Velarde[1], Feng-Pai Chou[1], Ahmad Daher[1], Fnu Tenzin[1], Takashi Tokino[2] and Dean S Rosenthal*[,1]

[1]*Department of Biochemistry and Molecular Biology, Georgetown University, School of Medicine, Washington, DC 20007, USA;*
[2]*Department of Molecular Biology, Sapporo Medical University School of Medicine, Sapporo 060-8556, Japan*

Solar ultraviolet B (UVB) acts as both an initiator and promoter in models of multistage skin carcinogenesis. We found that, whereas UVB induces apoptosis in human papillomavirus-16 E6/7-immortalized keratinocytes, it inhibits markers of differentiation in human foreskin keratinocytes (HFK). Potential mechanisms for this differential response were examined by DNA microarray, which revealed that UVB alters the expression of three of the four human inhibitor of differentiation/DNA binding (Id) proteins that comprise a class of helix–loop–helix family of transcription factors involved in proliferation, differentiation, apoptosis, and carcinogenesis. These results were verified by RT–PCR and immunoblot analysis of control and UVB-irradiated primary and immortalized keratinocytes. Whereas Id1 was down-regulated in both cell types, Id2 expression was upregulated in primary HFK, but not immortalized cells. In contrast, Id3 expression was significantly increased only in immortalized cells. The differential expression pattern of Id2 in response to UVB was recapitulated in reporter constructs containing the 5′ regulatory regions of this gene. Id2 promoter activity increased in response to UVB in HFK, but not in immortalized cells. To identify the regulatory elements in the Id2 promoter that mediate transcriptional activation by UVB in HFK, promoter deletion/mutation analysis was performed. Deletion analysis revealed that transactivation involves a 166 bp region immediately upstream to the Id2 transcriptional start site and is independent of c-Myc. The consensus E twenty-six (ETS) binding site at −120 appears to mediate UVB transcriptional activation of Id2 because point mutations at this site completely abrogated this response. Chromatin immunoprecipitation and electrophoretic mobility-shift assays verified that the Id2 promoter interacts with known Id2 promoter (ETS) binding factors Erg1/2 and Fli1, but not with c-Myc; and this interaction is enhanced after UVB exposure. Similar to the effects of UVB exposure, ectopic expression of Id2 protein in primary HFK resulted in inhibition of differentiation, as shown by decreased levels of the terminal differentiation marker keratin K1 and inhibition of involucrin crosslinking. Reduction of Id2 expression by small interfering RNAs attenuated the UVB-induced inhibition of differentiation in these cells. These results suggest that UVB-induced inhibition of differentiation of primary HFK is at least, in part, due to the upregulation of Id2, and that upregulation of Id2 by UVB might predispose keratinocytes to carcinogenesis by preventing their normal differentiation program.
Oncogene (2005) **24,** 5443–5458. doi:10.1038/sj.onc.1208709; published online 27 June 2005

Keywords: Id2; keratinocyte; differentiation; promoter; ETS

Introduction

The incidences of human skin cancers are on the rise and are now the most common of all human malignancies (Stratton, 2001; Cleaver and Crowley, 2002). Solar ultraviolet (UV) radiation has been shown to be the major etiological factor leading to the precancerous stage of actinic keratosis (AK) and to induction and progression of skin cancers (Armstrong and Kricker, 2001). Others and we have shown that ultraviolet B (UVB) irradiation induces apoptosis and altered differentiation in primary human keratinocytes; this may be potential mechanism for tumor promotion, which allows the preferential clonal expansion of initiated cells (Jonason *et al*., 1996; Karen *et al*., 1999; Mammone *et al*., 2000; Simbulan-Rosenthal *et al*., 2002). Differentiation is altered in skin carcinogenesis since squamous cell carcinomas (SCC) in UV-induced mice show altered markers of differentiation and proliferation compared to normal cells (Rundhaug *et al*., 2005). Disseminated superficial actinic porokeratosis (DSAP)-derived keratinocytes also exhibit inherent defects in the terminal differentiation program (D'Errico *et al*., 2004). Similarly, cell cycling, differentiation, and apoptosis are altered in basal cell carcinomas (BCCs), which have been correlated with mutations in Patched (PTCH) protein in the Hedgehog pathway (Brellier *et al*., 2004). Point mutations in the p53 gene from SCCs and BCCs,

*Correspondence: DS Rosenthal, Department of Biochemistry and Molecular Biology, Georgetown University School of Medicine, 3900 Reservoir Road NW, Washington, DC 20007, USA;
E-mail: rosenthd@georgetown.edu
Received 28 January 2005; revised 9 March 2005; accepted 9 March 2005; published online 27 June 2005

and the PTCH gene from BCC of xeroderma pigmentosum (XP) patients have been attributed to solar UV radiation (de Gruijl *et al*., 2001).

Whereas low UVB doses (50–200 J/m^2) induce apoptosis, UVB doses greater than 200 J/m^2 inhibit terminal differentiation in human HaCaT keratinocytes, as indicated by decreased levels of keratinocyte differentiation markers, including involucrin, keratin K1, and keratin K10 (Mammone *et al*., 2000). Consistent with results using monolayer cell cultures, UVB exposure of human skin grafted on to nude mice showed altered or delayed expression of differentiation markers involucrin, keratin K10, loricrin, keratinocyte transglutaminase, filaggrin, and induced the formation of abnormal horny layers. The basal cell-specific keratin K14 was increased, while hyperproliferative keratins K6, K16, K17, and K19 were induced, along with an increase in the epidermal proliferation rate (Del Bino *et al*., 2004). Similar results were obtained after UVB exposure of a model of human skin reconstructed *in vitro*. Induction of early UVB-DNA damage such as pyrimidine dimers, sunburn cells, and apoptotic keratinocytes was noted at 500 J/m^2. Subsequent changes included epidermal disorganization, parakeratotic epidermis characterized by nucleated horny layers, as well as the downregulation of major markers of keratinocyte differentiation including keratin K10, loricrin, filaggrin, and type I transglutaminase (Bernerd and Asselineau, 1997). Thus, in both cell culture and in models of human skin, UVB exposure induces apoptosis as well as the inhibition of keratinocyte differentiation.

Besides UV irradiation, human papillomavirus (HPV) has also been shown to be a risk factor for skin cancers. A variety of HPV types have been identified in BCC and SCC in immunosuppressed patients (Shamanin *et al*., 1996), as well as in AK and SCC in those with the inherited disorder epidermodysplasia verruciformis (EV) (Bouwes Bavinck *et al*., 2000). HPV is also involved in BCC and SCC from immunocompetent non-EV patients as well (Shamanin *et al*., 1996; zur Hausen, 1996). In most cases of nongenital HPV skin cancer, carcinomas occur in sun-exposed sites, indicating cooperation between UV and HPV. UV and HPV thus likely play roles in the early immortalization stage of carcinogenesis. While HPV-16 is implicated in anogenital cancer, between 16 and 25% of nongenital Bowen's disease of the skull, foot, and periungual regions of the finger is associated with HPV-16 (Guerin-Reverchon *et al*., 1990; Kettler *et al*., 1990). These sites are potential targets of solar radiation, and the latter lesion represents a significant fraction of all skin cancer cases (Eliezri *et al*., 1990).

We earlier examined the effects of the E6/7 oncoproteins of malignancy-associated HPV-16 and additional early immortalizing events on the UVB response of primary human foreskin keratinocytes (HFK). We transduced HFK with a retroviral vector expressing HPV16 E6/7, or with the empty vector alone (LXSN), and compared the UVB-induced response of HFK and HPV16-immortalized cells (p27 E6/7-HFK). Whereas immortalized HFK were induced into caspase-9-mediated apoptosis, primary HFK (LXSN) were more resistant (Simbulan-Rosenthal *et al*., 2002). We subsequently determined that UVB exposure was not killing the primary HFK, but rather inducing a differential response, inhibition of differentiation. Consistent with our results, primary keratinocytes, when irradiated with a single dose of 400 J/m^2 or with multiple low UVB doses (200 J/m^2), showed greater resistance to caspase-9-mediated apoptosis than SCC cells (SCC12B2) (Dazard *et al*., 2003). Microarray analysis of these UVB-exposed cells exhibited a protective response in primary keratinocytes as shown by upregulation of antiapoptotic genes Bcl2, AP15L1, IER3, and TNFAIP3, as well as downregulation of the differentiation genes filaggrin and transglutaminase 3 (Dazard *et al*., 2003). Similar microarray studies indicate that primary keratinocytes respond to a single low UVB dose by suppressing processes related to transcription, differentiation, and transport (Takao *et al*., 2002).

To examine potential mechanisms and which genes might be responsible for the differential UVB response of primary and HPV16 immortalized keratinocytes, we performed microarray analysis of the control and UVB-exposed primary (LXSN) and immortalized HFK. The data reveal significant differences in a number of genes involved in cellular structure/adhesion, DNA repair, transcription, differentiation, and apoptosis. Interestingly, three of the four known inhibitor of differentiation/DNA binding (Id) proteins (Id1, Id2, and Id3) exhibit significant changes following exposure to UVB. Id4 is not expressed in either primary or immortalized keratinocytes (Ohtani *et al*., 2001). Consistent with our results, Id2 has also been shown to be upregulated in primary keratinocytes after exposure to UVB (Dazard *et al*., 2003).

These four small Id proteins (149, 134, 119, and 161 aa residues) comprise one of five classes of helix–loop–helix (HLH) family of transcription factors involved in proliferation, differentiation, apoptosis, and carcinogenesis (Atchley and Fitch, 1997). The HLH motif allows for dimerization of different HLH family members (Murre *et al*., 1989a). The five HLH classes are divided according to their structure, expression patterns, and ability to form dimers with other HLH classes. Class V proteins, which include the four Id proteins, form inactive heterodimers with most class I (E2A gene products) and some class II proteins (MyoD, myogenin, Myf5, Myf6). Class I–IV bHLH proteins all contain a basic DNA-binding domain at the N-terminus and bind a consensus DNA sequence, CANNTG (E-box) (Murre *et al*., 1989b), found in regulatory regions of many genes involved in growth, differentiation, and apoptosis. In contrast, the Id proteins contain no basic region, and appear to act as dominant-negative inhibitors of class I and class II proteins. Id proteins exert their effects primarily by binding class I proteins, preventing their interaction with class II proteins, thereby blocking the activation of tissue and differentiation-specific genes (Norton, 2000). However, some class I and class II proteins can themselves act as transcriptional repressors, and therefore Id proteins can be either activators or

inhibitors of E-box-containing genes. Id2, for example, relieves the repression of the p75 NGFR gene by preventing the bHLH transcriptional repressor HEB from binding the E-box in the promoter (Chiaramello *et al*., 1995).

In addition to the role of Id proteins in sequestering class I bHLH transcription factors, Id proteins interact with other proteins as well. Id2 specifically binds to the hypophosphorylated forms of the Rb family of proteins, including Rb, p107, and p130 (Iavarone *et al*., 1994; Lasorella *et al*., 1996). As Id2 levels increase, Rb is eventually sequestered by Id2, DNA synthesis is promoted, and excess Id2 is free to interact with other proteins, including the class I bHLH factors (Lasorella *et al*., 1996). Ids also bind to E twenty-six (ETS) family proteins, including Ets2 (Ohtani *et al*., 2001), and Id2 has also been shown to homodimerize (Liu *et al*., 2000). The roles of Ids have been well studied in B-cell, T-cell, pancreatic, nerve, and muscle differentiation. The skeletal muscle bHLH factors MyoD, Myf5, myogenin, and Myf6 regulate each step of myogenesis by forming heterodimers with E12/E47 (Murre *et al*., 1989b; Brennan and Olson, 1990; Chakraborty *et al*., 1991a, b; French *et al*., 1991; Lassar *et al*., 1991). Similarly, the differentiation of hematopoietic cells (Hsu *et al*., 1991), presomitic mesoderm (Quertermous *et al*., 1994), and neural tissue (Akazawa *et al*., 1992; Brown and Baer, 1994) also depends on the interaction of E12/E47 with cell type-specific bHLH factors. However, little is known about their role in keratinocyte differentiation, although Id1 has been shown to exert potent effects on senescence in keratinocytes. Recent studies have shown that Id1 and Id3 delay or block senescence, as a result of the suppression of the p16/Ink4a promoter (Alani *et al*., 1999; Nickoloff *et al*., 2000). Lower levels of p16 relieve the inhibition of cyclin D/cdk4/6, allowing Rb to be phosphorylated, and progression from G1 to S.

In the current paper, the events related to UVB-induced modulation of Id2 expression in primary and HPV16 E6/7-immortalized HFK were assessed. The upstream regulation of Id genes has been studied in mouse and in humans primarily in response to mitogenic and differentiation signals, such as serum stimulation (Barone *et al*., 1994) and vitamin D treatment (Kawaguchi *et al*., 1992; Ezura *et al*., 1997), respectively. Regulation appears to be primarily at the level of transcription and all of the responses of the Id1, Id2, and Id3 genes appears to be contained within a 3 kb DNA segment 5′ to the transcriptional start site. Deletion analysis as well as electrophoretic mobility-shift assay (EMSA) and DAPA and chromatin cross-linking has revealed smaller consensus DNA sequences, which bind a number of other transcription factors. The Id promoters themselves contain E-boxes, and the Id2 promoter binds to and is responsive to Myc family proteins, and can regulate cell division induced by c-Myc and N-Myc (Lasorella *et al*., 2000). In the present paper, we demonstrate for the first time a striking upregulation of Id2 by UVB in primary, but not immortalized keratinocytes. Since Id2 is differentially induced by UVB only in primary HFK, we examined the downstream effects of Id2 in these cells. Ectopic expression of Id2 inhibited differentiation in primary HFK, partially recapitulating the effects of UVB on these cells. Id2 thus may have transient effects on HFK that mimic those of UVB, and many of the UVB effects (apoptosis, differentiation, and tumorigenesis) on keratinocytes may be mediated by Id2.

Results

UVB-induced changes in expression of genes of the Id family in primary HFK, and HPV16 E6/7-immortalized (p27) keratinocytes

Compared to primary HFK, immortalized (>p27) E6/7-expressing keratinocytes were exquisitely sensitive to UVB-induced apoptosis (Simbulan-Rosenthal *et al*., 2002). We subsequently determined that UVB exposure was not killing the primary HFK, but rather inducing a differential response, inhibition of differentiation. To examine which genes might be responsible for this differential response, the transcriptional profiles of HFK and immortalized E6/7 p27 cells before and 4 h after 480 J/m^2 UVB irradiation were examined by oligonucleotide microarray hybridization analysis as described in Materials and methods. Of 16 000 human genes monitored, 205 differentially expressed genes (0.63–0.68%) were identified (Table 1), which were primarily involved in cellular structure/adhesion, DNA repair, transcription, differentiation, and apoptosis.

DNA microarray analysis revealed that UVB strikingly alters the expression of three of the four human Id genes (Id1, Id2, and Id3; Table 1). Furthermore, the three Id genes were differentially regulated by UVB in primary versus immortalized keratinocytes. Id1 has been shown to induce immortalization or extend the lifespan of keratinocytes (Alani *et al*., 1999; Nickoloff *et al*., 2000). Whereas DNA microarray analysis revealed a downregulation of Id1 expression by 3.2- to 4.7- fold in both cell types in response to UVB, expression of Id2 protein was dramatically upregulated by 10-fold in primary HFK, but not in immortalized cells (Table 1). On the other hand, expression of Id3 was upregulated by fivefold in the immortalized cells. Consistent with these results, a marked decrease in transcript levels of Id1 in all three cell types, as shown by RT–PCR analysis (Figure 1a), correlates with decreased abundance of Id1 protein in these cells (Figure 1b). The upregulation of Id2 in primary HFK, but not in immortalized cells, as well as the increased expression of Id3 in immortalized cells were likewise confirmed by RT-PCR analysis (Figure 1a), and were also apparent at the protein level after immunoblot analysis (Figure 1b). In response to UVB, Id1 protein levels decreased to barely detectable levels in both primary and immortalized cells, while Id2 protein increased markedly in primary HFK and Id3 protein expression was significantly upregulated in immortalized E6/7-HFK. There were no differences in mRNA or protein levels of GAPDH, as normalization or loading control, in both cell types before or after

Table 1 Differential expression profiles of genes altered in response to UVB in primary HFK and E6/E7-immortalized HFK (grouped according to function)

Primary HFK		*E6/E7-immortalized HFK*	
Fold Δ	*Gene name/GenBank Accession number*	*Fold Δ*	*Gene name/GenBank Accession number*
−2.3	*integrin alpha 6B S66213*	*−8.4*	*integrin alpha 6B S66213*
−9.8	*plectin U53204*	*−28*	*plectin U53204*
−2.2	*AHNAK M80899*	*−3*	*AHNAK M80899*
−2.8	E-cadherin L08599	−3.3	p cadherin X63629
−4	integrin beta4E AF011375	−4.6	caldesmon M83216
−2.3	Desmoplakin I AL031058	−3.3	fibronectin M10905
−5.2	Has2 U54804	−4.9	integrin alpha 2 X17033
		−3.3	lamA3 L34155
		−3	lamc2 U31201
		−6.4	radixin L02320
Apoptosis/survival			
−2.8	MCL1 L08246	−5	semaphorin-E AB000220
−2.4	PQ-rich protein Z50194		
2.6	receptor 4-1BB ligand U03398		
Cell cycle			
−2.7	cyclin F Z36714	−6.8	ribonucleotide reductase small subunit X59618
Chromosomal assembly			
3.1	H2A.2 L19779	−4.8	nucleosome assembly protein NAP M86667
Cytokines, growth factors			
4.4	*B61 M57730*	*8.1*	*B61 M57730*
5.2	*IFN-beta 2a X04430*	*3.3*	*IFN-beta 2a X04430*
−4.5	*thrombospondin-1 X14787*	*−56.7*	*thrombospondin-1 X14787*
6.1	GRO-beta M36820	−5.2	insulin-like growth factor receptor-1 X04434
4.2	GRO-gamma M36821	−4.5	thromobomodulin J02973
3.2	IL8 M28130	−3.5	epiregulin D30783
−2.8	MEGF1 AB011535		
−2.7	VEGF (angiogenesis) AF024710		
2.9	p27 X67325		
DNA/RNA synthesis and repair			
−2.3	*spliceosomal protein 62 L21990*	*−7.3*	*spliceosomal protein (SAP 62) L21990*
∼18.7	CHOP U19765	−4.5	Gu protein U41387
∼17.1	GADD45beta AF078077	−3.2	TOPOISOMERASE IIB X68060
−5.4	Novel gene chomosome 1 BAT2 AL096857	−4.3	MSSP-1 HG2639-H
−3.3	RBP-MS/type 4 (rb) D84110	−4.5	Cell cycle reg. protein p95 NBS1 AF058696
4.9	RNA polymerase II L37127		
−3	RNA polymerase II largest subunit X63564		
−2.6	MSSP-2 X77494		
Differentiation			
−2	*tyrosine phosphatase (PRL-1) AF051160*	*−3.96*	*tyrosine phosphatase (PRL-1) AF051160*
−3.2	**Id-1 X77956**	**−4.7**	**Id-1 X77956**
10.1	**Id-2 D13891**	**5.1**	**Id-3 AL021154**
−4.8	NRP/B AF059611		
Oncogenes, tumor suppressors			
−3.4	*C-Myc, Alt. Splice 3, Orf 114 HG3523-HT*	*−3.5*	*C-Myc, Alt. Splice 3, Orf 114 HG3523-HT*
−2.6	*EGFPRE X00588*	*−7.9*	*EGFPRE X00588*
−2.2	*TMP U43916*	*−3.5*	*tumor-assoc. membrane protein homolog (TMP) U43916*
−4.3	*c-myc-P64 M13929*	*−3.8*	*c-myc-P64 M13929*
−2.6	*TACC1 AF049910*	*−3.9*	*TACC1 AF049910*
−7.1	c-myc oncogene V00568		
−2.2	KET Y16961		
∼−13.1	MN1 X82209		
Signal transduction			
−2	*cAMP-dep prot kin type I-alpha subunit M33*	*−3.6*	*cAMP-dep prot kin type I-alpha subunit M33336*
−4.6	*protein-tyrosine-phosphatase (testis) X93921*	*−27*	*protein-tyrosine-phosphatase X93921*
−2.8	80K-L protein (MARCKS- PKC substrate) D10522	−3.7	JAK-1 protein tyrosine kinase M64174
−3.3	beta-2-adrenergic receptor (rec) M15169	−5.4	ras GTPase-activating-like protein IQGAP1 L33075
−2.5	GRB-7 SH2 domain protein D43772	−4.8	bcl-1 M73554
−3	PI-4-phos 5-kinase type II beta U85245	−14.8	Rho associated protein kinasev p160rock U43195

Table 1 (*continued*)

Primary HFK		*E6/E7-immortalized HFK*	
Fold Δ	*Gene name/GenBank Accession number*	*Fold Δ*	*Gene name/GenBank Accession number*
−7.7	DUSP5 dual-specif. prot. phosphatase U15932		
−5.7	serum-inducible kinase AF059617		
Stress response			
2.5	microsomal glutathione S-transferase 3 AF026977	−3.3	cytochrome p-1-450 TCDD-inducible K03191
		−4.1	cytochrome p450 dioxin-inducible U03688
Transcription factors			
−3.5	*ERF-2 X78992*	*−4.9*	*ERF-2 X78992*
−2.3	*hFat protein X87241*	*−4.7*	*hFat protein X87241*
−2.3	*APRF (DNA-binding protein) L29277*	*−7.3*	*APRF L29277*
2.4	*atf4 AL022312:dJ1104E15.2*	*3.7*	*atf4 AL022312:dJ1104E15.2*
−2.5	*son-a X63753*	*−6.7*	*son-a X63753*
−2.6	nuclear factor RIP140 X84373	−19.8	AP2 X52611
−3.2	SOX9 Z46629	3.7	ATF3 L19871
−2.9	EGR alpha S81439	−3.1	BAF155 SWI/SNF U66615
−2.6	ERF-1 X79067	−5.5	DP-1 L23959
−2.6	MEN1 U93237	−3	Fuse-binding protein 3 U69127
−2.8	ROX protein X96401	−3.7	ISGF3 M97935
−2.8	transcript factor AREB6 D15050	25.2	my1 X63131
−2.7	TGFb inducible early protein AF050110	−3	p40 Y11395
		−3.1	ring-H2 protein RNF6 AJ010346
		−3.3	Smad 3 AB004922
		−3.6	trans factor CA150 AF017789
Other			
−3	*similarities to BAT2 M33509*	*−20*	*similarities to BAT2 M33509*
−3.1	peroxisome prolif. activated receptor L07592	−4.4	plasminogen activator inhibitor-1 J03764
		−4.6	SAM decarboxylase M21154
		−5.7	antizyme inhibitor B88674
		−3.3	eiF2 gamma L19161
		−3.2	ranbp7/importin 7 AF098799
		−7.7	SAM synthetase X68836
		−7.5	proteinase-activated receptor-2 U34038
		4.7	folate receptor alpha U78793

Fold Δ: fold increase or decrease in expression of genes in UVB-exposed cells relative to control unexposed cells. Italics indicates same gene altered in response to UVB in both primary and immortalized HFK. Normal indicates unique genes altered in response to UVB in primary or immortalized HFK. Bold values refers to the differential expression profiles for the Id protein family (Id-1, Id-2, and Id-3)

UVB exposure. The differential upregulation of Id2 by UVB in primary, but not in immortalized HFK is further confirmed by immunoblot analysis of extracts derived 24 h after irradiation of cells with increasing doses of UVB (Figure 1c).

Id2 promoter analysis in UVB-exposed HFK and immortalized E6/7-HFK

Given that Id2 expression in response to UVB was differentially regulated in normal HFK and immortalized E6/7-HFK, we next investigated whether a 5′ promoter of Id2 can recapitulate the differential response to UVB in these cell types. A –834 Id2-CAT fusion construct with the 5′ region of the Id2 gene cloned upstream of the CAT reporter gene was transiently cotransfected together with a CMV-luciferase construct into either primary or immortalized HFK, and then induced with UVB. CAT assays were performed 16 and 24 h after UVB exposure, as a measure of Id2 promoter activity, and normalized against transfection efficiencies by luciferase activity and total protein. The Id2 promoter activity was strongly upregulated in response to UVB in primary HFK; the increase was maximal (sevenfold higher than basal levels) 24 h after 480 J/m^2 UVB (Figure 2). In contrast, Id2 promoter activity in immortalized HFK did not exhibit any significant increase after UVB exposure. Thus, the UVB-induced cell-type-specific expression pattern of Id2 mRNA and protein as determined by reverse transcription–polymerase chain reaction (RT–PCR) and immunoblot analysis (Figure 1) is reproduced by that of the Id2 promoter (Figure 2). These results indicate that UVB either directly or indirectly upregulates Id2 expression at the level of transcription in primary HFK, but not in immortalized keratinocytes.

We next identified the regulatory elements in the Id2 promoter that may mediate transcriptional activation by UVB in primary HFK. Consensus ETS binding sequences (especially for Fli1) in the Id2 promoter have been identified at positions –2633, −120 and –60, where +1 represents the transcription start site; E-box c-Myc binding sites were identified at positions −1880 and −1570 (Nishimori *et al*., 2002; Figure 3a). To clarify the

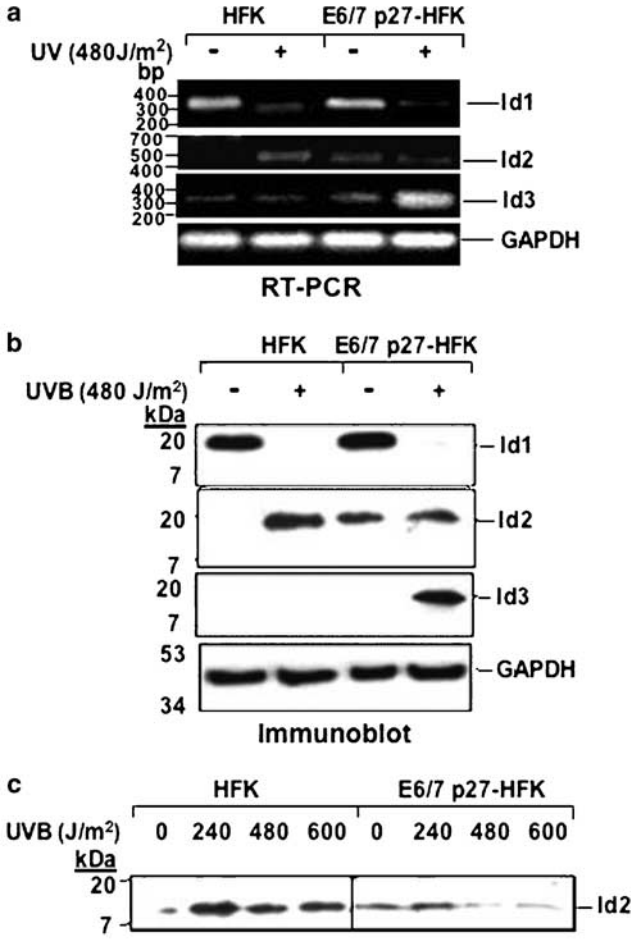

Figure 1 Differential expression of Id1, Id2, and Id3 in primary HFK and E6/7-immortalized HFK in response to UVB irradiation as revealed by RT–PCR (**a**) and immunoblot analysis (**b**). Cells were irradiated with the 480 J/m^2 of UVB and 4 h later RNA was prepared and subjected to RT–PCR analysis with specific primers for Id1, Id2, and Id3 mRNA (**a**) as described in Materials and methods. (**b, c**) At 4 h after cells were irradiated with the 480 J/m^2 (**b**) or the indicated doses (**c**) of UVB, cell extracts were prepared and subjected to immunoblot analysis with antibodies to Id1, Id2, Id3, or to GAPDH. The positions of the Id1, Id2, Id3, and GAPDH cDNA, as well as immunoreactive proteins and the molecular size standards are indicated

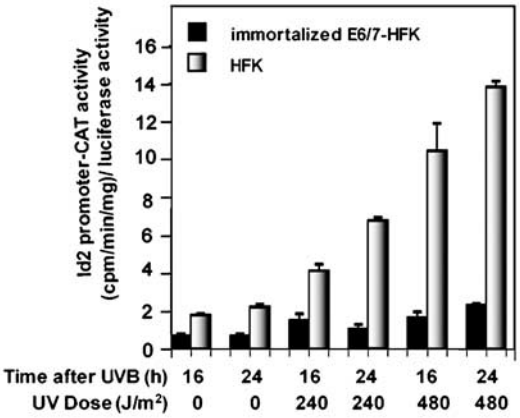

Figure 2 Transactivation of the Id2 promoter by UV irradiation in primary HFK, but not in immortalized E6/7-HFK. A plasmid containing the 843 bp upstream fragment of the Id2 gene fused to the CAT reporter was cotransfected with CMV-luciferase into primary (HFK; hatched boxes) or immortalized (p27 E6/E7-HFK; black boxes). Keratinocytes were then exposed to the indicated doses of UVB (J/m^2), and cell extracts were derived after either 16 or 24 h, analysed for CAT activity, and normalized for protein concentration (mg) and luciferase activity. A representative experiment is shown; essentially the same results were obtained in three independent experiments: Bars indicate means $\pm$ s.d.

role of these sites in Id2 induction mediated by UVB, primary HFK were cotransfected with a 2.7 kb Id2 promoter fragment (Id2-2755) or eight different deletion constructs (Id2-del 980, Id2-1329, Id2- 850, Id2-204, Id2-166, Id2-120, Id2-100, and Id2-60) inserted upstream of a luciferase reporter gene, together with a pSV$_2$CAT internal control vector. Id2 promoter activity was measured by luciferase assays 24 h after UVB irradiation (480 J/m^2), and normalized against transfection efficiencies by CAT activity. The Id2-60, Id2-100, and Id2-120 reporter constructs (encompassing –60 to +35, –120 to +35, and –100 to +35, respectively), containing the ETS box at –60 but lacking the ETS box at –120, conferred no significant luciferase activity with or without UVB exposure (Figure 3). Deletion of the ETS binding site at –120 markedly reduced the UV-mediated activation noted with reporter constructs Id2-166, Id2-204, and Id2-1329 in primary HFK. Consistent with previous studies (Nishimori *et al*., 2002), the region between –1329 and –2755 appears to act as a repressive element for Id2 transcription in primary HFK since inclusion of this region in Id2-del980 and Id2-2755 decreased UVB-mediated activation. UVB also activated the reporter construct Id2-1329, which lacks the c-Myc binding sites at –1880 and –1570 and the ETS binding site at –2633. These results together suggest that UVB-mediated transcriptional activation of Id2 in primary HFK involves the minimal Id2 promoter encompassing the two ETS binding sites at –60 and –120, requires the ETS box at –120, and is independent of c-Myc.

Mutation analysis of the ETS binding site at –120 in UVB-exposed primary HFK

Deletion analysis showed that UVB-mediated transcriptional activation of Id2 in primary HFK requires the ETS box at –120, and is independent of c-Myc. To clarify the requirement for this ETS binding site in the UVB-mediated activation of the Id2 promoter, we next investigated whether point mutations introduced in this site can abolish this UVB response. Two point mutations A-115T and G-113C were introduced in the ETS box (–120) in reporter constructs Id2-166, Id2-204, and Id2-2755 by site-directed mutagenesis. Primary HFK were cotransfected with Id2-166, Id2-204, Id2-2755, and their corresponding mutant constructs Id2-166mut, Id2- 204mut, and Id2-2755mut, together with a

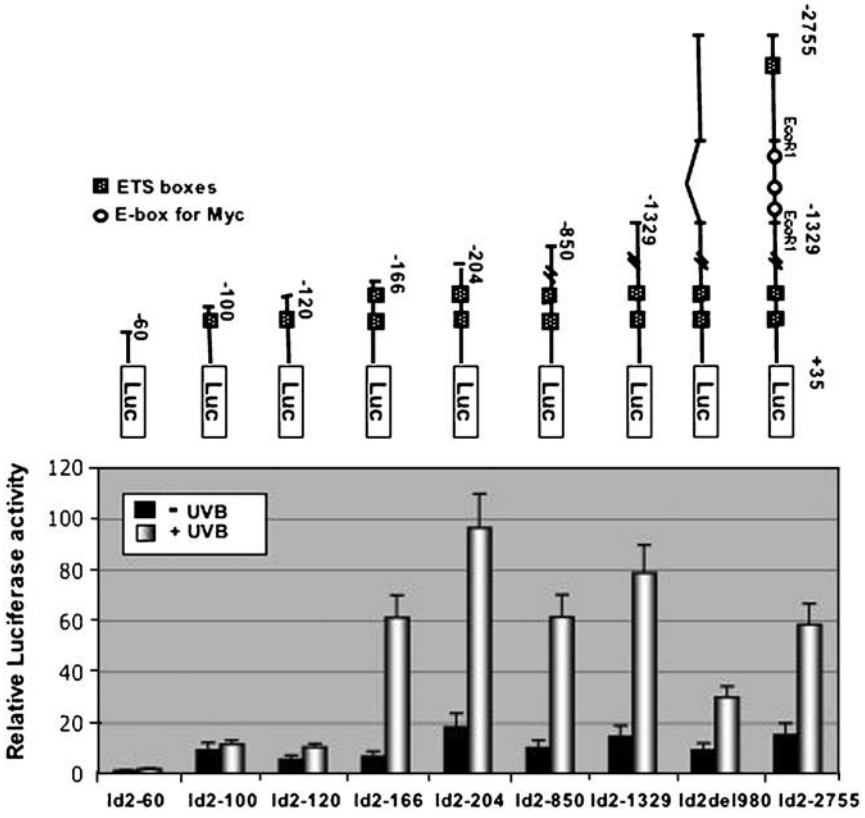

Figure 3 Identification of regulatory elements in the Id2 promoter that mediate transcriptional activation by UVB in primary HFK by deletion analysis. Schematic diagram of the Id2 promoter reporter constructs; nine fragments (Id2-2755 or deletion constructs Id2-del 980, Id2-1329, Id2-850, Id2-204, Id2-166, Id2-120, Id2-100, and Id2-60) containing different 5′ flanking regions of the Id2 gene subcloned upstream of a luciferase reporter gene in pGL3-basic vector; the transcription start site is +1; closed boxes, ETS-binding sites; circles, E-box consensus binding sequences for N-Myc or c-Myc (upper panel). Primary keratinocytes were cotransfected with each of the Id2 promoter reporter constructs together with a pSV2-CAT control plasmid, and exposed to 480 J/m^2 UVB. Cells were harvested 24 h after UVB exposure, followed by measurement of luciferase activity, normalized with CAT activity from the internal control plasmid in the same cell extracts. These experiments were performed in triplicates and repeated at least three times; the bars indicate means ±s.d.

pSV2CAT internal control vector. Id2 promoter activity was measured by luciferase assays 24 h after UVB irradiation (480 J/m^2), and normalized by CAT activity. As expected, site-directed mutagenesis of the ETS binding site at –120, even in the full-length Id2-2755 construct, largely abolished the UV-mediated activation of the Id2 promoter in primary HFK; thus, indicating that this UVB response in primary HFK requires the ETS binding site at –120 (Figure 4).

Id2, Fli1, and Erg1/2, but not c-Myc, selectively bind the Id2 promoter in primary HFK

Chromatin immunoprecipitation (ChIP) assays were performed to determine whether the ETS binding proteins Fli1 or Erg1/2 or E-box-binding protein c-Myc bind the Id2 promoter *in vivo*, providing a mechanism to facilitate Id2 transcription. After formaldehyde crosslinking and sonication of lysates from untreated or UVB-exposed primary HFK (Figure 5), protein–DNA complexes were immunoprecipitated with antibodies to Fli1, Erg1/2, c-Myc, or control IgG, and IP chromatin was subjected to PCR amplification using primers specific for the Id2 promoter fragment. Antibodies to Fli1 and Erg1/2 were able to precipitate the Id2 promoter, indicating the binding of these proteins to this element. In addition, the binding of Erg1/2 and Fli-1 to the Id2 promoter element increased significantly after UVB exposure. A strong signal was also detected after Id2 ChIP, suggesting that Id2 interacts with its own promoter, although this interaction may be indirect (data not shown). In contrast, no amplified product was detected with control IgG, verifying antibody specificity. Consistent with these results, when cell extracts derived from primary HFK prior to or 24 h after UVB irradiation (480 J/m^2) were subjected to immunoblot analysis with antibodies to Id2, Erg1/2, or GAPDH, an increase in both Id2 as well as Erg1/2 protein was observed following UVB irradiation of primary keratinocytes. No Id2 promoter sequences were amplified from c-Myc ChIP, suggesting that c-Myc does not bind to the Id2 promoter under these conditions. These results are in agreement with the promoter reporter assays showing that UVB-mediated-transcriptional activation of Id2 is independent of c-Myc

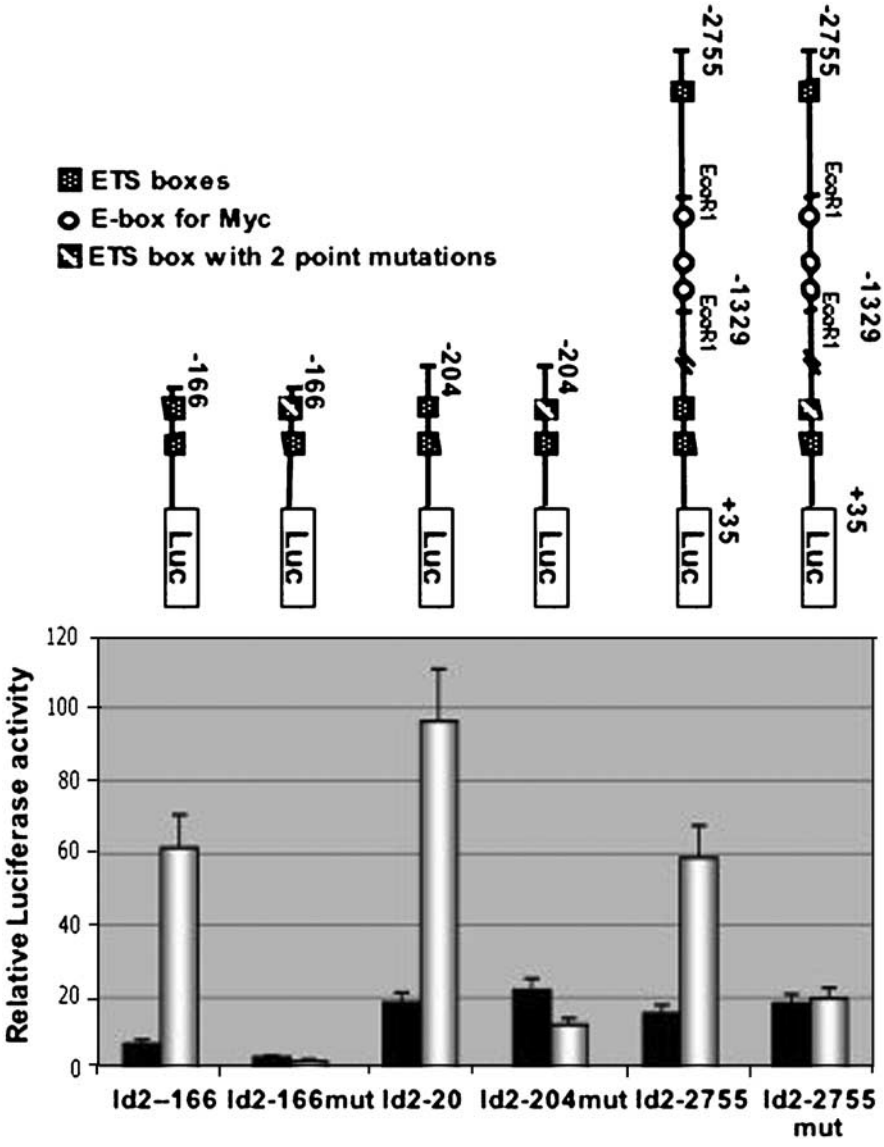

Figure 4 An intact ETS box at −120 from the transcription start site is required for UVB-induced activation of the Id2 promoter in primary HFK. Schematic representation of the Id2 promoter reporter constructs and their corresponding mutant constructs; the transcription start site is +1; closed boxes represent ETS-binding sites; open boxes represent ETS boxes with double-point mutations A-115T and G-113C introduced by site-directed mutagenesis; circles represent E-box consensus binding sequences for N-Myc or c-Myc (upper panel). Primary keratinocytes were cotransfected with Id2-166, Id2-204, Id2-2755, and their corresponding mutant constructs Id2-166mut, Id2-204mut, and Id2-2755mut, together with a pSV2CAT internal control vector. At 24 h after UVB irradiation (480 J/m^2), transient reporter assays were performed as described in Figure 3. Error bars represent means ± s.d. of three replicates of a representative experiment; essentially the same results were obtained in three independent experiments

and involves the minimal Id2 promoter encompassing the ETS binding sites for Fli1 and Erg1/2 at –120.

Fli1 binds the Id2 promoter in primary HFK in response to UVB

ETS genes encode eucaryotic transcription factors that share a conserved DNA-binding domain (ETS domain), which recognizes and binds to the purine-rich ETS binding site. The Ets family, which includes Erg and Fli1, holds a key role in regulating cellular proliferation and differentiation during embryonic development and in adults, and upon binding to the ETS recognition sequence, triggers transcription of several target genes including transcription factor genes, immune response genes, growth factors or their receptors (Sharrocks *et al*., 1997). To investigate whether ETS box binding proteins Erg and/or Fli1 bind to the ETS consensus sequence *in vitro* in response to UVB exposure, we performed EMSA assays with a biotin labeled 66-bp oligonucleotide probe containing the ETS consensus binding sequence. Primary HFK were exposed to UVB (480 J/m^2) and nuclear extracts were derived 4 h after UVB exposure. Nuclear extracts were first incubated with or without antibodies to Erg1/2 or Fli1, followed by incubation with the DNA probe in the presence or

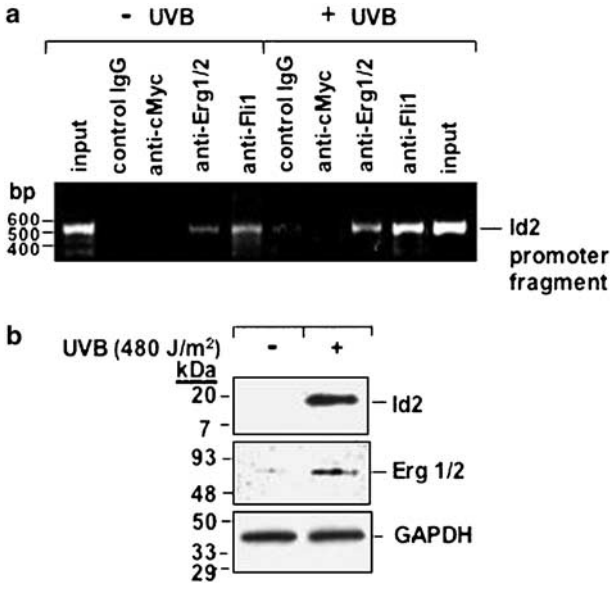

Figure 5 ChIP assay detects increased binding of ETS binding proteins Fli1 and Erg1/2 to the Id2 promoter after UVB irradiation of primary HFK. (**a**) ChIP assay of a genomic fragment containing the Id2 promoter was performed on primary HFK that were untreated (lanes 1–5) or harvested 4 h after UVB exposure (lanes 6–10). After precipitation of the protein–DNA complexes with antibodies to Fli1 (lanes 5 and 9), Erg1/2 (lanes 4 and 8), c-Myc (lanes 3 and 7), or a control IgG (lanes 2 and 6), PCR amplification of the Id2 fragment was performed using Id2 promoter primers. A positive signal is noted with anti-Erg1/2 and anti-Fli1, but not with anti-c-Myc or control IgG. Lanes 1 and 10, input refers to the DNA from untreated or UVB-exposed HFK. (**b**) Cell extracts derived from primary HFK prior to or 24 h after UVB irradiation (480 J/m^2) were subjected to immunoblot analysis with antibodies to Id2, Erg1/2, or GAPDH. Positions of the immunoreactive proteins and the molecular size standards (in kilodaltons) are indicated

absence of excess nonbiotinylated probe. The DNA–protein complexes were then analysed by electrophoresis, followed by transfer to nylon membranes, and detection of biotin-labeled DNA by chemiluminescence (Figure 6). While complexes of nuclear proteins from unexposed control HFK and the DNA probe were detected as a major shifted band (lane 2), a second larger protein–DNA complex was noted in extracts from UVB-exposed cells (lane 5). Competition with excess nonbiotinylated control probe completely abolished the DNA–protein interaction, verifying the specificity of the interaction (lanes 6, 8, and 10). Whereas incubation of the extracts from unexposed control HFK with antibodies to Erg and Fli1 did not supershift the DNA–protein complexes (lanes 3 and 4), extracts from UVB-exposed cells preincubated with anti-Fli1 exhibited a supershifted antibody–protein–DNA complex (lane 9). These results indicate that Fli1 specifically binds the Id2 promoter in primary HFK in response to UVB.

Id2 overexpression has no effect on apoptosis, but inhibits differentiation markers in primary HFK

To further delineate the role of Id2 in the UVB response of primary human keratinocytes, we next determined the effect of overexpression of the Id2 protein in primary HFK. Id expression vectors were constructed under the control of CMV promoter by inserting full-length coding regions of Id2 into the *Xho*/*Xba*1 site of the mammalian expression vector pCMSEGFP. Cells were transfected with Id2 or with an empty vector (pCMSEGFP). Immunoblot analysis with antibodies to Id2 of cell extracts derived 24 h after transfection confirmed the overexpression of Id2 in HFK (Figure 7a, inset). Visualization of GFP in transfected cells by fluorescence microscopy indicated a transfection efficiency of approximately ~50%, essentially the same as transfection efficiencies with Id2 and the pCMSEGFP vector; these values were confirmed by FACS analysis (data not shown). Cells were exposed to 480 J/m^2 UVB 24 h after transfection. Phosphatidylserine, exposed on the surface of apoptotic cells, was detected by binding to Annexin V 24 h after UVB exposure by subjecting untreated and UVB-exposed cells to AnnexinV-PE and 7-actinomycin D (7AAD) staining, followed by FACS analysis. Although UVB exposure induced an increase in the number of apoptotic cells, overexpression of Id2 did not induce an apoptotic response in primary HFK (Figure 7a).

To further clarify the role of Id2 in the UVB response of primary HFK, we next determined the effect of increased expression of the Id2 protein on differentiation markers in primary HFK. Immunoblot analysis with antibodies specific to the differentiation markers keratin HK1 and involucrin revealed that Id2 overexpression in primary HFK inhibits HK1 expression and cross-linking of involucrin (Figure 7b). UVB exposure of primary HFK, which upregulates Id2

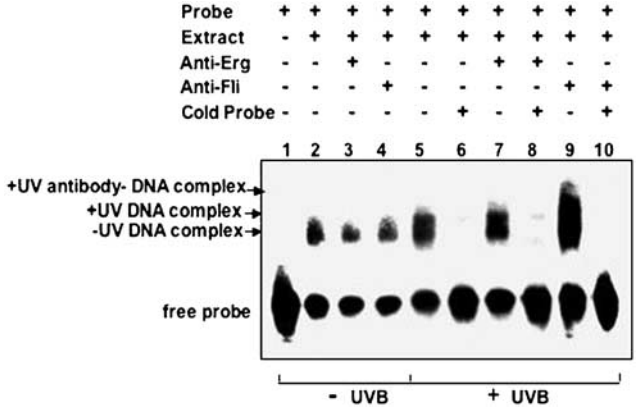

Figure 6 Specific binding of Fli1 to the Id2 promoter in primary HFK in response to UVB. Nuclear extracts from unirradiated HFK (lanes 1–4)) or UVB-exposed HFK (4 h, 480 J/m^2, lanes 5–10) were subjected to gel supershift assays with antibodies to Erg or Fli1 and a biotin-labeled 66-bp oligonucleotide probe containing the ETS consensus binding sequence. Control EMSA was performed with excess nonbiotinylated control probe (lanes 6, 8, and 10) to confirm specificity of DNA binding. Lane 1, probe alone; lanes 2 and 5, probe with extract; lanes 3 and 7, probe with extract and anti-Erg; lanes 4 and 9, probe with extract and anti-Fli1; lane 6, probe with extract and excess control probe; lane 8, probe with extract, anti-Erg, and excess control probe; lane 10, probe with extract, anti-Fli1, and excess control probe

expression, also induced a similar decrease in the abundance of HK1 as well as in involucrin crosslinking (Figure 7c). Thus, similar to the effects of UVB exposure, the ectopic expression of Id2 protein in primary HFK results in inhibition of differentiation, as shown by decreased abundance of the terminal differentiation marker keratin K1 and involucrin crosslinking. These results indicate that effects of UVB can be mimicked by overexpression of Id2 and might be mediated by upregulation of Id2 by UVB in primary HFK.

Reduction of Id2 protein expression by siRNAs attenuates UVB-induced inhibition of differentiation in primary HFK

In order to further clarify the potential roles of Id2 protein in mediating the UVB response of human keratinocytes, we utilized small interfering RNA (siRNAs) targeting Id2 to reduce the expression of this Id protein in primary HFK after UVB exposure. Since different siRNAs targeting the same gene can vary in efficiency, three siRNAs against the open reading frame of Id2 mRNA were designed and tested in primary HFK for their effects on Id2 protein expression.

To examine the effects of Id2 siRNA on the UVB-induced inhibition of differentiation in primary HFK, cell extracts were derived 24 h after 480 J/m^2 UVB exposure and immunoblot analysis with antibodies to Id2 and differentiation markers was performed. Compared with a scrambled control siRNA, transfection with Id2 siRNA resulted in significant downregulation of Id2 expression; intracellular Id2 protein concentrations were reduced to $\sim$5% of the levels in scrambled siRNA-transfected cells (Figure 7d, top). Similar to untransfected cells (Figure 7c), UVB irradiation of scrambled siRNA-transfected HFK resulted in decreased levels of HK1. Transfection with Id2 siRNA abrogated this response and maintained higher HK1 levels. siRNA targeting Id2 reduces Id2 protein, which may attenuate UVB-induced inhibition of differentiation in primary HFK (Figure 7d), thus suggesting that this UVB response of these cells may at least in part be mediated by the Id2.

Discussion

In the present study, we demonstrated that the expression of Id1, Id2, and Id3 is differentially regulated by UVB in primary and HPV-immortalized HFK. While Id1 is downregulated in both cell types, Id2 is induced in primary human keratinocytes, and Id3 is induced in HPV-16 E6/7-immortalized keratinocytes. Since Id2 proteins have been shown to play important roles in differentiation, apoptosis, and tumorigenesis in a variety of other cell types, we further examined the regulation and effects of Id2 in primary and immortalized HFK. We showed that the preferential induction of Id2 by UVB in primary HFK versus immortalized HFK could be reproduced in promoter constructs. Furthermore, deletion analysis indicated that the UVB-inducible

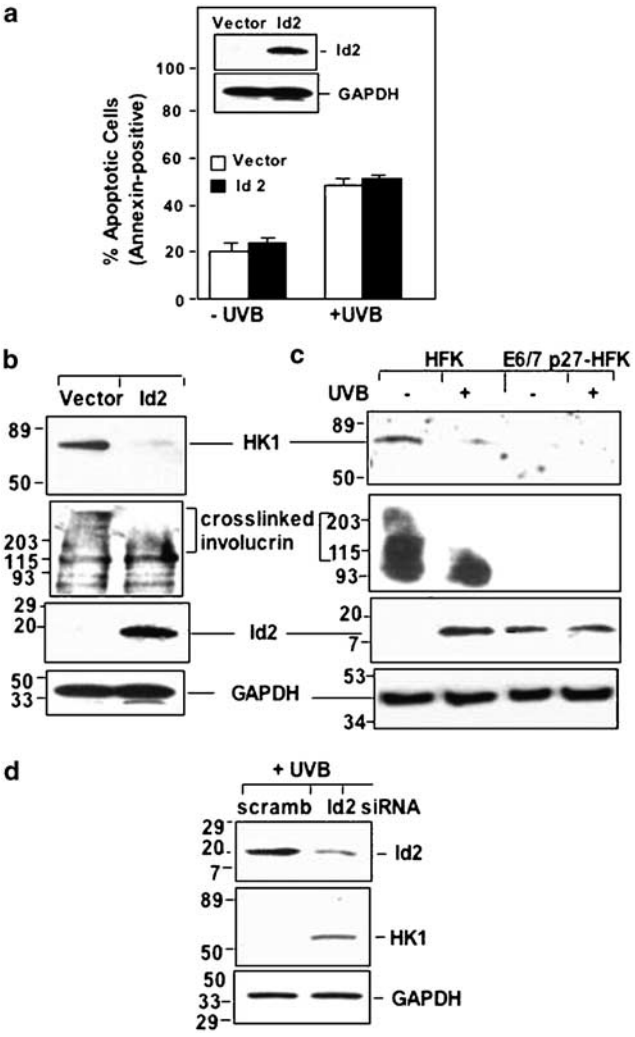

Figure 7 Overexpression of Id2 and UVB irradiation both inhibit differentiation markers HK1 and involucrin crosslinking in primary HFK; reduction of Id2 expression by siRNAs attenuates this response. (**a**) HFK were transfected with Id2-EGFP, or the empty vector pCMS-EGFP (vector); cell lysates were subjected to immunoblot analysis with antibodies to Id2 24 h after transfection, and membranes were reprobed with antibodies to GAPDH for loading control (inset). HFK were exposed to UVB (480 J/m^2) 24 h after transfection, and assayed for GFP, Annexin V-PE and 7AAD staining by FACS analysis 24 h after UVB exposure. Percentages of GFP-expressing cells that are positive for Annexin V-PE staining (apoptotic) are shown and presented as means$\pm$s.d. of three replicates of a representative experiment; essentially the same results were obtained in three independent experiments. (**b**) HFK were transfected with Id2-EGFP or empty vector as in (**a**); 24 h after transfection, cell lysates were subjected to immunoblot analysis with antibodies to the differentiation markers keratin HK1 and involucrin (upper panels) or to Id2 or GAPDH (loading control). (**c**) Cell extracts derived from primary or immortalized HFK prior to or 24 h after UVB irradiation (480 J/m^2) were subjected to immunoblot analysis with antibodies to HK1, involucrin, Id2, or GAPDH. (**d**) Primary HFK were transfected with siRNAs against the open reading frame of Id2 or with a scrambled siRNA control vector (scramb). Cells were exposed to 480 J/m^2 UVB 48 h after transfection; cell extracts were derived and subjected to immunoblot analysis with antibodies to Id2 (top), HK1 (middle), or GAPDH (bottom). Positions of the immunoreactive proteins and the molecular size standards (in kilodaltons) are indicated

region was localized to the 166 bp proximal promoter, containing consensus-binding sequences for the ETS transcription factors Fli1 and Erg1/2. Id2 was also found to interact with its own proximal promoter. Since Id2 lacks a DBD, we believe that this interaction is indirect, perhaps through one of the ETS proteins, as Ets has been shown to bind directly to Id2 in a complex with the telomerase promoter (Xiao *et al*., 2003). Using point mutation analysis, the regulatory region was further localized to an ETS box consensus sequence located 120 bp upstream of the transcriptional start site. The increased binding of the ETS factors Fli1 and Erg in response to UVB were confirmed by (1) loss of UVB-induced activity of the −120 bp ETS mutant in the −166, −204, and even the −2755 promoter constructs; (2) EMSA analysis demonstrating the specific complexes in the −120 bp region that were supershifted by anti-Erg and anti-Fli antibodies; and (3) ChIP analysis showing increased Erg and Fli1 binding after UVB exposure.

c-Myc plays no role in the UVB inducibility of Id2 since (1) ChIP analysis detects no c-Myc binding in the promoter region (Figure 5); (2) deletion of the E boxes required for Myc family binding did not alter the UVB-inducible response (Figure 3); and (3) c-*myc* RNA levels are decreased following UVB exposure as determined by microarray analysis (Table 1). These results are consistent with those of other investigators who found that Id2 functions in a Myc-independent pathway in the epidermis (Murphy *et al*., 2004).

Primary keratinocytes differ from E6/7 immortalized keratinocytes in that both Rb and p53 pathways are perturbed in the latter, but a direct role for either of these pathways in the induction of the Id2 promoter has not yet been described. The reason for the selective induction of Id2 in primary keratinocytes is thus unclear. Mutation, EMSA, and ChIP analyses demonstrated the importance of Erg1/2 and Fli1 binding to the Id2 minimal promoter in primary keratinocytes. We did not observe an upregulation of Fli1 or Erg1/2 in the microarray, although an increase in Erg1/2 protein was observed following UVB irradiation of primary keratinocytes by immunoblot analysis (Figure 5). Whether UVB-induced levels or post-translational modifications of Erg1/2 and Fli1 proteins lead to upregulation of Id2 remains to be determined. Some modifications known to affect ETS transcription factor activity include phosphorylation, glycosylation, sumoylation, acetylation and ubiquitination (for a review, see Tootle and Rebay, 2005). Erg1/2 has been shown to be a substrate for PKC, but the effect of this phosphorylation was undetermined (Murakami *et al*., 1993). However, many of the other ETS family members are phosphorylated by MAPK, JUNK, PKC, or CAMKII, and these and other transcription factors can alter the activities of Erg1/2 and Fli1 by forming complexes with different activities. For example, Fli1 has been shown to heterodimerize with ETS-member Tel to form an inactive complex (Kwiatkowski *et al*., 1998), while the subcellular localization and activity of the latter is in turn determined by phosphorylation via MAPK (Maki *et al*., 2004).

The cause of the selective upregulation of Id-3 in immortalized keratinocytes is similarly unknown. A previous functional analysis of the mouse Id3 promoter showed that only 180 bp upstream was sufficient for its activity in proliferating C2C12 cells (Yeh and Lim, 2000). We have also observed cell cycle alterations in immortalized cells compared to primary keratinocytes following UVB exposure (Simbulan-Rosenthal *et al*., 2002). Whether Id3 is a cause or effect of these cell cycle alterations remains to be determined, although we have noted that ectopic expression of Id3 induces an apoptotic response in immortalized keratinocytes (Simbulan-Rosenthal *et al*., manuscript in preparation). Yeh and Lim, (2000) utilized the TRANSFAC program (Wingender *et al*., 2000) for sequence comparison between 200 nucleotides immediately upstream of the human and mouse Id3 promoters and noted conserved putative transcription factor binding sites including an ATF site. In our study, we found that ATF3, a stress-inducible transcription factor that can act as a transcriptional activator or repressor depending on its splice form (Chen *et al*., 1994), is only upregulated in immortalized keratinocytes, while transcriptional repressor ATF4 is upregulated in both cell types (Table 1). Most other transcription factors were down-regulated by UVB, including Smad3, which is down-regulated only in immortalized keratinocytes suggesting changes in TGFβ signaling following UVB exposure. It was previously shown that TGFβ-activated Smad3 directly induced *ATF3* expression; ATF3 and Smad3 then formed a complex that directly mediated repression of Id1 and possibly Id2 and Id3 as well, in human epithelial cells (Kang *et al*., 2003). In contrast, Kee *et al*. (2001) showed that TGFβ rapidly induced transient Id3 mRNA and protein expression in mouse B-lymphocyte precursors, via activation of the Smad pathway. We performed a recent TESS/TRANSFAC 4.0 (Wingender, 2004) homology search utilizing the –200 bp promoter region of Id3 and found a partial consensus sequence for Erg1/2 but not for Fli1, thus suggesting a more important role for Fli1 in the selective induction of Id2 but not Id3 in primary keratinocytes. Studies to determine which of these or other putative binding sites and transcription factors may be involved in the regulation of the *Id3* gene are in progress.

The most important etiologic agent for skin cancer is UV. While UVC (<280 nm) is filtered by the ozone layer of the earth's atmosphere, UVB (280–320 nm) and UVA (320–400 nm) penetrate to the surface and cause skin cancer through a series of cellular changes that are not all identified. However, it is clear that in addition to genetic alterations, inappropriate or altered growth, differentiation, and/or apoptotic responses play key roles in this process. Consistent with other studies, we found that both UVB and Id2 inhibit keratinocyte differentiation (Figure 7); our demonstration that Id2 siRNA can partially block the UVB inhibition of differentiation suggests that UVB acts in part via an

Id2-dependent pathway in primary HFK. Overexpression of Id1 has also been shown to result in either immortalization (Alani *et al*., 1999) or extended lifespan (Nickoloff *et al*., 2000) specifically in keratinocytes, while overexpression of Id2 increased lifespan and suppressed differentiation (Alani *et al*., 1999).

Carcinogenesis is a multistep process during which key genes are up- or down-regulated during tumor progression. The type and number of genes involved in human nonmelanoma skin cancer (NMSC) are still unclear (Tsai and Tsao, 2004). The p53, Rb, and Ras pathways are important in BCC, SCC as well as in melanoma. While a study with Id2-knockout mice did not demonstrate a role for Id2 in Myc-mediated skin carcinogenesis (Murphy *et al*., 2004; although curiously, Hacker *et al*. (2003) found that Id2-deficient mice lacked epidermis-specific Langerhans cells), we speculate that it may in fact play a role in the early stages of UVB carcinogenesis. Id2 knockout studies clearly support a role for Id2 in the Rb pathway since in Id2/Rb double knockouts, there is a compensation of Rb−/− defects in neurogenesis and hematopoiesis, as well as a temporary rescue of Rb−/− embryonic lethality (Lasorella *et al*., 2000). The direct role of Rb in turn has been studied in skin tumorigenesis in which Rb−/− mice displayed hyperplasia, hyperkeratosis, and altered differentiation in the skin (Ruiz *et al*., 2004).

With the caveat that alterations of Id genes have not as yet been identified in primary human tumors to currently validate them as true cellular proto-oncogenes, Id proteins have been implicated in regulating a variety of cellular processes that regulate tumorigenesis, including growth, senescence, differentiation, apoptosis, and angiogenesis (for a review, see Sikder *et al*., 2003). In particular, Id2 has been frequently found increased in human neoplasias, including that of Ewing's sarcoma (Nishimori *et al*., 2002; Fukuma *et al*., 2003), colorectal cancer (Wilson *et al*., 2001), astrocytic tumors (Vandeputte *et al*., 2002), pancreatic cancer (Kleeff *et al*., 1998; Maruyama *et al*., 1999), testicular seminomas (Sablitzky *et al*., 1998), and squamous cell cancer (Langlands *et al*., 2000). With respect to Id2 in SCC, while not shown to be mutated, Id2 expression has been shown to be upregulated during tumor development and progression in the epidermis (Langlands *et al*., 2000). The authors found that Id2 staining was nuclear in normal epidermal tissue sections, and the basal layer appeared to show the greatest levels of expression, with downregulation as cells transited to the stratum corneum. Id2 mRNA was also found to be downregulated during differentiation in cultured keratinocytes. In contrast to normal skin, strong Id2 protein immunoreactivity was observed in the majority of malignant keratinocytes in SCC. The increase in proliferative lifespan of keratinocytes induced by ectopic Id2 also supports a role for Id2 in the early stages of cutaneous carcinogenesis (Alani *et al*., 1999). The notion that Id2 may play a role in the early stages of radiation carcinogenesis in the epidermis is also supported by a recent study (Baghdoyan *et al*., 2005) in which the authors found that Id2 was upregulated in keratinocytes by ionizing radiation, and played roles both in inducing proliferation and increasing radioresistance.

Chronic inhibition of differentiation might force cells into increased proliferation beyond their normal capacity, thus increasing the probability of further mutations, including those involving p53, Rb, and hTERT pathways. UV induces specific p53 mutations in both SCC and BCC (Tornaletti *et al*., 1993; Wikonkal and Brash, 1999) as well as in normal sun-exposed skin (Ling *et al*., 2001). Immortalization of primary cells is an important step in carcinogenesis. Unlike most other cell types, keratinocytes require the inactivation of the p16/Rb pathway to achieve immortalization (Kiyono *et al*., 1998; Dickson *et al*., 2000). Similar to other cell types, keratinocytes appear for the most part to require the stable expression of the catalytic subunit of telomerase (hTERT), although immortalization of keratinocytes has also been shown to occur in the absence of telomerase, via an alternative pathway of telomere maintenance (ALT) (Opitz *et al*., 2001). Other groups have also reported alternate mechanisms of maintaining telomere length in other cell types (Perrem *et al*., 1999; Reddel *et al*., 2001; Rizki and Lundblad, 2001; Henson *et al*., 2002). HPV E6 upregulates the gene and promoter of hTERT, at least temporarily (Klingelhutz *et al*., 1996; Veldman *et al*., 2001), while E7 inactivates Rb. However, additional genetic changes are required for immortalization. These other genes may be related to the stable expression of hTERT (Steenbergen *et al*., 2001), since loss of a region of chromosome 6 derepresses telomerase expression in HPV-immortalized cells. Nonrandom allelic losses at 3p, 11p, and 13q have also been observed during HPV-mediated immortalization (Steenbergen *et al*., 1998), while evidence for loss of a senescence locus within the chromosomal region 10p14–p15 has been shown in HFK-expressing HPV 16 E6/7 genes (Poignee *et al*., 2001). We have also observed the amplification of chromosome 20q in HFK immortalized by HPV E6/7 (data to be published elsewhere).

Thus UVB, via Id2, may inactivate the Rb pathway in the short-term promotion phase of carcinogenesis until genetic or epigenetic changes (p16-Ink4a gene mutation or methylation; Brown *et al*., 2004) or cooperation with HPV (E7-mediated inactivation of Rb) lead to the stable inactivation of this pathway. This theme is very similar to that found in keratinocytes expressing HPV-16 or -18 E6 which, in addition to inactivating p53, also upregulates the hTERT promoter (Klingelhutz *et al*., 1996; Veldman *et al*., 2001), prior to the stable upregulation of hTERT due to stable genetic changes, including losses of suppressors on other chromosomes (Steenbergen *et al*., 1998; Poignee *et al*., 2001).

In summary, we have demonstrated that UVB preferentially induces Id2 in primary HFK, but not in immortalized HFK. Thus, upregulation of Id2 by UVB might predispose primary keratinocytes to carcinogenesis by preventing their normal differentiation program, rendering them susceptible to carcinogenesis and may therefore represent an important therapeutic target for intervention.

Materials and methods

Cells, plasmids, and transfection

Primary human keratinocytes (HFK) were derived from neonatal foreskins and grown in KSF medium supplemented with human recombinant EGF and bovine pituitary extract (Gibco BRL). Primary HFK were infected with an amphotropic LXSN (Clontech) retrovirus expressing the HPV-16 E6, and E7 genes. Retrovirus-infected cells were selected in G418 (100 μg/ml) for 10 days, and G418-resistant colonies were pooled from each transduction and passaged every 3–4 days. Cells were transiently transfected at high density with human Id2, or with Id2 promoter reporter constructs, using Lipofectamine 2000 (Life Tech) according to the manufacturer's protocols.

For overexpression of the Id2 protein, expression vectors were constructed under the control of a CMV promoter by inserting the full-length coding regions of Id2 cDNA into pCMSEGFP (Clontech) at the *Xho*I and *Xba*I sites. Correct insertion of the Id2 cDNA in the pCMSEGFP vector was confirmed by digestion with *Xho*1 and *Xba*1 (to yield 500 or 800 bp fragments corresponding to Id2 and Id3 cDNA, respectively), as well as by DNA sequencing. For promoter activity assays, the Id2 reporter gene plasmid (pId-CAT), containing the 5′ flanking region corresponding to -834 to $+30$ in front of the CAT reporter in pId was utilized (Kurabayashi *et al*., 1995). To test the regulatory elements of the Id2 promoter that mediate transcriptional activation, a 2.7 kb Id2 promoter fragment containing three ETS-binding sequences and two E-box sequences with c-Myc binding sites (Id2-2755), along with a series of deletion constructs inserted upstream of the luciferase reporter gene in pGL3 basic vector (Id2-del960, Id2-1329, Id2-166, Id2-100, and Id2-60) were used in reporter assays (Nishimori *et al*., 2002). For more precise localization of the regulatory elements involved in the UVB-inducible response, additional deletion constructs were made, including Id2-120, Id2-204, and Id2-850 and subsequently used in reporter assays together with the other constructs.

Mutagenesis

For mutation analysis, point mutations were introduced in the ETS box (-120) of Id2-166, Id2-204 and Id2-2755; (Nishimori *et al*., 2002) using a site-directed mutagenesis kit (Stratagene). Template-specific mutagenic primers (-127) 5′-GCCCACCA ATGGTACCGCCCGCTCGTCT-3′ (forward) (-100) and 5′-AGACGAGCGGGCGGTACCATTGGTGGGC-3′ (reverse) were utilized to introduce two point mutations A-115 T and G-113C at the ETS box, creating an artificial *Kpn*I site. The presence of the point mutations in the promoter constructs (Id2-166mut, Id2-204mut, and Id2-2755mut) was confirmed by restriction digest and sequencing.

UVB irradiation

Primary and HPV-16 E6/7-immortalized HFK were grown under identical conditions to 70–80% confluency, trypsinized before UVB exposure, and replated at equal cell densities. Cells were allowed to recover and were irradiated with indicated doses with ultraviolet light, using a UVB source with a peak wavelength of 312 nm FS40 sunlamp (Philips) with a Kodacel cutoff filter (Kodak, France) to eliminate UV wavelengths shorter than 290 nm. At indicated time points after UVB irradiation, cells were harvested for further analyses.

Oligonucleotide microarray hybridization

Human keratinocytes were grown under identical conditions to $\sim$60% confluency and irradiated as described above. Total RNA was then isolated from the control and UVB-irradiated cells 4 h after UVB exposure and subjected to reverse transcription. The resulting cDNA was subjected to *in vitro* transcription in the presence of biotinylated nucleoside triphosphates. Biotinylated cRNAs were hybridized to Hu16 K oligonucleotide arrays (Affymetrix, Santa Clara, CA, USA), which contain probes for 16 000 known human genes and expressed sequence tags (ESTs). According to stringent criteria, only those differences in RNA abundance between the control and UVB-treated cells that were reproducible in independent replicates and represented a change of 2.5-fold or greater were considered further.

Reverse transcription–polymerase chain reaction

Unique oligonucleotide primer pairs for Id1, Id2, Id3, and GAPDH mRNA were designed and prepared. Total RNA, purified from cell pellets with Trizol Reagent (Gibco BRL), was subjected to RT–PCR with a Perkin Elmer Gene Amp EZ rTth RNA PCR kit. The reaction mix (50 μl) contained 300 μM each of dGTP, dATP, dTTP, and dCTP, 0.45 μM of each primer, 1 μg of total RNA, and rTth DNA polymerase (5 U). RNA was transcribed at 65°C for 40 min, and DNA was amplified by an initial incubation at 95°C for 2 min, followed by 30 cycles of 95°C for 1 min, 60°C for 1.5 min, and 65°C for 0.5 min, and a final extension at 70°C for 22 min. The PCR products were then separated by electrophoresis in 1.5% agarose gel and visualized by ethidium bromide staining.

Immunoblot analysis

SDS–PAGE and transfer of separated proteins to nitrocellulose membranes were performed according to standard procedures. Membranes were stained with Ponceau S (0.1%) to verify equal loading and transfer of proteins. They were then incubated with antibodies specific to Id1, Id2, Id3, human keratin HK1 (1 : 500; BabCo), involucrin (1 : 200; Sigma), Erg1/2 (1 : 200; Santa Cruz Biotech), or to GAPDH for loading control (1 : 1000; Abcam). Immune complexes were detected by incubation with appropriate horseradish peroxidase–conjugated antibodies to mouse or rabbit IgG (1 : 3000) and enhanced chemiluminescence (Pierce).

Id2 promoter activity assays

For CAT assays, HFK or p27 E6/7-HFK were transiently cotransfected with the pId-CAT reporter gene together with a CMV-luciferase construct, and then induced with UVB. At 24 h after UVB exposure, cell extracts were derived and assayed for chloramphenicol acetyl transferase (CAT) activity by incubating equal volumes of cell extracts and [3H]-acetyl-CoA and chloramphenicol, followed by liquid scintillation spectroscopy. CAT activity was normalized by mg protein in the assays, as well as luciferase activity in the same cell extracts, as monitored with a luciferase assay kit (Promega). The Id2 promoter reporter constructs used subsequently included nine fragments containing parts of the 5′ flanking regions of the Id2 gene subcloned upstream of a luciferase reporter gene in pGL3-basic vector. HFK or immortalized E6/7-HFK were cotransfected with Id2-2755, or with a series of deletion constructs Id2-del980, Id2-1329, Id2-850, Id2-204, Id2-166, Id2-120, Id2-100, and Id2-60 in pGL3, together with a pSV2-CAT control plasmid, and then exposed to UVB. Cells were harvested 24 h after UVB exposure, followed by measurement of luciferase activity as well as CAT activity using a luciferase reporter assay system (Promega). Luciferase activity from the pGL3 reporter constructs was normalized

with CAT activity from the internal control plasmid in the same cell extracts.

ChIP assays

At 4 h after UVB exposure, cells were fixed in 1% formaldehyde, neutralized with glycine, washed, lysed in 1% SDS lysis buffer with protease inhibitors, and then sonicated to generate DNA fragments, as previously described (Veldman *et al*., 2003). After centrifugation, the supernatant was incubated with antibodies to Id2, Fli1, Erg1/2, or c-Myc (5 μg, Santa Cruz Biotech), or a control IgG. Immune complexes were then precipitated, washed extensively, eluted, and the DNA–protein crosslinks were reversed by heating at 65°C overnight. After extraction and purification of DNA from the samples, 5 μl of each sample was used as template for PCR amplification of the Id2 promoter region, using the primers: 5′-TCTAAGGTGTG TAGGGCTTGG-3′ (forward); 5′-TGCTGAGCTAGCTGCG CTT-3' (reverse).

Electrophoretic mobility-shift assay

Nuclear extracts were obtained from cells according to standard protocols, using the NE-PER nuclear and cytoplasmic extraction reagent (Pierce). EMSA analysis was performed at RT using the Lightshift Chemiluminescent EMSA kit (Pierce) according to the manufacturer's specifications. Biotinylated oligonucleotide probes containing the ETS consensus binding sequences were designed, purchased from Invitrogen, and used in EMSA assays. Cell extracts (10 μg of protein) were preincubated with excess poly(dI:dC) (1 μg) in DNA binding buffer (Pierce), 2.5% glycerol, 5 mM MgCl2, 0.05% NP40, in the presence or absence of appropriate antibodies (1 μg; anti-Erg1/2, anti-Fli1) for 20 min. The binding reactions (20 μl) were then incubated for 5 min with excess nonbiotinylated probes (4 pmol/ reaction; for competition assays) and an additional 20 min with biotinylated probes (40 fmol/binding reaction). The DNA–protein complexes were then analysed by electrophoresis on native 5% polyacrylamide gels in Tris-borate-EDTA buffer, followed by electrophoretic transfer of binding reactions to nylon membranes at 380 mA for 30 min, UV crosslinking of the DNA to the membrane, and detection of biotin-labeled DNA by chemiluminescence.

Flow cytometry and apoptosis assays

For apoptosis assays, floating and attached cells were harvested at indicated times after UV exposure, and stained with Annexin V-PE (Biovision) and 7-Actinomycin D (7AAD; Sigma) according to the manufacturer's specifications. Flow cytometric analysis on cells gated for GFP-positive fluorescence was then performed on a Becton-Dickinson FACStar Plus flow cytometer equipped with a 100 mW air-cooled argon laser.

siRNA construction and transfection

siRNA was synthesized according to protocols for the Silencer siRNA Construction Kit (Ambion Inc.). The following sequences for Id2 were used for the sense and antisense templates, respectively:

5′-AACAGGATGCTGATATCCGTGCCTGTCTC-3′ and 5′AACACGGATATCAGCATCCTGCCTGTCTC-3′.

Primary keratinocytes were transfected for 4 h with the synthesized Id2 siRNA or a scrambled control siRNA (140 μg/ 10 cm plate) using oligofectamine (Invitrogen). Cells were then incubated for 48 h, cells were then derived and subjected to immunoblot analysis with antibodies to differentiation markers.

Abbreviations

Id, inhibitor of differentiation/DNA binding; HFK, human foreskin keratinocytes; UVB, ultraviolet B; HPV, human papillomavirus.

Acknowledgements

We thank Danith Ly (Carnegie Mellon University) and Xuefeng Liu (Pathology Deptartment, Georgetown University) for help with the DNA microarray analysis and with the ChIP assay, respectively. This work was supported in part by the National Cancer Institute Grant 5RO1 CA100443-02 and the US Army Medical Research and Materiel Command contract DAMD17-00-C-0026 (to DSR).

References

Akazawa C, Sasai Y, Nakanishi S and Kageyama R. (1992). *J. Biol. Chem.*, **267,** 21879–21885.

Alani RM, Hasskarl J, Grace M, Hernandez MC, Israel MA and Munger K. (1999). *Proc. Natl. Acad. Sci. USA*, **96,** 9637–9641.

Armstrong BK and Kricker A. (2001). *J. Photochem. Photobiol. B*, **63,** 8–18.

Atchley WR and Fitch WM. (1997). *Proc. Natl. Acad. Sci. USA*, **94,** 5172–5176.

Baghdoyan S, Lamartine J, Castel D, Pitaval A, Roupioz Y, Franco N, Duarte M, Martin MT and Gidrol X. (2005). *J. Biol. Chem.*, **3,** 3.

Barone MV, Pepperkok R, Peverali FA and Philipson L. (1994). *Proc. Natl. Acad. Sci. USA*, **91,** 4985–4988.

Bernerd F and Asselineau D. (1997). *Dev. Biol.*, **183,** 123–138.

Bouwes Bavinck JN, Stark S, Petridis AK, Marugg ME, Ter Schegget J, Westendorp RG, Fuchs PG, Vermeer BJ and Pfister H. (2000). *Br. J. Dermatol.*, **142,** 103–109.

Brellier F, Marionnet C, Chevallier-Lagente O, Toftgard R, Mauviel A, Sarasin A and Magnaldo T. (2004). *Cancer Res.*, **64,** 2699–2704.

Brennan TJ and Olson EN. (1990). *Genes Dev.*, **4,** 582–595.

Brown L and Baer R. (1994). *Mol. Cell. Biol.*, **14,** 1245–1255.

Brown VL, Harwood CA, Crook T, Cronin JG, Kelsell DP and Proby CM. (2004). *J. Invest. Dermatol.*, **122,** 1284–1292.

Chakraborty T, Brennan T and Olson E. (1991a). *J. Biol. Chem.*, **266,** 2878–2882.

Chakraborty T, Brennan TJ, Li L, Edmondson D and Olson EN. (1991b). *Mol. Cell. Biol.*, **11,** 3633–3641.

Chen BP, Liang G, Whelan J and Hai T. (1994). *J. Biol. Chem.*, **269,** 15819–15826.

Chiaramello A, Neuman K, Palm K, Metsis M and Neuman T. (1995). *Mol. Cell. Biol.*, **15,** 6036–6044.

Cleaver JE and Crowley E. (2002). *Front. Biosci.*, **7,** d1024–d1043.

Dazard JE, Gal H, Amariglio N, Rechavi G, Domany E and Givol D. (2003). *Oncogene*, **22,** 2993–3006.

de Gruijl F, van Kranen HJ and Mullenders LH. (2001). *J. Photochem. Photobiol. B*, **63,** 19–27.

Del Bino S, Vioux C, Rossio-Pasquier P, Jomard A, Demarchez M, Asselineau D and Bernerd F. (2004). *Br. J. Dermatol.*, **150,** 658–667.

D'Errico M, Teson M, Calcagnile A, Corona R, Didona B, Meschini R, Zambruno G and Dogliotti E. (2004). *Br. J. Dermatol.*, **150,** 47–55.
Dickson MA, Hahn WC, Ino Y, Ronfard V, Wu JY, Weinberg RA, Louis DN, Li FP and Rheinwald JG. (2000). *Mol. Cell. Biol.*, **20,** 1436–1447.
Eliezri YD, Silverstein SJ and Nuovo GJ. (1990). *J. Am. Acad. Dermatol.*, **23,** 836–842.
Ezura Y, Tournay O, Nifuji A and Noda M. (1997). *J. Biol. Chem.*, **272,** 29865–29872.
French BA, Chow KL, Olson EN and Schwartz RJ. (1991). *Mol. Cell. Biol.*, **11,** 2439–2450.
Fukuma M, Okita H, Hata J and Umezawa A. (2003). *Oncogene*, **22,** 1–9.
Guerin-Reverchon I, Chardonnet Y, Viac J, Chouvet B, Chignol MC and Thivolet J. (1990). *J. Cancer Res. Clin. Oncol.*, **116,** 295–300.
Hacker C, Kirsch RD, Ju XS, Hieronymus T, Gust TC, Kuhl C, Jorgas T, Kurz SM, Rose-John S, Yokota Y and Zenke M. (2003). *Nat Immunol*, **4,** 380–386.
Henson JD, Neumann AA, Yeager TR and Reddel RR. (2002). *Oncogene*, **21,** 598–610.
Hsu HL, Cheng JT, Chen Q and Baer R. (1991). *Mol. Cell. Biol.*, **11,** 3037–3042.
Iavarone A, Garg P, Lasorella A, Hsu J and Israel MA. (1994). *Genes Dev.*, **8,** 1270–1284.
Jonason AS, Kunala S, Price GJ, Restifo RJ, Spinelli HM, Persing JA, Leffell DJ, Tarone RE and Brash DE. (1996). *Proc. Natl. Acad. Sci. USA*, **93,** 14025–14029.
Kang Y, Chen CR and Massague J. (2003). *Mol. Cell*, **11,** 915–926.
Karen J, Wang Y, Javaherian A, Vaccariello M, Fusenig NE and Garlick JA. (1999). *Cancer Res.*, **59,** 474–481.
Kawaguchi N, DeLuca HF and Noda M. (1992). *Proc. Natl. Acad. Sci. USA*, **89,** 4569–4572.
Kee BL, Rivera RR and Murre C. (2001). *Nat. Immunol.*, **2,** 242–247.
Kettler AH, Rutledge M, Tschen JA and Buffone G. (1990). *Arch. Dermatol.*, **126,** 777–781.
Kiyono T, Foster SA, Koop JI, McDougall JK, Galloway DA and Klingelhutz AJ. (1998). *Nature*, **396,** 84–88.
Kleeff J, Ishiwata T, Friess H, Buchler MW, Israel MA and Korc M. (1998). *Cancer Res.*, **58,** 3769–3772.
Klingelhutz AJ, Foster SA and McDougall JK. (1996). *Nature*, **380,** 79–82.
Kurabayashi M, Jeyaseelan R and Kedes L. (1995). *Gene*, **156,** 311–312.
Kwiatkowski BA, Bastian LS, Bauer Jr TR, Tsai S, Zielinska-Kwiatkowska AG and Hickstein DD. (1998). *J. Biol. Chem.*, **273,** 17525–17530.
Langlands K, Down GA and Kealey T. (2000). *Cancer Res.*, **60,** 5929–5933.
Lasorella A, Iavarone A and Israel MA. (1996). *Mol. Cell. Biol.*, **16,** 2570–2578.
Lasorella A, Noseda M, Beyna M, Yokota Y and Iavarone A. (2000). *Nature*, **407,** 592–598.
Lassar AB, Davis RL, Wright WE, Kadesch T, Murre C, Voronova A, Baltimore D and Weintraub H. (1991). *Cell*, **66,** 305–315.
Ling G, Persson A, Berne B, Uhlen M, Lundeberg J and Ponten F. (2001). *Am. J. Pathol.*, **159,** 1247–1253.
Liu J, Shi W and Warburton D. (2000). *Biochem. Biophys. Res. Commun.*, **273,** 1042–1047.
Maki K, Arai H, Waga K, Sasaki K, Nakamura F, Imai Y, Kurokawa M, Hirai H and Mitani K. (2004). *Mol. Cell. Biol.*, **24,** 3227–3237.
Mammone T, Gan D, Collins D, Lockshin RA, Marenus K and Maes D. (2000). *Cell Biol. Toxicol.*, **16,** 293–302.
Maruyama H, Kleeff J, Wildi S, Friess H, Buchler MW, Israel MA and Korc M. (1999). *Am. J. Pathol.*, **155,** 815–822.
Murakami K, Mavrothalassitis G, Bhat NK, Fisher RJ and Papas TS. (1993). *Oncogene*, **8,** 1559–1566.
Murphy DJ, Swigart LB, Israel MA and Evan GI. (2004). *Mol. Cell. Biol.*, **24,** 2083–2090.
Murre C, McCaw PS and Baltimore D. (1989a). *Cell*, **56,** 777–783.
Murre C, McCaw PS, Vaessin H, Caudy M, Jan LY, Jan YN, Cabrera CV, Buskin JN, Hauschka SD, Lassar AB, Weintraub H and Baltimore D. (1989b). *Cell*, **58,** 537–544.
Nickoloff BJ, Chaturvedi V, Bacon P, Qin JZ, Denning MF and Diaz MO. (2000). *J. Biol. Chem.*, **275,** 27501–27504.
Nishimori H, Sasaki Y, Yoshida K, Irifune H, Zembutsu H, Tanaka T, Aoyama T, T, Kawaguchi S, Wada T, Hata J, Toguchida J, Nakamura Y and Tokino T. (2002). *Oncogene*, **21,** 8302–8309.
Norton JD. (2000). *J. Cell Sci.*, **113,** 3897–3905.
Ohtani N, Zebedee Z, Huot TJ, Stinson JA, Sugimoto M, Ohashi Y, Sharrocks AD, Peters G and Hara E. (2001). *Nature*, **409,** 1067–1070.
Opitz OG, Suliman Y, Hahn WC, Harada H, Blum HE and Rustgi AK. (2001). *J. Clin. Invest.*, **108,** 725–732.
Perrem K, Bryan TM, Englezou A, Hackl T, Moy EL and Reddel RR. (1999). *Oncogene*, **18,** 3383–3390.
Poignee M, Backsch C, Beer K, Jansen L, Wagenbach N, Stanbridge EJ, Kirchmayr R, Schneider A and Durst M. (2001). *Cancer Res.*, **61,** 7118–7121.
Quertermous EE, Hidai H, Blanar MA and Quertermous T. (1994). *Proc. Natl. Acad. Sci. USA*, **91,** 7066–7070.
Reddel RR, Bryan TM, Colgin LM, Perrem KT and Yeager TR. (2001). *Radiat. Res.*, **155,** 194–200.
Rizki A and Lundblad V. (2001). *Nature*, **411,** 713–716.
Ruiz S, Santos M, Segrelles C, Leis H, Jorcano JL, Berns A, Paramio JM and Vooijs M. (2004). *Development*, **131,** 2737–2748.
Rundhaug JE, Hawkins KA, Pavone A, Gaddis S, Kil H, Klein RD, Berton TR, McCauley E, Johnson DG, Lubet RA, Fischer SM and Aldaz CM. (2005). *Mol. Carcinog.*, **42,** 40–52.
Sablitzky F, Moore A, Bromley M, Deed RW, Newton JS and Norton JD. (1998). *Cell Growth Differ.*, **9,** 1015–1024.
Shamanin V, zur Hausen H, Lavergne D, Proby CM, Leigh IM, Neumann C, Hamm H, Goos M, Haustein UF, Jung EG, Plewig G, Wolff H and de Villiers EM. (1996). *J. Natl. Cancer Inst.*, **88,** 802–811.
Sharrocks A, Brown A, Ling Y and Yates PR. (1997). *Int. J. Biochem. Cell Biol.*, **29,** 1371–1387.
Sikder HA, Devlin MK, Dunlap S, Ryu B and Alani RM. (2003). *Cancer Cell*, **3,** 525–530.
Simbulan-Rosenthal CM, Velena A, Veldman T, Schlegel R and Rosenthal DS. (2002). *J. Biol. Chem.*, **277,** 24709–24716.
Steenbergen RD, Hermsen MA, Walboomers JM, Meijer GA, Baak JP, Meijer CJ and Snijders PJ. (1998). *Int. J. Cancer*, **76,** 412–417.
Steenbergen RD, Kramer D, Meijer CJ, Walboomers JM, Trott DA, Cuthbert AP, Newbold RF, Overkamp WJ, Zdzienicka MZ and Snijders PJ. (2001). *J. Natl. Cancer Inst.*, **93,** 865–872.
Stratton SP. (2001). *Curr. Oncol. Rep.*, **3,** 295–300.
Takao J, Ariizumi K, Dougherty II and Cruz Jr PD. (2002). *Photodermatol. Photoimmunol. Photomed.*, **18,** 5–13.
Tootle TL and Rebay I. (2005). *Bioessays*, **27,** 285–298.

Tornaletti S, Rozek D and Pfeifer GP. (1993). *Oncogene*, **3,** 2051–2057.

Tsai KY and Tsao H. (2004). *Am. J. Med. Genet.*, **131C,** 82–92.

Vandeputte DA, Troost D, Leenstra S, Ijlst-Keizers H, Ramkema M, Bosch DA, Baas F, Das NK and Aronica E. (2002). *Glia*, **38,** 329–338.

Veldman T, Horikawa I, Barrett JC and Schlegel R. (2001). *J. Virol.*, **75,** 4467–4472.

Veldman T, Liu X, Yuan H and Schlegel R. (2003). *Proc. Natl. Acad. Sci. USA*, **100,** 8211–8216.

Wikonkal NM and Brash DE. (1999). *J. Investig. Dermatol. Symp. Proc.*, **4,** 6–10.

Wilson JW, Deed RW, Inoue T, Balzi M, Becciolini A, Faraoni P, Potten CS and Norton JD. (2001). *Cancer Res.*, **61,** 8803–8810.

Wingender E. (2004). *In Silico Biol.*, **4,** 55–61; Epub 2004, Mar 16.

Wingender E, Chen X, Hehl R, Karas H, Liebich I, Matys V, Meinhardt T, Pruss M, Reuter I and Schacherer F. (2000). *Nucleic Acids Res.*, **28,** 316–319.

Xiao X, Athanasiou M, Sidorov IA, Horikawa I, Cremona G, Blair D, Barret JC and Dimitrov DS. (2003). *Exp. Mol. Pathol.*, **75,** 238–247.

Yeh K and Lim RW. (2000). *Gene*, **254,** 163–171.

zur Hausen H. (1996). *Biochim. Biophys. Acta.*, **1288,** F55–F78.

Experimental Dermatology 2005: 00: 1–12
Blackwell Munksgaard . Printed in Singapore

Experimental Dermatology
ISSN 0906-6705

Apoptosis induced by ultraviolet B in HPV-immortalized human keratinocytes requires caspase-9 and is death receptor independent

Daher A, Simbulan-Rosenthal CM, Rosenthal DS. Apoptosis induced by ultraviolet B in HPV-immortalized human keratinocytes requires caspase-9 and is death receptor independent.
Exp Dermatol 2005: 00: 1–12. © The Authors 2005. Journal compilation © 2005 Blackwell Munksgaard

Abstract: Ultraviolet B (UVB) induces both apoptosis and skin cancer. We found that human keratinocytes (KC) immortalized by HPV16 E6/E7 were sensitized to UVB-induced apoptosis, possibly representing a transient regression-prone precancerous stage equivalent to actinic keratosis. To further examine which caspases are apical and essential, we utilized retroviral constructs expressing dominant-negative caspase-9 (caspase-9-DN) or Fas-associated protein with death domain (FADD)-DN as well as caspase inhibitor peptides. Caspase-9-DN and zLEHD-fmk both suppressed caspase-9, -3, and -8 activity after UVB exposure, as well as proteolytic processing of procaspase-3 into its active form, DNA fragmentation factor 45 cleavage, and internucleosomal DNA fragmentation. By contrast, stable expression of FADD-DN in HPV-immortalized KC did not inhibit UVB-induced activation of caspases-9, -3, and -8 nor downstream apoptotic events, although inhibition of caspase-8 with zIETD-fmk attenuated apoptosis. This study indicates that caspase-9 activation is upstream of caspases-3 and -8 and that UVB-induced apoptosis in HPV-immortalized human KC is death receptor (DR) independent and requires both caspase-9 upstream and caspase-8 downstream for maximal apoptosis. These studies further indicate that cell type as well as transformation state determine the sensitivity and mode of cell death (DR vs. mitochondrial apoptotic pathways) in response to UVB and explain the high regression rates of premalignant lesions.

Ahmad Daher, Cynthia M. Simbulan-Rosenthal and Dean S. Rosenthal

Department of Biochemistry and Molecular Biology, Georgetown University School of Medicine, Washington, DC, USA

Key words: apoptosis – caspase – death receptor – FADD – HPV – immortalization – keratinocyte – mitochondria – skin

Dean S. Rosenthal
Department of Biochemistry and Molecular Biology
Georgetown University School of Medicine
3900 Reservoir Road, NW
Washington, DC 20007
USA
Tel.: +1 202 687 1056
Fax: +1 202 687 4632
e-mail: rosenthd@georgetown.edu

Accepted for publication 7 October 2005

Introduction

Nonmelanoma skin cancer, the most common of human malignancies, is caused primarily by chronic exposure to solar ultraviolet B (UVB) radiation (280–320 nm) through a series of cellular changes that are not all identified (1,2). While the process of photocarcinogenesis is still not fully characterized at the molecular level, genetic alterations, inappropriate or altered differentiation, and apoptosis have been shown to play key roles in this process. Others and we have shown that UVB irradiation induces apoptosis and altered differentiation in primary human keratinocyte (KC) (3–7). This is a potential mechanism for tumor promotion and progression, which allows the preferential clonal expansion of mutant cells, as normal KCs have been shown to block progression of malignant cells (8), while UVB appears to selectively induce

Abbreviations: BCC, basal cell carcinoma; DISC, death-inducing signaling complex; DN, dominant-negative; DR, death receptor; FADD, Fas-associated protein with death domain; KC, keratinocytes; LHCX, Retroviral expression vector carrying hygromycin resistance; SBC, sunburn cells; SCC, squamous cell carcinoma; TBE, Tris-Borate-EDTA; TNFR, tumor necrosis factor receptor; TRAIL, tumor necrosis factor-related apoptosis-inducing ligand; UVB, ultraviolet B.

apoptosis in normal KC, allowing the malignant population to expand (9). UVB exposure of KC, human skin, or human skin equivalents reconstructed *in vitro* induces DNA damage and apoptotic KC or "sunburn" cells (SBCs) (10,11), reviewed in (12), which ensures elimination of UV-damaged cells that potentially could become tumorigenic. Conversely, apoptosis of initiated cells would lead to tumor regression, as occurs in the majority of actinic keratoses (13). As dysregulation of UVB-induced apoptotic pathways and disruption of the balance between survival and apoptogenic factors in the mitochondrial death pathway leads to development of skin malignancies, a better understanding of this UVB response in initiated immortalized cells is crucial to the development of effective therapeutic strategies to control skin photocarcinogenesis.

Two main signaling pathways have been proposed to contribute to UV-induced apoptosis in KC, an extrinsic death receptor (DR)-mediated pathway and an intrinsic mitochondrial pathway; the two are not necessarily mutually exclusive and cross-talk may occur between them as a mechanism of amplification. The first signaling pathway is initiated by clustering and activation of the membrane DR, formation of a death-inducing signaling complex (DISC) containing the adaptor protein Fas-associated protein with death domain (FADD), which recruits and leads to autocatalytic activation of initiator procaspase-8; caspase-8 then cleaves and activates effector caspases-3 and -7.

The potential role for DR, including Fas, tumor necrosis factor receptor 1 (TNFR1), and tumor necrosis factor-related apoptosis-inducing ligand (TRAIL) receptors, as well as DR ligand mediation of UVB apoptosis in KC has been reviewed (14). UVB may induce clustering of TNFR1, sensitizing KC to DR-mediated apoptosis (15). A potential role for TNF-a was demonstrated in intact animals; subcutaneous injection of a TNF-α neutralizing antibody after UVB exposure reduced numbers of SBC significantly (but not completely (16). Using knockout animals, TNFR1 was shown to play a role in mediating the apoptotic response of mouse KC to UVB-induced apoptosis; the importance of the ligand–DR interaction was further demonstrated by showing that TNF-α neutralizing antibodies reduced the level of apoptosis of wild-type KC to that of the TNFR1 knockout cells (17).

Fas has also been suggested to play a role in mediating the apoptotic response of KC to UV. Exposure of HaCaT KC to UVA or UVB induces Fas upregulation (18). UV irradiation induced both Fas and FasL expression in KC, and FasL neutralizing antibody significantly reduced the apoptotic response to UV (19). The role of Fas–FasL interaction was also indicated using FasL (*gld*/*gld*) knockout animals (20); FasL-deficient mice had significant reduction in SBC cell formation and a 14-fold higher incidence of p53 mutation accumulation in the epidermis. The importance of DR clustering and recruitment of FADD was shown to mediate UV apoptosis of HaCaT KC (21). As Fas-neutralizing antibodies were unable to block this effect, it was suggested that UV light directly induces clustering of DR and the activation of the apoptotic cascade. The role of UVB in sensitizing cells to TRAIL signaling has also been demonstrated (22).

TRAIL is also expressed in intact human skin (23), and several studies have shown that *in vivo* UVB irradiation induces upregulation and clustering of DR (24,25). Bang et al. (25) showed that UVB-irradiated normal human volunteers demonstrated cutaneous clustering of Fas within 30 min of irradiation and recruitment of FADD; TUNEL staining was only observed in Fas-positive cells. Other investigators have also shown a direct upregulation of FADD itself by UV with a corresponding increase in caspase-8 cleavage and apoptosis (26). Furthermore, adenoviral expression of antisense FADD reduced KC apoptosis. Consistent with the importance of FADD, Wu et al. (27) found that overexpression of a dominant-negative (DN) mutant of FADD inhibited UV-induced apoptosis of human embryonic kidney 293 epithelial cells.

The mitochondrial pathway of apoptosis induced by UVB occurs primarily, although not solely, as the result of DNA-damaging effects of radiation (28). In exposed areas of human skin, UVB radiation induces cyclobutane pyrimidine dimers, 6-4 photoproducts, and cytosine photohydrates in DNA, as well as DNA strand breaks and DNA cross-links (29,30). DNA damage signaling to the mitochondria in some cases subsequently results in the release of cytochrome c and other apoptogenic factors (e.g. Smac/Diablo), which, together with Apaf-1 and ATP/dATP, triggers formation of the apoptosome and procaspase-9 activation; caspase-9 then cleaves and activates effector caspases-3 and -7, orchestrating downstream apoptotic events. The "commitment" to the release of proapoptotic factors from the mitochondria depends primarily on the balance between proapoptotic and antiapoptotic members of the Bcl2 family of proteins; Bcl2 and BclxL stabilize mitochondrial integrity, while Bax

and Bak destabilize this organelle. Bax has been shown to be induced and inserts into the mitochondrial outer membrane following UVB irradiation (31). Conversely, Bcl2 overexpression in HaCaT KC blocks the effects of UVB-induced Bax activation, cytochrome c release, and apoptosis, suggesting that the DR pathway does not play a dominant role in this response in this system (32). UVB-induced DNA damage can upregulate Bax via p53-dependent or p53-independent pathways. For example, UVB induces ATR-mediated phosphorylation and stabilization of p53, which in turn can induce Bax (33), while UVB can also induce p38MAPK Bax activation in the absence of p53 (34). Thus, both normal and p53-mutated initiated cells can be induced to undergo apoptosis, and the latter may be one mechanism for the elimination of mutated cells (34).

We have shown that UVB activates caspase-8 prior to caspase-9 in primary human KC, while in KC immortalized with HPV E6/7, caspase-9 is much more rapidly activated as a result of Bcl2 downregulation and proposed that resistance to apoptosis occurs at a subsequent stage (6), reminiscent of conversion of regression-prone actinic keratoses to squamous cell carcinoma (SCC) by the upregulation of survivin (35). There is abundant experimental support for the idea that tumors evade apoptosis by acquiring inactivating mutations in proapoptotic genes (36) or expressing inhibitor of apoptosis (IAP) proteins such as survivin (37). The endogenous constitutive activation of Akt found in some cell lines derived from SCC has been shown to block UVB-induced apoptosis, indicating that a deregulated Akt pathway also can play a role in tumor progression during photocarcinogenesis (38).

In the present study, we further delineated the molecular events that follow UVB irradiation in immortalized KC. To clarify whether both apical caspases-8 and -9 were necessary for UVB-induced apoptosis, we pursued a specific DN approach. Retroviral constructs were utilized expressing a FADD-DN mutant to block the Fas/TNF/TRAIL DR pathway or a caspase-9-DN. Stable expression of FADD-DN in immortalized KC failed to inhibit UVB-induced activation of caspases-9, -3, and -8, and downstream apoptotic events, while inhibition of caspase-8 with zIETD-fmk blocked apoptosis. Caspase-9-DN and zLEHD-fmk both significantly suppressed caspases-9, -3, and -8 activity after UVB exposure, as well as proteolytic processing of procaspase-3 into its active form. Furthermore, UVB-induced internucleosomal DNA fragmentation and caspase-3-mediated DNA fragmentation factor (DFF) 45 cleavage was observed in UVB-treated control retroviral expression vector carrying hygromycin resistance (LHCX) KC but not in caspase-9-DN cells.

The results presented in this study identify a critical role for caspase-9 activation in the cellular response of immortalized KC to UVB-induced DNA damage. The execution of UVB-induced apoptosis requires a mitochondrial-driven pathway that depends on caspase-9 activation upstream of caspases-3 and -8 and that UVB-induced apoptosis in HPV-immortalized human KC is DR independent but requires both caspase-9 upstream and caspase-8 downstream, perhaps as part of an amplification mechanism.

Materials and methods

Cells

Primary KC were derived from neonatal human foreskins and grown in KSF medium supplemented with human recombinant EGF and bovine pituitary extract (Life Technologies Inc., Rockville, MD, USA). The primary cells were infected with an amphotropic LXSN retrovirus expressing the HPV-16 open-reading frame of E6 plus E7 genes. Retrovirus-infected cells were selected in G418 (100 μg/ml) for 10 days, and G418-resistant colonies were pooled from each transduction and passaged every 3–4 days. Primary and HPV16 E6/7-immortalized p30 human KC were grown under identical conditions to 70–80% confluency and passaged 1:4 at equal cell densities.

Plasmids and recombinant viruses; infection of KC with retroviral constructs

Replication-deficient recombinant retrovirus constructs were cloned and utilized in this study. These retrovirus constructs expressing constitutively active FADD-DN mutant lacking the N-terminal death effector domain (FADD-DN) and caspase-9-DN were constructed by subcloning the cDNA for these genes into the retroviral vector pLHCX. These retroviral constructs, as well as empty vector pLHCX, were then packaged and propagated in the amphotropic producer cell line ϕNX by transfection with 25 μg of the retroviral constructs using Lipofectamine 2000 (Life Technologies Inc.); viral supernatants were derived, filtered, and used to infect immortalized KC in 100-mm plates in the presence of polybrene (10 μg/ml) for 4 h. Retrovirus-infected cells were selected in hygromycin (10 μg/ml) for 10 days, and hygromycin-resistant colonies were pooled from each transduction and passaged every 4 days. Immunoblot analysis was performed on expanded pooled cells to confirm FADD-DN and caspase-9-DN expression.

UVB irradiation

KC were grown under identical conditions to 70–80% confluency and replated at equal cell densities before UVB exposure. Cells were allowed to recover and were irradiated with indicated doses with UV light, using a UVB source with a peak wavelength of 312 nm (FS40 sunlamp (Philips)] with a Kodacel cutoff filter (Kodak, France) to eliminate UV wavelengths

shorter than 290 nm. Irradiation intensity was monitored by IL1400A radiometer/photometer. The doses used were selected to be within the physiological range of UV exposure of human skin, representing about three times the minimal erythema dose equivalent to moderate sunburn. In selected experiments, cells were pretreated with peptide inhibitors for caspases-3, -8, or -9 (z-DEVD-fmk, z-IETD-fmk, z-LEHD-fmk, respectively; BD 9 Biosciences) 30 min prior to exposure to UVB. Peptides are *O*-methylated at the P1 position of aspartic acid for enhanced stability and increased cell permeability. At indicated time points after UVB irradiation, cells were harvested for further analyses.

Fluorometric assay of caspase activity

Cytosolic extracts were derived from pooled floating and attached cells and subjected to fluorometric caspase-3 activity assays using fluorescent tetrapeptide substrate specific for cas- 10 pase-3 [Ac-DEVD-aminomethylcoumarin (AMC), BioMol] as previously described (6). For the fluorometric caspases-8 and -9 activity assays, the tetrapeptide substrates specific for caspases-8 and -9 (Ac-IETD-AMC and Ac-LEHD-AMC, respectively; BioMol) were utilized in essentially the same reaction assay conditions as for caspase 3. Free AMC, generated as a result of cleavage of the aspartate–AMC bond, was monitored over 11 30 min with a Wallac Victor^{3}V fluorometer (Perkin Elmer) at excitation and emission wavelengths of 360 and 460 nm, respectively. The emission from each sample was plotted against time, and linear regression analysis of the initial velocity (slope) for each curve yielded the activity.

Immunoblot analysis

SDS-PAGE and transfer of separated proteins to nitrocellulose membranes were performed according to standard procedures. Membranes were stained with Ponceau S (0.1%) to verify equal loading and transfer of proteins. They were then incubated with antibodies to procaspase-3 (1:1000; BioMol) and the p17 subunit of caspase-3 (1:100; Cell Signaling), to DFF45 (1:500; BD 12 13 14 PharMingen), to caspase-9 (1:1000; Calbiochem), or to FADD (1:500; Calbiochem). Immune complexes were detected by subsequent incubation with appropriate horseradish peroxidase-conjugated antibodies to mouse or rabbit immunoglobulin G (1:3000) and enhanced chemiluminescence (Pierce, Rockford, IL, USA).

Analysis of DNA fragmentation

Cells were harvested and lysed in 0.5 ml of 7 M guanidine hydrochloride. The lysate was mixed with 1 ml of Wizard Miniprep resin (Promega, Madison, WI, USA), incubated at room temperature for 15 min with occasional mixing, and then centrifuged. The resulting pellet was resuspended in 2 ml of washing solution [90 mM NaCl, 9 mM Tris–HCl (pH 7.4), 2.25 mM EDTA, 55% (v/v) ethanol)], drawn by vacuum through a Wizard Minicolumn (Promega) mounted onto a vacuum manifold, washed twice with 4 ml of washing solution, and dried by centrifugation. DNA was eluted from the column with deionized H_2O, and residual RNA was removed in the eluate by incubation with 10 µg of RNase A at 37°C for 30 min. DNA samples were then loaded onto a 1.5% agarose gel in Tris-Borate-EDTA buffer and subjected to electrophoresis at 4 V/cm. DNA ladders were visualized by staining with ethidium bromide (0.5 µg/ml), and images were captured with the Kodak EDAS 120 (Kodak) gel documentation system.

Statistical analysis

For caspase activity assays, data derived from three experiments were compared using two-way ANOVA tests with Bonferroni post-tests for significance. P values of <0.05 were considered statistically significant. The results are representative of at least three independent experiments with reproducible results.

Results

Expression of a DN form of caspase-9 attenuates UVB-induced apoptosis in HPV-immortalized KC

We investigated whether the initiator caspase for the mitochondrial pathway, caspase-9, is indispensable for UVB-induced apoptosis by cloning and utilizing retroviral constructs constitutively expressing a caspase-9-DN. The DN form of caspase-9 was designed by making a point mutation in a critical position in the active site of the catalytic domain of caspase-9. Because the CARD domain of caspase-9 is present, replacing cysteine 287 (QACGG) by a serine (QASGG) and producing the mutant form DN9-C287S allows binding between caspase-9, Apaf1, and cytochrome c but suppresses caspase-9 processing by forming an inactive apoptosome (39,40). Overexpression of this DN caspase-9 mutant titers the endogenous caspase-9, thus, blocking the mitochondrial pathway in apoptotic cells. Immunoblot analysis with antibodies specific to caspase-9 confirms the increased expression of the mutant form DN9-C287S, which is the same size as caspase-9, in caspase 9-DN cells (Fig. 2a). Whereas control LHCX cells had no significant effect on the activation of caspases-9 or -3 in response to UVB, stable expression of this DN form of caspase-9 completely abrogated this UVB response (Fig. 1a,b). Caspase-3 activation, therefore, occurs downstream of caspase-9 and is dependent on caspase-9 activation. The effects of caspase-9-DN on caspase 3-mediated cleavage of DFF45 were also assessed. Immunoblot analysis with antibodies to the intact form of DFF45 revealed caspase-3-mediated cleavage of DFF45, as shown by the disappearance of the intact form, in control LHCX cells after UVB exposure (Fig. 2b). By contrast, this proteolytic cleavage 15 of DFF45 was completely suppressed in UVB-irradiated cells stably expressing caspase-9-DN. To further analyze the effect of caspase-9-DN on the proteolytic activation of caspase-3, immunoblot analysis of extracts from LHCX or caspase-9-DN cells exposed to UVB was performed using an antibody specific for the p17 subunit of caspase-3. In UVB-irradiated LHCX cells, caspase-3 is proteolytically processed to its active

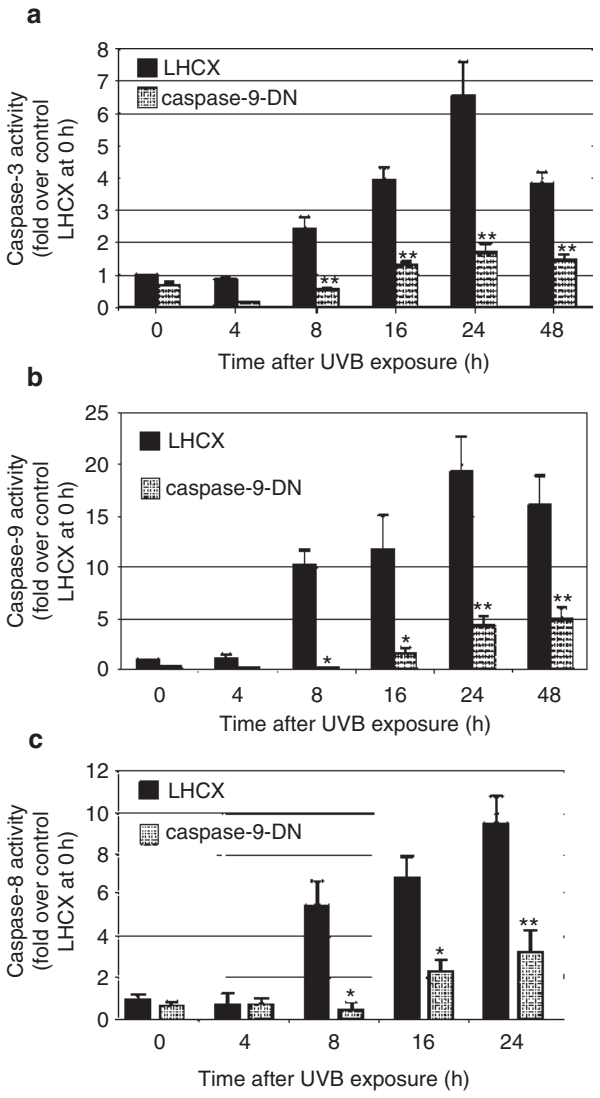

Figure 1. Stable expression of dominant-negative caspase-9 (caspase-9-DN) blocks ultraviolet (UV) B-induced activation of caspases-3 and -9 in HPV-immortalized keratinocyte (KC). Retroviral constructs constitutively expressing caspase-9-DN were cloned in pLHCX and used to infect HPV16 E6/7-immortalized KC; retrovirus-infected cells were selected in hygromycin as described in *Materials and methods*. Control retroviral expression vector carrying hygromycin resistance (LHCX) and caspase-9-DN cells were irradiated with the 480 J/m^2 UVB, and after the indicated times, cytosolic extracts were assayed for caspase-3 activity with the specific substrate DEVD-aminomethylcoumarin (AMC) (a), for caspase-9 activity with LEHD-AMC (b), or for caspase-8 activity with the specific substrate IETD-AMC (c). All data are presented as means ± SEM of three replicates of a representative experiment; essentially the same results were obtained in three independent experiments. *$P < 0.01$, **$P < 0.001$ for all figures.

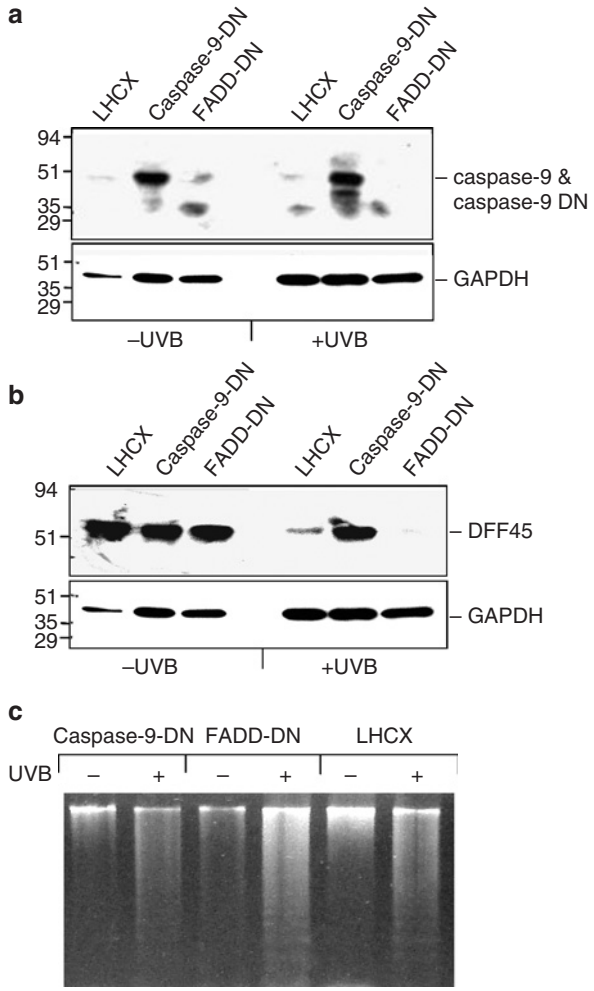

Figure 2. Expression of dominant-negative caspase-9 (caspase-9-DN), but not Fas-associated protein with death domain (FADD)-DN, suppresses caspase-3-mediated proteolytic cleavage of DNA fragmentation factor (DFF) 45 and internucleosomal DNA fragmentation in HPV-immortalized keratinocyte (KC). Retroviral constructs constitutively expressing caspase-9-DN or FADD-DN were cloned in pLHCX and used to infect HPV16 E6/7-immortalized KC; retrovirus-infected cells were selected in hygromycin as described in *Materials and methods*. Cells were irradiated with 480 J/m^2 ultraviolet (UV) B, and after the 16 h, cytosolic extracts were assayed for the presence of caspase-9-DN by immunoblot analysis (a); the immunoblot in (a) was stripped of antibodies and reprobed with antibodies to full-length DFF45 (b) or to GAPDH (protein-loading control). (c) Caspase-9-DN-, FADD-DN-, and retroviral expression vector carrying hygromycin resistance (LHCX)-expressing cells were irradiated with 480 J/m^2 UVB. After 16 h, DNA was isolated, resolved by 1% agarose gel electrophoresis, and visualized by ethidium bromide staining. All data in panel (a) are presented as means ± SEM of three replicates of a representative experiment; essentially the same results were obtained in three independent experiments.

form (p17), but this processing is completely blocked in caspase-9-DN cells (Fig. 3a,b).

Cytosolic extracts from LHCX and caspase-9-DN cells were then derived at different times after UVB exposure and subjected to caspase-8 activity assays. UVB exposure of control LHCX cells, but not caspase-9-DN cells, induced a time-dependent increase in caspase-8 activity (Fig. 1c), providing further evidence that caspase-8 acts downstream of caspase-9 activation. To examine internucleosomal cleavage of DNA, another

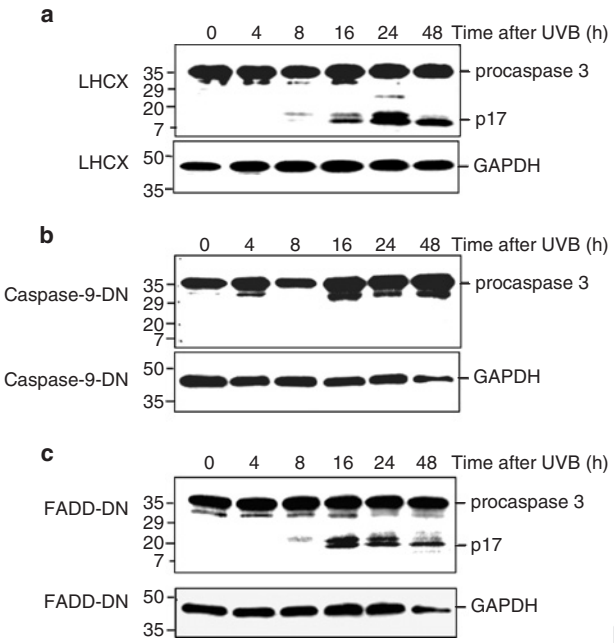

Figure 3. Expression of dominant-negative caspase-9 (caspase-9-DN) suppresses proteolytic cleavage of caspase-3 to its active form in HPV-immortalized keratinocyte (KC). Retroviral expression vector carrying hygromycin resistance (LHCX) control retroviral constructs (a) or LHCX retroviral constructs constitutively caspase-9-DN (b) or Fas-associated protein with death domain (FADD)-DN (c) were used to infect HPV16 E6/7-immortalized KC; retrovirus-infected cells were selected in hygromycin as described in *Materials and methods*. Cells were irradiated with 480 J/m^2 ultraviolet (UV) B, and after the indicated times, cytosolic extracts were assayed for the presence of the large active p17 subunit of caspase-3 or GAPDH (loading control) by immunoblot analysis.

hallmark of apoptosis, we exposed LHCX and caspase-9-DN cells to UVB, after which DNA was extracted and resolved by agarose gel electrophoresis. A characteristic pattern of apoptotic internucleosomal DNA fragmentation is observed in control LHCX (and FADD-DN, below) cells exposed to UVB, which is attenuated in caspase-9-DN cells (Fig. 2c). These results together indicate that the mitochondrial pathway and caspase-9 activation is required and plays a pivotal role in UVB-induced apoptosis in immortalized human KC.

UVB-induced apoptosis is independent of DR signaling in HPV-immortalized KC

Immortalized KC stably expressing a FADD-DN mutant were next employed to confirm or exclude involvement of DR signaling via FADD in UVB-induced activation of caspases-9 and -3. Immunoblot analysis with antibodies to FADD revealed that FADD-DN cells express both the wild-type and the truncated FADD-DN protein lacking the N-terminal DED domain required for recruitment and activation of procaspase-8 at the DISC (Fig. 4a). In contrast, control LHCX cells

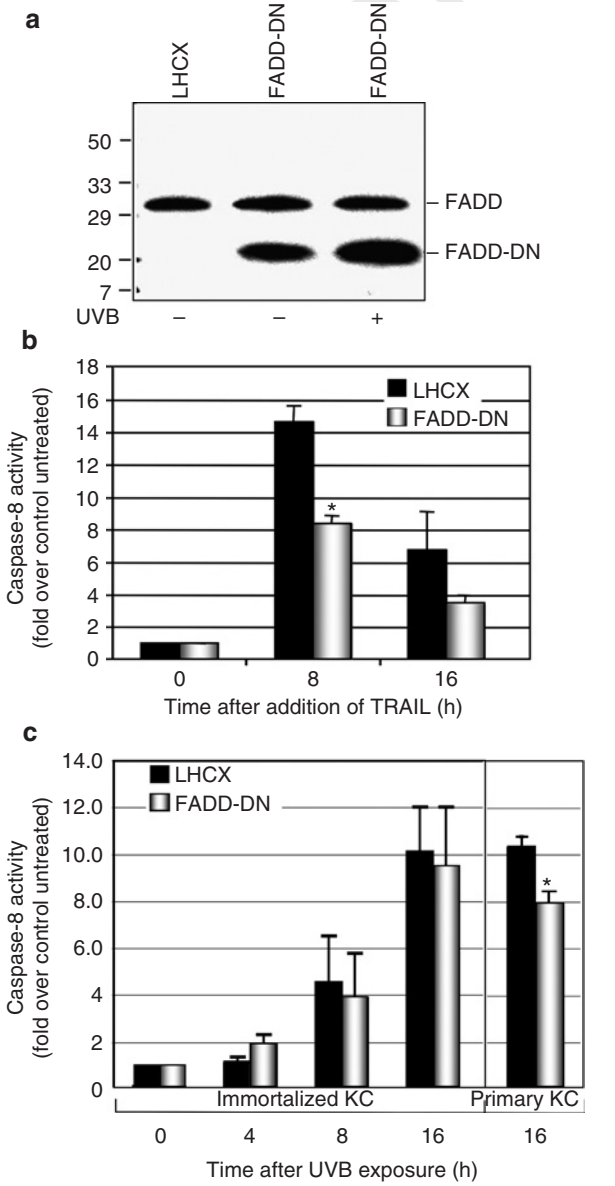

Figure 4. Stable expression of Fas-associated protein with death domain (FADD)- dominant negative (DN) suppresses tumor necrosis factor-related apoptosis-inducing ligand (TRAIL)- but not ultraviolet (UV) B-induced caspase-8 activation in HPV-immortalized keratinocyte (KC). Retroviral constructs constitutively expressing FADD-DN were cloned in pLHCX and used to infect HPV16 E6/7-immortalized KC; retrovirus-infected cells were selected in hygromycin as described in *Materials and methods*. Control retroviral expression vector carrying hygromycin resistance (LHCX) and FADD-DN-expressing cells were exposed to UVB for 16 h (a) or for the indicated times (c), or treated with 100 ng/ml of soluble TRAIL (b), and after the indicated times, cytosolic extracts were assayed for the presence of FADD-DN by immunoblot analysis (a) or for caspase-8 activity with the specific substrate IETD-aminomethylcoumarin (b, c). All data in panels b and c are presented as means ± SEM of three replicates of a representative experiment; essentially the same results were obtained in three independent experiments.

express only the endogenous wild-type FADD protein. We have utilized similar FADD-DN constructs to impair recruitment of procaspase-8 to the DISC and effectively block apoptosis and vesication of KC exposed to the DNA alkylating agent sulfur mustard (41).

We first tested whether expression of FADD-DN could in fact suppress DR-mediated caspase-8 activation. Control LHCX or FADD-DN cells were incubated with soluble TRAIL to induce DR-mediated apoptosis, and cytosolic extracts were derived at different times after addition of TRAIL and analyzed for caspase-8 activity. Following incubation with TRAIL, caspase-8 activity was significantly suppressed in cells expressing FADD-DN (Fig. 4b). However, FADD-DN (Fig. 4c) did not block UVB-induced caspase-8 activation in immortalized KC, indicating that caspase-8 is activated, not via FADD signaling but downstream of caspase-9.

Control LHCX and FADD-DN KC were then exposed to 480 J/m^2 UVB for the indicated times, and cytosolic extracts were analyzed for caspases-9 and -3 activity (Fig. 5). Although FADD-DN cells exhibited reduced caspase-8 activity after treatment with TRAIL, stable expression of FADD-DN had no significant effect on UVB-induced activation of caspases-9 and -3, thus, excluding a role of DR signaling in this response. To examine the effect of FADD-DN on the proteolytic processing of procaspase-3, we next performed immunoblot analysis using the antibody
17 specific for the p17 subunit of caspase-3. Consistent with the results of the fluorometric assays, both LHCX and FADD-DN cells exhibited proteolytic processing of procaspase-3 to its active form (p17) in response to UVB (Fig. 3c). Expression of FADD-DN also did not block caspase-3-mediated cleavage of DFF45, as shown by immunoblot analysis of UVB-irradiated LHCX or FADD-DN cells with antibodies to the intact form of DFF45 (Fig. 2b). Internucleosomal DNA fragmentation was also not blocked by FADD-DN (Fig. 2c). Caspase-3 activation, DFF45 cleavage, and apoptotic DNA fragmentation are thus independent of DR signaling and occur downstream of caspase-9 in UVB-irradiated immortalized KC.

To further analyze the functional role of the initiator caspases-8 and -9 as well as lysosomal proteases in the caspase cascade during UVB-induced apoptosis, we utilized cell-permeable peptide inhibitors specific for caspases-3, -8, or -9 or cathepsin to block activation of these proteases. Immortalized KC were preincubated for 30 min prior to exposure to UVB with z-DEVD-fmk, z-IETD-fmk, z-LEHD-fmk (50 μM; peptide inhibitors for caspase-3, -8, or -9, respectively; BD Biosciences), or z-FA-fmk (inhibitor of cathepsins B and L). Cells were then exposed to 480 J/m^2 UVB, harvested at 16 h after UVB irradiation, and cytosolic extracts were derived and subjected to quantitative fluorometric DEVDase assay to measure caspase-3 activity as a measure of UVB-induced apoptosis. UVB exposure of immortalized KC induced a 4-fold increase in caspase-3 activity, which was attenuated by peptide inhibitors for caspases-3, 8, or 9 (Fig. 6a). The protective effects of the peptide caspase inhibitors were also confirmed in time–course experiments (Fig. 6b). In contrast, z-FA-fmk did not

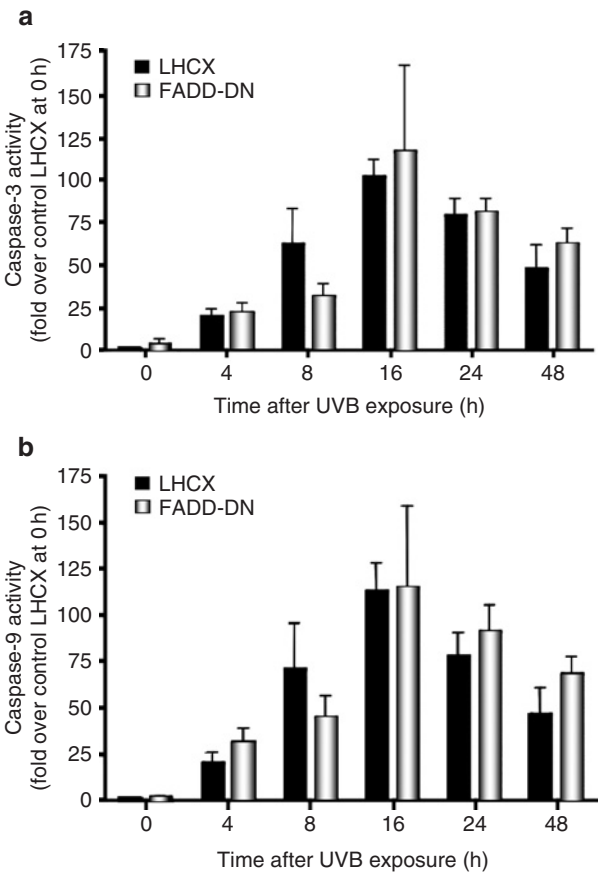

Figure 5. Stable expression of Fas-associated protein with death domain (FADD)-DN does not block ultraviolet (UV) B-induced activation of caspasse-3 and -9 in HPV-immortalized keratinocyte (KC). Retroviral constructs constitutively expressing FADD-DN were cloned in pLHCX and used to infect HPV16 E6/7-immortalized KC; retrovirus-infected cells were selected in hygromycin as described in *Materials and methods*. Control retroviral expression vector carrying hygromycin resistance (LHCX) and FADD-DN cells were irradiated with the 480 J/m^2 UVB, and after the indicated times, cytosolic extracts were assayed for caspase-3 activity with the specific substrate DEVD-aminomethylcoumarin (AMC) (a) or for caspase-9 activity with LEHD-AMC (b). All data are presented as means ± SEM of three replicates of a representative experiment; essentially the same results were obtained in three independent experiments.

Colour Figure

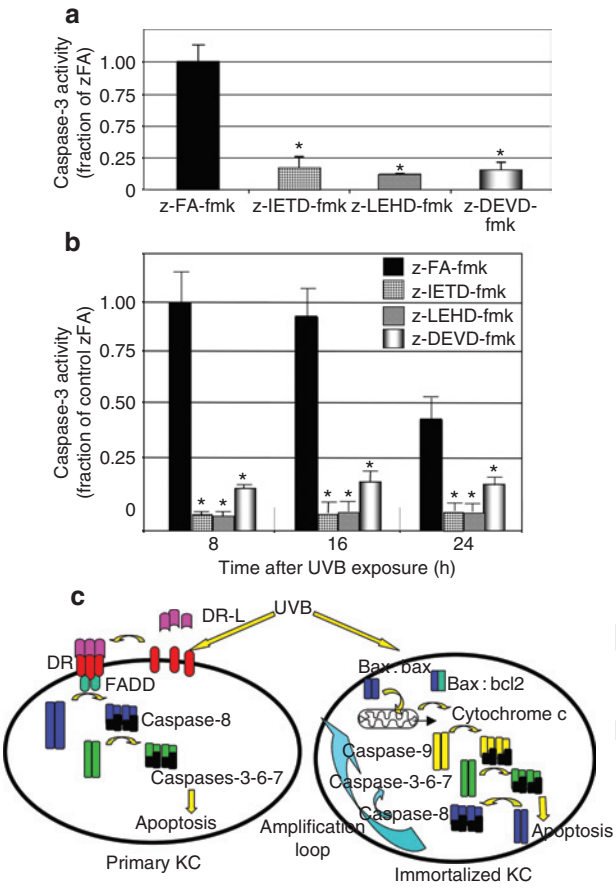

27 *Figure 6*. Preincubation of HPV-immortalized keratinocyte (KC) with peptide inhibitors of caspases-9, -8, and -3 suppresses ultraviolet (UV) B-induced activation of caspase-3 and suggests an amplification loop. Immortalized KC were preincubated for 30 min prior to exposure to UVB with z-DEVD-fmk, z-IETD-fmk, z-LEHD-fmk (50 μM; peptide inhibitors for caspases-3, -8, or -9, respectively), or with z-FA-fmk (inhibitor of cathepsins B and L). Cells were then exposed to 480 J/m^2 UVB, harvested at 16 h (a) or at the indicated times (b) after UVB irradiation, and cytosolic extracts were derived and subjected to quantitative fluorometric DEVDase assay to measure caspase-3 activity. All data are presented as means ± SEM of three replicates of a representative experiment; essentially the same results were obtained in three independent experiments. (c) Proposed pathway of apoptosis in immortalized KC, including amplification loop dependent upon caspase-8. *$P < 0.001$.

25 26

protect KC from UVB-mediated killing, thus, excluding a role for lysosomal proteases cathepsin B/l in this response, in contrast with a previous study showing that overexpression of hurpin, a cytosolic inhibitor of cathepsin L, protects KC from UVB apoptosis (42). These results also indicate that activation of caspases-3, -8, and -9 are necessary for the maximal UVB response. Thus, while caspase-9 is the apical caspase in UVB apoptosis, activation of caspases-3 and -8 is also absolutely required, perhaps as an amplification mechanism for the apoptotic response (Fig. 6c).

Discussion

Normal KCs have been shown to block progression of malignant cells in organotypic models (8), while UVB appears to selectively induce apoptosis in normal KC, allowing the malignant population to expand (9). Thus, apoptosis of normal KC may contribute to tumor progression, while apoptosis of initiated/immortalized cells could result in tumor regression. The pathways involved in each of these processes are of obvious importance to the understanding of carcinogenesis. However, different studies have yielded seemingly conflicting results concerning the relative contributions of the DR vs. the mitochondrial pathway of apoptosis. It is certainly conceivable that cell type determines the mode of cell death. Based upon our previous studies suggesting that upon HPV immortalization, caspase-9 is activated earlier and at lower doses of UVB; we have now tested the individual contributions of FADD and caspase-9 using DN retroviral expression vectors as well as with peptide inhibitors. Our results indicate that caspase-9-DN suppresses UVB apoptosis in KC immortalized with HPV16 E6/7 and that the DR plays no role in the process in these cells. Our results using physiologically relevant HPV-immortalized cells (see below) are in agreement with those of Sitailo et al. (43) who found that caspase-9-DN blocked UVB-induced apoptosis in spontaneously immortalized HaCaT cells, as well as in primary human KC. Additionally, as other studies have also implicated Fas/TNF/TRAIL DR in this process, we have also tested the individual contribution of DR to the apoptotic response using FADD-DN. To our knowledge, this study is the first to use both of these highly specific DNs and peptide inhibitors in one cell type to test each of these pathways side-by-side in response to UVB. Furthermore, we show that while caspase-8 activation is an event that occurs only downstream of the mitochondrial pathway in immortalized cells (as caspase-9-DN, but not FADD-DN is able to block the activation of caspase-8), caspase-8 is nonetheless required for the maximal apoptotic response. Other studies have also shown that caspase-8 can be activated downstream of caspase-9 via both caspase-3-dependent (44) and caspase-3-independent pathways (45). DR-independent FADD has also been implicated in caspase-8 activation downstream of mitochondrial events during anoikis (46) or following treatment with anticancer drugs (47,48). As FADD-DN did not block UVB-induced caspase-8 activation in our system, downstream

cleavage via a caspase-3-dependent pathway rather than induced proximity (FADD dependent) may be involved in the activation of caspase-8 by UVB. Importantly, when caspase-8 activity is blocked by IETD-fmk (Fig. 6), apoptosis is attenuated, demonstrating a role for caspase-8 in amplifying UVB-induced apoptosis of HPV-immortalized KC, possibly via cleavage and activation of Bid.

While solar-simulated light was not utilized in the present study, a filter that mimics the earth's atmosphere by eliminating UVC was employed. Additionally, we used a UVB irradiance of 480 J/m^2 which is equivalent to approximately twice the 18 minimal erythema dose (about one-half hour summertime exposure in Baltimore, MD (49). Nonetheless, UVA has been shown to contribute to both KC apoptosis and photocarcinogenesis (50). Thus, additional studies utilizing both UVA and UVB, as well as human skin grafted onto nude mice are currently underway to determine the relative role of DR and mitochondrial pathways in apoptosis and carcinogenesis of primary and immortalized KC.

Immortalization is thought to be an early step in this process that involves the selection of a population of cells that express hTERT and progress to the next stage of cancer; thus, preneo- 19 plastic (AK and porokeratosis) as well as neoplastic nonmelanoma [(SCC and basal cell carcinoma (BCC)] skin lesions express hTERT (35). We chose to use HPV16 immortalization because of its physiological relevance as well as its utility as a defined agent for immortalization. A number of different HPV types are found in high percentage of BCC and SCC in immunosuppressed individuals (51). Similarly, a range of HPV types have been isolated from actinic keratoses and SCC from epidermodysplasia verruciformis (EV) patients (52). Furthermore, HPV may likely play a role in these cutaneous carcinomas from immunocompetent non-EV patients as well (51,53). While long implicated in the etiology of anogenital cancer, HPV16 and HPV18 are now associated with up to 25% of nongenital Bowen's Disease of the skull, foot, and periungual regions of the finger (54,55); the latter lesion represents a significant fraction of all skin cancer cases (56). As sensitive, strain-specific detection methods become more commonly utilized, HPV-16 is being found in other skin cancers as well, including SCC of the lip (57). In most cases of these nongenital HPV skin cancers, carcinomas occur in sun-exposed sites, indicating cooperation between UV and HPV, including HPV16. As the HPV16 E6 protein participates in the degradation of p53 (58), E6 may in part play the same role as UV-induced p53 mutations during the initiation phase of skin carcinogenesis (59). Interestingly, while E6 derived from HPVs that are more traditionally classified as cutaneous, including HPV77, do not degrade p53, they do interfere with its ability to upregulate the expression of certain key proapoptotic genes in response to UVB, including Fas, PUMAβ, Apaf-1, and PIG3 (60). In most epidermal malignancies, the p16-Rb pathway is also inactivated; in our system, Rb is inactivated by E7. In addition to UVB p53-independent activation of p38 MAPK and Bax (34), sequestering of Rb by E7 would allow E2F1 to upregulate p73 (61,62), Apaf1 (63), as well as a number of BH3-only family members, including PUMA, Noxa, Hrk/DPS, and Bim (64), which coupled with lower Bcl2 levels in HPV16 E6/7 immortalized KC would lead to activation of caspase-9. E2F1 also induces other less well-studied inducers of apoptosis via p53-independent pathways including galectin and actinin a [which activates the apoptotic DNAse Y (65)].

Previous studies comparing the response of primary KC with their immortalized counterparts have utilized cells that are tumor derived or that have been cultured for long periods of time, such as spontaneously immortalized HaCaT cells. The use of immortalized cell lines such as HaCaT involve a number of undefined changes that occur over time in culture. We also found that NcoI cells, KC immortalized with HPV16 E6/7 but cultured for an undetermined period of time in the presence of intermediate calcium (0.5 vs. 0.1 mM), were completely resistant to UVB-induced apoptosis (data not shown). NcoI cells may therefore represent a later irreversible stage of tumorigenesis coinciding with, among other things a loss of the apoptotic response, and that the earliest stages, i.e. immortalization, correspond with decreased cell-cycle control and DNA repair, and concomitant selection for a population with decreased genomic stability. To 20 avoid cell culture artifacts that may arise from the use of well-established lines such as HaCaT cells, we immortalized cells with a defined and physiologically relevant agent, HPV16 E6/7 21 (above), and utilized at passage 30 (60 population doublings), a minimum passage to be considered immortal (66,67). In addition, immortalized cells used in these studies were derived from pooled clones as KCs were transduced with a high-titer retroviral vector expressing HPV16 E6/7.

The idea that the antiapoptotic phenotype arises or continues to evolve after immortalization is

supported by *in vivo* studies in which it was found that p53, p63 (a p53 homolog expressed in replicating KC), and hTERT are expressed in the preneoplastic lesions AK and porokeratosis, as well as in SCC *in situ* and invasive SCC. However, upregulation of the IAP survivin, which is abundantly expressed in most solid and hematologic malignancies, is only found in SCC but not in AK or porokeratosis (35). Similarly, Akt is constitutively activated in some SCC and blocks UVB-induced apoptosis (38). Akt activation phosphorylates the proapoptotic protein Bad, sequestering it in the cytosol with 14-3-3 proteins and consequently preventing cytochrome c release and activation of caspases-9 and -3 (68). The importance of these antiapoptotic proteins involved primarily in the mitochondrial pathway in cutaneous carcinogenesis has been verified in animal models. KC of transgenic mice overexpressing survival proteins Bcl2 or BclxL exhibit a UVB-resistant phenotype as well as a predisposition to skin cancer (69). Survivin, which is undetectable in adult skin but upregulated in malignant KC, when expressed transgenically in skin leads to resistance to UVB-induced cell death by suppression of mitochondrial apoptosis (70). Conversely, UVB-sensitivity to apoptosis is increased by alteration of NF-κB signaling in KC or transgenic expression of a super suppressor IκB in skin (69). Akt activates the NF-κB pathway and is itself a downstream target of NF-κB (71,72).

We postulate that in addition to p53-dependent apoptosis, KCs have a built in fail-safe (almost) mechanism whereby immortalizing agents render cells extremely sensitive to apoptosis, and only further stable genetic or epigenetic events (e.g. upregulation of survivin or constitutive Akt activation) allow the progression of a small subset of immortalized cells, whereas the majority undergo p53-independent apoptosis and regression.

Acknowledgements

This work was supported in part by the National Cancer Institute grant 5RO1 CA100443-02 and the US Army Medical Research and Materiel Command, under contract DAMD17-00-C-0026 (to DSR). Authors thank Yuri Lazebnik (Cold Spring Harbor, NY) for pUC18-caspase-9-DN, Vishva Dixit (Genentech) for pcDNA- FADD-DN and Richard Schlegel (Department of Oncology, Georgetown University) for the HPV16-E6/7 retroviral vectors.

References

1. Cleaver J E Crowley E. UV damage, DNA repair and skin carcinogenesis. Front Biosci 2002: 7: d1024–1043.
2. Stratton S P. Prevention of non-melanoma skin cancer. Curr Oncol Rep 2001: 3: 295–300.
3. Jonason A S, Kunala S, Price G J et al. Frequent clones of p53-mutated keratinocytes in normal human skin. Proc Natl Acad Sci USA 1996: 93: 14025–14029.
4. Karen J, Wang Y, Javaherian A, Vaccariello M, Fusenig N E, Garlick J A. 12-O-tetradecanoylphorbol-13-acetate induces clonal expansion of potentially malignant keratinocytes in a tissue model of early neoplastic progression. Cancer Res 1999: 59: 474–481.
5. Mammone T, Gan D, Collins D, Lockshin R A, Marenus K, Maes D. Successful separation of apoptosis and necrosis pathways in HaCaT keratinocyte cells induced by UVB irradiation. Cell Biol Toxicol 2000: 16: 293–302.
6. Simbulan-Rosenthal C M, Velena A, Veldman T, Schlegel R, Rosenthal D S. HPV-16 E6/7 immortalization sensitizes human keratinocytes to ultraviolet B by altering the pathway from caspase-8 to caspase-9-dependent apoptosis. J Biol Chem 2002: 277: 24709–24716.
7. Simbulan-Rosenthal C M, Trabosh V, Velarde A et al. Id2 protein is selectively upregulated by UVB in primary, but not in immortalized human keratinocytes and inhibits differentiation. Oncogene 2005: 4: 5443–5458.
8. Vaccariello M, Javaherian A, Wang Y, Fusenig N E, Garlick J A. Cell interactions control the fate of malignant keratinocytes in an organotypic model of early neoplasia. J Invest Dermatol 1999: 113: 384–391.
9. Mudgil A V, Segal N, Andriani F, Wang Y, Fusenig N E, Garlick J A. Ultraviolet B irradiation induces expansion of intraepithelial tumor cells in a tissue model of early cancer progression. J Invest Dermatol 2003: 121: 191–197.
10. Bernerd F, Asselineau D. Successive alteration and recovery of epidermal differentiation and morphogenesis after specific UVB-damages in skin reconstructed in vitro. Dev Biol 1997: 183: 123–138.
11. Laethem A V, Claerhout S, Garmyn M, Agostinis P. The sunburn cell: regulation of death and survival of the keratinocyte. Int J Biochem Cell Biol 2005: 37: 1547–1553 (Epub March 8 2005).
12. Sheehan J M, Young A R. The sunburn cell revisited: an update on mechanistic aspects. Photochem Photobiol Sci 2002: 1: 365–377.
13. Rehman I, Takata M, Wu Y Y, Rees J L. Genetic change in actinic keratoses. Oncogene 1996: 12: 2483–2490.
14. Zhuang L, Wang B, Sauder D N. Molecular mechanism of ultraviolet-induced keratinocyte apoptosis. J Interferon Cytokine Res 2000: 20: 445–454.
15. Wehrli P, Viard I, Bullani R, Tschopp J, French L E. Death receptors in cutaneous biology and disease. J Invest Dermatol 2000: 115: 141–148.
16. Schwarz A, Bhardwaj R, Aragane Y et al. Ultraviolet-B-induced apoptosis of keratinocytes: evidence for partial involvement of tumor necrosis factor-alpha in the formation of sunburn cells. J Invest Dermatol 1995: 104: 922–927.
17. Zhuang L, Wang B, Shinder G A, Shivji G M, Mak T W, Sauder D N. TNF receptor p55 plays a pivotal role in murine keratinocyte apoptosis induced by ultraviolet B irradiation. J Immunol 1999: 162: 1440–1447.
18. Banerjee G, Gupta N, Kapoor A, Raman G. UV induced bystander signaling leading to apoptosis. Cancer Lett 2005: 223: 275–284 (Epub 23 November 2004).

19. Leverkus M, Yaar M, Gilchrest B A. Fas/Fas ligand interaction contributes to UV-induced apoptosis in human keratinocytes. Exp Cell Res 1997: 232: 255–262.
20. Hill L L, Ouhtit A, Loughlin S M, Kripke M L, Ananthaswamy H N, Owen-Schaub L B. Fas ligand: a sensor for DNA damage critical in skin cancer etiology. Science 1999: 285: 898–900.
21. Aragane Y, Kulms D, Metze D et al. Ultraviolet light induces apoptosis via direct activation of CD95 (Fas/APO-1) independently of its ligand CD95L. J Cell Biol 1998: 140: 171–182.
22. Zeise E, Weichenthal M, Schwarz T, Kulms D. Resistance of human melanoma cells against the death ligand TRAIL is reversed by ultraviolet-B radiation via downregulation of FLIP. J Invest Dermatol 2004: 123: 746–754.
23. Stander S, Schwarz T. Tumor necrosis factor-related apoptosis-inducing ligand (TRAIL) is expressed in normal skin and cutaneous inflammatory diseases, but not in chronically UV-exposed skin and non-melanoma skin cancer. Am J Dermatopathol 2005: 27: 116–121.
24. Bang B, Rygaard J, Baadsgaard O, Skov L. Increased expression of Fas on human epidermal cells after in vivo exposure to single-dose ultraviolet (UV) B or long-wave UVA radiation. Br J Dermatol 2002: 147: 1199–1206.
25. Bang B, Gniadecki R, Larsen J K, Baadsgaard O, Skov L. In vivo UVB irradiation induces clustering of Fas (CD95) on human epidermal cells. Exp Dermatol 2003: 12: 791–798.
26. Kim P K, Weller R, Hua Y, Billiar T R. Ultraviolet irradiation increases FADD protein in apoptotic human keratinocytes. Biochem Biophys Res Commun 2003: 302: 290–295.
27. Wu S, Loke H N, Rehemtulla A. Ultraviolet radiation-induced apoptosis is mediated by Daxx. Neoplasia 2002: 4: 486–492.
28. Kulms D, Schwarz T. Independent contribution of three different pathways to ultraviolet-B-induced apoptosis. Biochem Pharmacol 2002: 64: 837–841.
29. Brash D E. Sunlight and the onset of skin cancer. Trends Genet 1997: 13: 410–414.
30. de Gruijl F R, van Kranen H J, Mullenders L H. UV-induced DNA damage, repair, mutations and oncogenic pathways in skin cancer. J Photochem Photobiol B 2001: 63: 19–27.
31. Miyashita T, Reed J C. Tumor suppressor p53 is a direct transcriptional activator of the human bax gene. Cell 1995: 80: 293–299.
32. Assefa Z, Garmyn M, Vantieghem A et al. Ultraviolet B radiation-induced apoptosis in human keratinocytes: cytosolic activation of procaspase-8 and the role of Bcl-2. FEBS Lett 2003: 540: 125–132.
33. Shiloh Y. ATM and related protein kinases: safeguarding genome integrity. Nat Rev Cancer 2003: 3: 155–168.
34. Van Laethem A, Van Kelst S, Lippens S et al. Activation of p38 MAPK is required for Bax translocation to mitochondria, cytochrome c release and apoptosis induced by UVB irradiation in human keratinocytes. FASEB J 2004: 18: 1946–1948 (Epub 23 September 2004).
35. Park H R, Min S K, Cho H D, Kim K H, Shin H S, Park Y E. Expression profiles of p63, 53, survivin, and hTERT in skin tumors. J Cutan Pathol 2004: 31: 544–549.
36. Evan G I, Vousden K H. Proliferation, cell cycle and apoptosis in cancer. Nature 2001: 411: 342–348.
37. Altieri D C. Survivin, versatile modulation of cell division and apoptosis in cancer. Oncogene 2003: 22: 8581–8589.
38. Decraene D, Van Laethem A, Agostinis P et al. AKT status controls susceptibility of malignant keratinocytes to the early-activated and UVB-induced apoptotic pathway. J Invest Dermatol 2004: 123: 207–212.
39. Pan G, O'Rourke K, Dixit V M. Caspase-9, Bcl-XL, and Apaf-1 form a ternary complex. J Biol Chem 1998: 273: 5841–5845.
40. Fearnhead H O, Rodriguez J, Govek E E et al. Oncogene-dependent apoptosis is mediated by caspase-9. Proc Natl Acad Sci USA 1998: 95: 13664–13669.
41. Rosenthal D S, Velena A, Chou F P et al. Expression of dominant-negative Fas-associated death domain blocks human keratinocyte apoptosis and vesication induced by sulfur mustard. J Biol Chem 2003: 278: 8531–8540 (Epub 12 December 2002).
42. Welss T, Sun J, Irving J A et al. Hurpin is a selective inhibitor of lysosomal cathepsin L and protects keratinocytes from ultraviolet-induced apoptosis. Biochemistry 2003: 42: 7381–7389.
43. Sitailo L A, Tibudan S S, Denning M F. Activation of caspase-9 is required for UV-induced apoptosis of human keratinocytes. J Biol Chem 2002: 277: 19346–19352 (Epub 27 March 2002).
44. Slee E A, Harte M T, Kluck R M et al. Ordering the cytochrome c-initiated caspase cascade: hierarchical activation of caspases-2, -3, -6, -7, -8, and -10 in a caspase-9-dependent manner. J Cell Biol 1999: 144: 281–292.
45. Pirnia F, Schneider E, Betticher D C, Borner M M. Mitomycin C induces apoptosis and caspase-8 and -9 processing through a caspase-3 and Fas-independent pathway. Cell Death Differ 2002: 9: 905–914.
46. Rytomaa M, Martins L M, Downward J. Involvement of FADD and caspase-8 signalling in detachment-induced apoptosis. Curr Biol 1999: 9: 1043–1046.
47. Micheau O, Solary E, Hammann A, Dimanche-Boitrel M T. Fas ligand-independent, FADD-mediated activation of the Fas death pathway by anticancer drugs. J Biol Chem 1999: 274: 7987–7992.
48. Wesselborg S, Engels I H, Rossmann E, Los M, Schulze-Osthoff K. Anticancer drugs induce caspase-8/FLICE activation and apoptosis in the absence of CD95 receptor/ligand interaction. Blood 1999: 93: 3053–3063.
49. Heisler G M, Grant R H, Gao W, Slusser J R. Solar ultraviolet-B radiation in urban environments: the case of Baltimore, Maryland. Photochem Photobiol 2004: 80: 422–428.
50. Larsson P, Andersson E, Johansson U, Ollinger K, Rosdahl I. Ultraviolet A and B affect human melanocytes and keratinocytes differently. A study of oxidative alterations and apoptosis. Exp Dermatol 2005: 14: 117–123.
51. Shamanin V, zur Hausen H, Lavergne D et al. Human papillomavirus infections in nonmelanoma skin cancers from renal transplant recipients and nonimmunosuppressed patients. J Natl Cancer Inst 1996: 88: 802–811.
52. Bouwes Bavinck J N, Stark S, Petridis A K et al. The presence of antibodies against virus-like particles of epidermodysplasia verruciformis-associated humanpapillomavirus type 8 in patients with actinic keratoses. Br J Dermatol 2000: 142: 103–109.
53. zur Hausen H. Papillomavirus infections – a major cause of human cancers. Biochim Biophys Acta 1996: 1288: F55–F78.

54. Guerin-Reverchon I, Chardonnet Y, Viac J, Chouvet B, Chignol MC, Thivolet J. Human papillomavirus infection and filaggrin expression in paraffin-embedded biopsy specimens of extragenital Bowen's disease and genital bowenoid papulosis. J Cancer Res Clin Oncol 1990: 116: 295–300.
55. Kettler A H, Rutledge M, Tschen J A, Buffone G. Detection of human papillomavirus in nongenital Bowen's disease by in situ DNA hybridization. Arch Dermatol 1990: 126: 777–781.
56. Eliezri Y D, Silverstein S J, Nuovo G J. Occurrence of human papillomavirus type 16 DNA in cutaneous squamous and basal cell neoplasms. J Am Acad Dermatol 1990: 23: 836–842.
57. Kawashima M, Favre M, Obalek S, Jablonska S, Orth G. Premalignant lesions and cancers of the skin in the general population: evaluation of the role of human papillomaviruses. J Invest Dermatol 1990: 95: 537–542.
58. Thomas M, Pim D, Banks L. The role of the E6-p53 interaction in the molecular pathogenesis of HPV. Oncogene 1999: 18: 7690–7700.
59. Sedman S A, Hubbert N L, Vass W C, Lowy D R, Schiller J T. Mutant p53 can substitute for human papillomavirus type 16 E6 in immortalization of human keratinocytes but does not have E6-associated trans-activation or transforming activity. J Virol 1992: 66: 4201–4208.
60. Giampieri S, Garcia-Escudero R, Green J, Storey A. Human papillomavirus type 77 E6 protein selectively inhibits p53-dependent transcription of proapoptotic genes following UV-B irradiation. Oncogene 2004: 23: 5864–5870.
61. Irwin M, Marin MC, Phillips A C et al. Role for the p53 homologue p73 in E2F-1-induced apoptosis. Nature 2000: 407: 645–648.
62. Stiewe T, Putzer B M. Role of the p53-homologue p73 in E2F1-induced apoptosis. Nat Genet 2000: 26: 464–469.
63. Furukawa Y, Nishimura N, Satoh M et al. Apaf-1 is a mediator of E2F-1-induced apoptosis. J Biol Chem 2002: 277: 39760–39768 (Epub 30 July 2002).
64. Hershko T, Ginsberg D. Up-regulation of Bcl-2 homology 3 (BH3)-only proteins by E2F1 mediates apoptosis. J Biol Chem 2004: 279: 8627–8634 (Epub 18 December 2003).
65. Li Z, Stanelle J, Leurs C, Hanenberg H, Putzer B M. Selection of novel mediators of E2F1-induced apoptosis through retroviral expression of an antisense cDNA library. Nucleic Acids Res 2005: 33: 2813–2821.
66. Rheinwald J G, Green H. Serial cultivation of strains of human epidermal keratinocytes: the formation of keratinizing colonies from single cells. Cell 1975: 6: 331–343.
67. Kiyono T, Foster S A, Koop J I, McDougall J K, Galloway D A, Klingelhutz A J. Both Rb/p16INK4a inactivation and telomerase activity are required to immortalize human epithelial cells. Nature 1998: 396: 84–88.
68. Wang H Q, Quan T, He T, Franke T F, Voorhees J J, Fisher G J. Epidermal growth factor receptor-dependent, NF-kappaB-independent activation of the phosphatidylinositol 3-kinase/Akt pathway inhibits ultraviolet irradiation-induced caspases-3, -8, and -9 in human keratinocytes. J Biol Chem 2003: 278: 45737–45745 (Epub 2 September 2003).
69. Nickoloff B J, Qin J Z, Chaturvedi V, Bacon P, Panella J, Denning M F. Life and death signaling pathways contributing to skin cancer. J Investig Dermatol Symp Proc 2002: 7: 27–35.
70. Grossman D, Kim P J, Blanc-Brude O P et al. Transgenic expression of survivin in keratinocytes counteracts UVB-induced apoptosis and cooperates with loss of p53. J Clin Invest 2001: 108: 991–999.
71. Madrid L V, Mayo M W, Reuther J Y, Baldwin A S Jr. Akt stimulates the transactivation potential of the RelA/p65 subunit of NF-kappa B through utilization of the Ikappa B kinase and activation of the mitogen-activated protein kinase p38. J Biol Chem 2001: 276: 18934–18940 (Epub 20 March 2001).
72. Meng F, Liu L, Chin P C, D'Mello S R. Akt is a downstream target of NF-kappa B. J Biol Chem 2002: 277: 29674–29680 (Epub 6 June 2002).